THE INFLUENCE OF HYDROXYL ION CONTENT ON THE MECHANICAL PROPERTIES OF A SODA-LIME-SILICA GLASS

by

ADAM CHLEBIK

Submitted for the Degree of Doctor of Philosophy

UNIVERSITY OF WARWICK

Department of Physics

DECEMBER 1983

TABLE OF CONTENTS

LIST OF TABLES

LIST OF FIGURES

MEMORANDUM

This dissertation is submitted to the University of Warwick in support of my application for admission to the degree of Doctor of Philosophy. It contains an account of my work carried out at the Department of Physics of the University of Warwick in the period October 1976 to October 1979 under the general supervision of Prof. P.W. McMillan. No part of it has been used previously in a degree thesis submitted to this or any other University. The work described is the result of my own independent research except where specifically acknowledged in the text.

December 1983.

Adam Chlebik.

ACKNOWLEDGEMENTS

I would like to take this opportunity to thank the Science Research Council for providing the financial support for this study, and also to thank the Department of Physics for making the facilities available for the research work. In addition my thanks go to Prof. P W McMillan for his advice and guidance, and to my colleagues in the Glass Ceramics Section for their helpful discussions.

I would also like to acknowledge the help and practical assistance provided by Pilkington Brothers Ltd, and to thank G Copley for being my industrial supervisor. Finally, I am especially grateful to R Gaskell for his considerable help in the preparation of the glasses used in this study.

SUMMARY

A range of soda-lime-silica glasses based on the composition 16% Na_2O, 10% CaO and 74% SiO_2 have been prepared with hydroxyl ion contents which varied from 59 to 780 ppm. The hydroxyl ion contents were determined using transmission Infra-red spectroscopy.

The mechanical strength properties were investigated using the constant moment, double cantilever beam arrangement for fracture mechanics studies, and under atmospheres of 1% and 60% relative humidity. Four point bend studies under liquid nitrogen, and at room temperature were carried out using a number of different loading rates. In addition extensive Hertzian fracture and Vickers hardness testing has been carried out.

The results of these experiments were analysed in terms of a continuum model of mechanical strength based on fracture mechanics concepts. The fracture mechanics experiments indicated that fracture toughness increased slightly with increasing hydroxyl ion content. Under Stage I subcritical slow crack growth at 60% relative humidity, crack velocities were greater in high hydroxyl ion content glasses than in low hydroxyl ion content glasses.

In addition the effects of hydroxyl ion content on the low temperature viscosity, D.C. conductivity and elastic moduli, have been investigated. The viscosity was observed to decrease with increasing hydroxyl ion content, as did the activation energy for viscous flow. The D.C. conductivity decreased with increasing hydroxyl ion content.

The mechanical strength results were interpreted in terms of stress-corrosion behaviour, influenced by alkali ion diffusion to the crack tip.

SUMMARY

A range of soda-lime-silica glasses based on the composition 16% Na_2O, 10% CaO and 74% SiO_2 have been prepared with hydroxyl ion contents which varied from 59 to 780 ppm. The hydroxyl ion contents were determined using transmission Infra-red spectroscopy.

The mechanical strength properties were investigated using the constant moment, double cantilever beam arrangement for fracture mechanics studies, and under atmospheres of 1% and 60% relative humidity. Four point bend studies under liquid nitrogen, and at room temperature were carried out using a number of different loading rates. In addition extensive Hertzian fracture and Vickers hardness testing has been carried out.

The results of these experiments were analysed in terms of a continuum model of mechanical strength based on fracture mechanics concepts. The fracture mechanics experiments indicated that fracture toughness increased slightly with increasing hydroxyl ion content. Under Stage I subcritical slow crack growth at 60% relative humidity, crack velocities were greater in high hydroxyl ion content glasses than in low hydroxyl ion content glasses.

In addition the effects of hydroxyl ion content on the low temperature viscosity, D.C. conductivity and elastic moduli, have been investigated. The viscosity was observed to decrease with increasing hydroxyl ion content, as did the activation energy for viscous flow. The D.C. conductivity decreased with increasing hydroxyl ion content.

The mechanical strength results were interpreted in terms of stress-corrosion behaviour, influenced by alkali ion diffusion to the crack tip.

CHAPTER 1

INTRODUCTION

1.1 GENERAL BACKGROUND

Glass is in many ways the most versatile and potentially useful material available. However the biggest single limitation to the use of glass, particularly as a structural material, is its relatively low mechanical strength in tension.

The mechanical strength of glass can be broadly defined by two effects:

(1) The tendency to undergo fast catastrophic failure (brittle fracture) at stresses low compared to the theoretical strength.

(2) A pronounced susceptibility to fatigue especially in the presence of water. Fatigue will be taken to mean either a tendency to fail after some time at a constant load (static fatigue) or a tendency for the failure stress to be stress rate dependant, (dynamic fatigue).

Considering the first characteristic, the fracture of materials can be considered as being of two types, i.e. ductile or brittle. In ductile fracture a considerable amount of energy is expended and substantial irreversible deformation occurs prior to fracture. In contrast, in the brittle mode there is little or no irreversible deformation prior to fracture and the amount of energy absorbed is

correspondingly smaller. Whether a material will fail in a brittle or ductile mode can depend both on the material and on the conditions of testing, i.e. temperature, strain rate, test geometry.

Glasses fail in a brittle mode for two reasons. Firstly their atomic structure and bonding prohibits the presence of the irreversible deformation mechanisms which are present in metals. Secondly, the presence of flaws in the glass surface will influence failure in a britale mode.

The presence of flaws was first postulated by Griffith (1921) who investigated the strength of glass tubes with flaws of known size introduced into the surface. From his experiments he was able to conclude that flaws were present in all the glass tubes, even the tubes which had not been scratched to deliberately introduce flaws. These flaws are thought to be microscopic cracks in the glass surface which are introduced even by normal handling of the glass.

The other characteristic of the mechanical strength of glass is that fatigue readily occurs. As previously stated there are two types of fatigue behaviour, i.e. static and dynamic fatigue, although these terms more correctly describe the mode of testing rather than the mechanisms involved.

In static fatigue studies specimens are maintained at a fixed load and the time to failure recorded. In dynamic fatigue studies, however, the failure load or stress is recorded as a function of loading rate.

The results of these studies show that as the load is increased in static fatigue the time to failure decreases. Dynamic fatigue studies show that the load for failure increases as the rate of load application increases. These two results have a number of common characteristics, namely that as the time for which a glass surface is exposed to a tensile stress increases then the final stress that the glass will be able to sustain decreases. In addition, the presence of water in the surrounding environment also serves to decrease the failure stress in both types of study.

These two main effects, namely brittle fracture and fatigue susceptibility, have been studied for over sixty years. Over this time, a considerable amount of effort has been expended on defining and understanding the parameters which influence the mechanical strength of glass. There is however one noticeable gap in the body of information available, and this is on the compositional dependence of mechanical strength. Some studies have been performed but these have mostly compared different glass forming systems and there is very little information available concerning systematic studies within a glass forming system. The aim of this project is to try and rectify this situation by studying the effects of variations in just one component i.e. the hydroxyl ion within a glass. The hydroxyl ion content is a particularly interesting component because it is present only in small quantities but is known to have highly significant and to a certain extent anomolous effects on some of the physical properties of glasses.

1.2 AIMS OF THE WORK AND PLAN OF THESIS

As previously stated the aim of this work is to study the influence of hydroxyl ion content upon the mechanical strength of a soda-lime-silica glass.

The first stage of such a study will be to prepare glasses of differing hydroxyl ion content. The techniques considered and the experimental details of this aspect of the work are considered in Chapter 4.

The next stage of the work will be to characterise the prepared glasses with regard to their mechanical strengths. However, since the mechanical strength of glass is an essentially macroscopic property of the material, although it is influenced by the glass structure, the approach that it is proposed to adopt is to firstly define the mechanical strengths of the prepared glasses. Secondly, since the effects of glass structure and composition on mechanical strength are so poorly understood, it is proposed to study the microscopic and structural effects of hydroxyl ions by other experiments where the compositional dependance is more fully understood. To this end the experimental work will be divided into two chapters, 5 and 6. In Chapter 5 the experimental details of mechanical strength studies are presented and in Chapter 6 the other experiments performed are discussed. The results obtained from the techniques described in Chapters 5 and 6 will be presented in Chapter 7.

In order to introduce this dual approach the following chapter will present a review of the macroscopic view of mechanical strength studies, and in Chapter 3 the microscopic and structural aspects will be considered.

CHAPTER 2

REVIEW OF MACROSCOPIC STUDIES OF MECHANICAL STRENGTH

2.1 INTRODUCTION

The purpose of this chapter is to describe the current theories of mechanical strength of glass and to review the major experimental results of previous studies.

A review of this sort is necessary for two reasons. Firstly by considering the theories of mechanical strength of glass it is hoped to be able to show how composition may have an influence. Secondly the previous experimental studies which have been carried out should give guidance as to the experiments which are necessary for this study in order to define accurately the mechanical strength of glass.

The mechanical strength of glass has been studied extensively over the last sixty to seventy years. Recently there have been a number of good review articles relevant to an understanding of the mechanical strength of glass.

The book by Lawn and Wilshaw (1975) contains many of the basic tools required for an understanding of the fracture behaviour of brittle solids. The review by Lacourse (1972) presents a detailed view of the Griffith theory and of many of the relevant experimental results. Wachtman Jr (1974) has given a good general

review of the fracture mechanics approach to brittle fracture. Static fatigue behaviour has been reviewed by Adams and McMillan (1977). It is clear that with such a large amount of information on the subject of mechanical strength of glass, it would be impossible to describe the previous studies exhaustively. Hence this review chapter will try to describe the major theoretical tools available to analyse the fracture behaviour of glass.

As previously stated the two major phenomena which characterise the mechanical strength of glass are brittle fracture and fatigue susceptability.

The first of these to be considered will be brittle fracture which will be considered in two parts: firstly, the approaches aimed at characterising strength in terms of an intrinsic material parameter will be described. Secondly, the nature of the flaws and flaw inducing processes which contribute to the low mechanical strength of glass will be considered.

2.2 BRITTLE FRACTURE

2.2.1 Background

Glass is conventionally described as a perfectly brittle solid which fractures at low stress levels and low strains (1%. There have been a number of attempts to calculate the mechanical strength of glass from first principles e.g. Naray-Szabo and Ladik (1960).

These calculations have been based on the force-separation characteristics of the Si-O bond, and have given answers for a theoretical failure stress of the order of one tenth of the Young's modulus E. The observed breaking stress of bulk glass however is of the order of one thousandth of the Young's modulus. This discrepancy between theory and experimental results was first accounted for by Griffith (1920).

An important precursor to the Griffith theory of failure was described by Inglis in 1913. Inglis considered the stresses and strains around an elliptical hole with its major axis perpendicular to the applied uniform stress. Inglis evaluated the expression

$$\frac{\sigma_{max}}{\sigma_{applied}} = 2\sqrt{\frac{L}{\rho}} \qquad (2.2.1)$$

where σ_{max} is the maximum stress experienced, L is half the major axis length and ρ is the radius of curvature at the end of the major axis. Thus the stress experienced around such a hole is a sensitive function of the length and shape of the hole.

Using this theory the major step forward in the study of brittle fracture was made by Griffith in 1920. Griffith considered two interrelated phenomena i.e. the initiation of brittle failure by flaws and the propagation of a crack to catastrophic failure. Although the initiation process precedes crack propagation it is more instructive to consider propagation before initiation.

Griffith considered thermodynamically the situation of a crack extending infinitesimally and reversibly in a body of isotropic perfectly elastic material under the action of a uniform tension normal to the major axis of the crack. Considering the total energy of the system U in terms of the stored elastic strain energy U_E, W_L the work done by the external loading system, and U_S the surface energy required to produce two new surfaces, then

$$U = (U_E - W_L) + U_S \qquad (2.2.2)$$

And for equilibrium to be maintained i.e. for the crack to remain of constant length the dU/dc must be zero. Considering the case of an elliptical crack in uniform tension of σ_L Griffiths was able to show that the crack would extend when

$$\sigma_L = \left(\frac{2E\gamma}{\pi C}\right)^{\frac{1}{2}} \qquad (2.2.3)$$

where E = Young's modulus of glass

C = ½ total crack length

γ = Surface energy for each surface

Griffith then went on to investigate experimentally the failure of glass bulbs with introduced defects of known size. From these results he was able to estimate the surface energy and was thus able to conclude that, as received, glass specimens contained defects of at least 2μm.

Thus Griffith had investigated the two fundamental events of brittle fracture i.e. initiation and propagation and had laid the foundations of the science of fracture. In practical terms the equations developed by Griffith were limited by the need to know the fracture surface energy as a material parameter for any glass of interest.

The next major advance in the science of fracture lay in the development of the fracture mechanics techniques.

2.2.2 Fracture Mechanics

As the work of Inglis (1913) had been a precursor to the theories put forward by Griffith (1920), so the work of Westergaard (1939) was necessary before further developments could take place. Westergaard considered a sharp slit under a stress field tending to produce crack extension by three possible modes i.e. Mode I tension, Mode II shear and Mode III antiplane shear, Fig. 2.1. Mode I (crack opening in tension) is the simplest mode to consider both conceptually and analytically and discussions in this work will be confined to this mode. Westergaard described the stresses around a crack tip under Mode I loading by an equation of the form:

$$\sigma_{ij} = K_I (2\pi r)^{\frac{1}{2}} f_{ij} (\theta) \qquad (2.2.4)$$

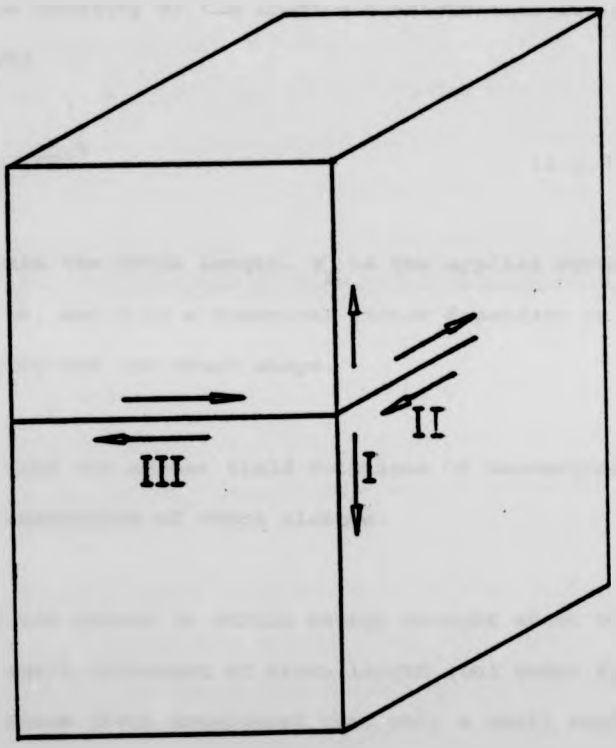

Fig 2.1 Crack Opening Modes

where σ_{ij} is the stress in the usual cartesian co-ordinate system, r is the radial distance from the crack tip and θ is the angle between r and the crack plane.$(2\pi r)^{\frac{1}{2}}$. $f_{ij}(\theta)$ is a function which describes the spatial distribution of the stress and K_I is a parameter which defines the intensity of the stress field. K_I represents the stress intensity fracture under Mode I loading. K_I depends on the geometry of the loading configuration but in general takes the form:

$$K_I = m\,\sigma_L\,(\pi C)^{\frac{1}{2}} \qquad (2.2.5)$$

where C is again the crack length, σ_L is the applied stress in uniform tension, and m is a numerical factor dependant on the exact loading geometry and the crack shape.

Irwin (1957) used the stress field solutions of Westergaard to consider the energetics of crack closure.

He considered the change in strain energy brought about by the closing of a small increment of crack length (δa) under fixed grip conditions. Hence Irwin considered that only a small region close to the crack tip would influence the change in strain energy. Irwin thus evaluated that:

$$G\delta a = \int_0^{\delta a} \sigma_{11}\,\mu_{11}\,\delta r \qquad (2.2.6)$$

where the 1 direction is normal to the crack plane and G is the strain energy release rate per unit increment of crack advance. By incorporating the Westergaard stress field solutions it is possible to show that:

$$G = \frac{K^2}{E} (1-\nu^2) \text{ for plain strain condition.} \qquad (2.2.7)$$

Thus the stress intensity factor assumes a considerable importance in that a parameter dependent purely on geometry and external loading can be used to evaluate the strain energy release rate as a crack advances. There is a strain energy release rate at which catastrophic failure occurs i.e. when G is greater than the surface energy required to create two new surfaces, and hence there is a critical value of K at which fracture occurs. The suggestion that K_{IC} (the critical stress intensity factor under Mode I loading) is a material parameter is of particular significance because it is much easier to evaluate K_{IC} rather than surface energies.

These developments by Irwin form the basis of the linear-elastic fracture mechanics approach to brittle fracture. Fracture mechanics itself has developed considerably to include elastic-plastic effects pertinent to metal structures, however for the purposes of this work these sophisticated techniques are not relevant.

It is however, necessary to consider how the crack tip region behaves even within this continuum model. The Westergaard (1939)

stress field solution is based on a sharp slit approximation, which upon loading will produce a parabolic crack tip implying infinite strains and hence stresses at the crack tip. In order to overcome the crack tip singularity Irwin (1958) and Orawan (1955) independantly postulated the model that the crack tip is surrounded by a small non-linear region. Since the elastic strain energy is not highly localised about the crack tip it was possible to postulate that the reversible system strain energy release rates would remain a good approximation. Since the non-linear region is small and highly localised it will be insensitive to the way in which the external boundary loadings are applied and hence remain a material characteristic. Thus the Griffith energy balance, eqn. 2.2.2 can still be applied. However the surface energy term Us now contains not only the surface energy to produce the two new surfaces which is proportional to area but also a term which contains the non-linear volume. This combined term is thus a fracture resistance rather than a surface energy. Physically the crack tip can be viewed as cusp shaped and hence retaining the sharp slit.

In glasses the size of this non-linear zone will be small. The theories which try to include these non-linear effects are described in section 2.3.

In applying fracture mechanics to a study of compositional effects on mechanical strength two approaches are possible. In the following section it is proposed to consider the nature of the

flaws present in glass and the flaw inducing processes which give rise to different types of flaws.

Firstly, it is possible to carry out the Griffith type of experiment which essentially considers microscopic defects under fast catastrophic failure in order to infer K_{IC} (the critical stress intensity factor). This technique has the disadvantage that K_{IC} can only be measured under fast loading rates or at very low (liquid nitrogen) temperatures where fatigue crack growth is absent. In addition it will be difficult to isolate the effect of composition on flaw generation by this approach.

The alternative technique is to consider the growth of a macroscopic crack particularly under conditions where fatigue crack growth is present. These techniques are discussed more fully in section 2.3.3 and in Chapter 5. Briefly these techniques consider the stress intensity factor which is assymptotic to the crack velocity/stress intensity relationship as being the critical stress intensity factor K_{IC}. Chapter 5 discusses details of the experimental techniques considered for the evaluation K_{IC} whilst Chapter 3 gives a review of compositional variations for K_{IC}.

2.2.3 The Nature of Flaws

It was concluded in the previous section that K_{IC} (the critical stress intensity factor) was the parameter which most completely

defined the inherent fracture resistance of a glass. However, it is the presence of cracks or flaws (either microscopic or macroscopic) which produces the stress intensification.

The nature of the flaws in glass is a subject which has aroused interest since Griffith (1920) first suggested that flaws were present. Griffith postulated that the microscopic flaws present were a localised rearrangement of molecules within the glass network with these local inhomogeneties capable of initiating full scale fracture. This view however, has been largely superceded and the flaws present in a glass are considered to be microscopic and sub-microscopic cracks present on the surface of the glass, and most commonly caused by contact damage and abrasion.

In studying flaws in the glass surface two basic approaches have been adopted. The first approach has been the phenomenological studies which have consisted of carrying out different surface abrasions and studying the resultant strength after abrasion. In contrast a more fundamental approach has been developed by Lawn and Co-workers who have tried to model the flaw production process by macroscopically simulating the controlling damage situation and then observing the resultant macroscopic cracks and their effect on fracture strength.

The phenomenological approach to the brittle strength of glass has been pursued since the work of Griffith (1920). Whilst there have been many papers reporting strength studies under differing

abrasion conditions, two factors have hampered the achievement of a coherent body of information concerning the nature of flaws. The first of these factors is that whilst within any particular study care is taken to produce a reproducible abrasion technique, the techniques used cannot in general be quantitatively compared with the results of other works in this field.

The second factor limiting the usefulness of these studies is that in general the studies which have been performed have been trying to investigate other aspects of mechanical strength e.g. fatigue behaviour rather than the nature of the flaws themselves. The most extensive and systematic study of the nature of flaws and flaw induced failure was performed by Mould and Southwick (1959). They identified four main areas of study as being important: flaw geometry, flaw production, flaw statistics and flaw growth.

Much of their work was devoted to flaw growth which will be discussed in the section concerned with fatigue. In considering flaw geometry and flaw production these two fields are clearly interrelated with the resultant flaw geometry being a function of the method of production. Mould and Southwick used two different abrasion processes.

The first of these was to drag fresh abrasive paper of a given grit size over the surface of the specimen in a direction either parallel or perpendicular to the principal tensile axis under four point bend testing. The result of such an abrasion technique was

to produce extended linear abrasions on the surface, with the liquid nitrogen strengths varying by a factor of two depending on the orientation of the abrasions, with the abrasions parallel to the stress axis giving the greater strengh.

The other abrasion process was to impact the glass surface with a stream of carborundum particles propelled using nitrogen at a known pressure, in order to produce abrasions of a point like nature. After abrasion, specimens were again tested at liquid nitrogen temperature where fatigue behaviour is absent and so a reasonable indication of flaw size can be obtained using equation 2.2.1. The principal result of these experiments was to show that the size of abrasion particle was linearly correlated to the size of the flaws evaluated by equation 2.2.1.

Just as it is possible to decrease the strength of glass by introducing flaws, attempts have also been made to remove flaws and hence increase strength. The most widely investigated technique for strength increase has been to etch the glass surface using primarily hydroflouric acid solutions. Proctor (1962) presented results for the relationship between dissolved surface layer depth and failure stress for soda-lime-silica, Pyrex and silica rods of various sizes. For 4mm diameter rods of soda-lime-silica glass, he observed that a doubling of strength was achieved for only a 50-100μm surface removal but that etching to much greater depths produced only a smaller subsequent strength increase. Proctor

(1962) postulated two models for the method by which etching altered flaw geometry as defined in eqn 2.2.1. The first model proposed was that only the depth of a crack changed and that there was no effect on width or radius of curvature. However, since this model predicts very high strengths for almost no surface removal it was discounted. The second model considered was that the etchant widened the crack and increased the radius of curvature at the same rate as removing the outside surface, i.e. the initial depth remains constant but the crack becomes more rounded. Whilst this model gave a strength increase/surface depth removal relationship comparable to that observed experimentally, the values of crack length and radius of curvature predicted were not credible for large diameter rods. This model was refined by Pavelchik and Doremus (1974) who postulated that for a crack the acid solution at the crack tip would rapidly become exhausted and so the radius of curvature would show only a slow rate of increase until an advanced stage of crack width extension had been reached.

There have been attempts to observe directly the flaws present in a glass surface, particularly one which is not heavily abraded. A technique which was originally thought to offer considerable scope in this field was to expose a glass surface to a high temperature sodium vapour treatment e.g. Andrade and Tsien (1937). This technique invariably produced a pattern of cracks on the glass surface which were thought to be possibly Griffith flaws. Ernsberger (1966), however, concluded that the cracks produced were simply an artefact of the sodium vapour treatment. He arrived at

this conclusion by observing the glass surface during the vapour treatment and noting that the surface cracks are only formed on cooling and that a subsequent reheating will produce a pattern of surface cracks. Ernsberger (1966) attributed the formation of these cracks to the ion exchange which occurs when a glass is exposed to an alkali metal vapour and which can result in a tensile layer being formed on the surface.

As previously stated Mould and Southwick (1959) considered flaw statistics to be one of the important characteristics of a glass surface. Since much of the work which has been carried out in the investigation of flaw statistics has been based on the Hertzian fracture test, which also forms the historical basis of the indentation fracture mechanics of Lawn and co-workers, these two topics will be discussed together in the following section.

2.2.4. The Hertzian Fracture Test, Indentation Fracture Mechanics and Flaw Statistics

The Hertzian fracture test has over the last twenty years given considerable impetus to the study of the fracture of glass. It has been the basis of considerable work into the theories of flaw statistics and forms the basis of indentation fracture mechanics.

Hertz (1896) first predicted quantitatively the surface stresses which result when a sphere in contact with a glass surface is compressed. The result of applying this loading is ultimately to

produce a cone crack as shown in Fig 2.2. In examining the Hertzian fracture the stress field will clearly play a significant role.

The full stress field which was analysed by Huber (1904) consists of two major regions both axisymmetric about the axis of loading. The volume of glass immediately below the area of contact consists of a compressive region which extends to approximately 2a below the indenter. The tensile stresses have a maximum at the surface and decrease rapidly into the bulk of the glass. The radial surface tensile stress is given by

$$\sigma = \frac{1-2\nu}{2} \left(\frac{a}{r}\right)^2 P_o \qquad (2.2.8)$$

where ν = Poisson's ratio

r = distance from the centre of the point of contact

a = radius of contact

and P_o = is given by

$$P_o = \frac{P}{\alpha \pi a^2} \qquad (2.2.9)$$

where P is the normally applied load and α is a dimensionless constant reflecting the indenter geometry, for axially symmetric indenters $\alpha = 1$.

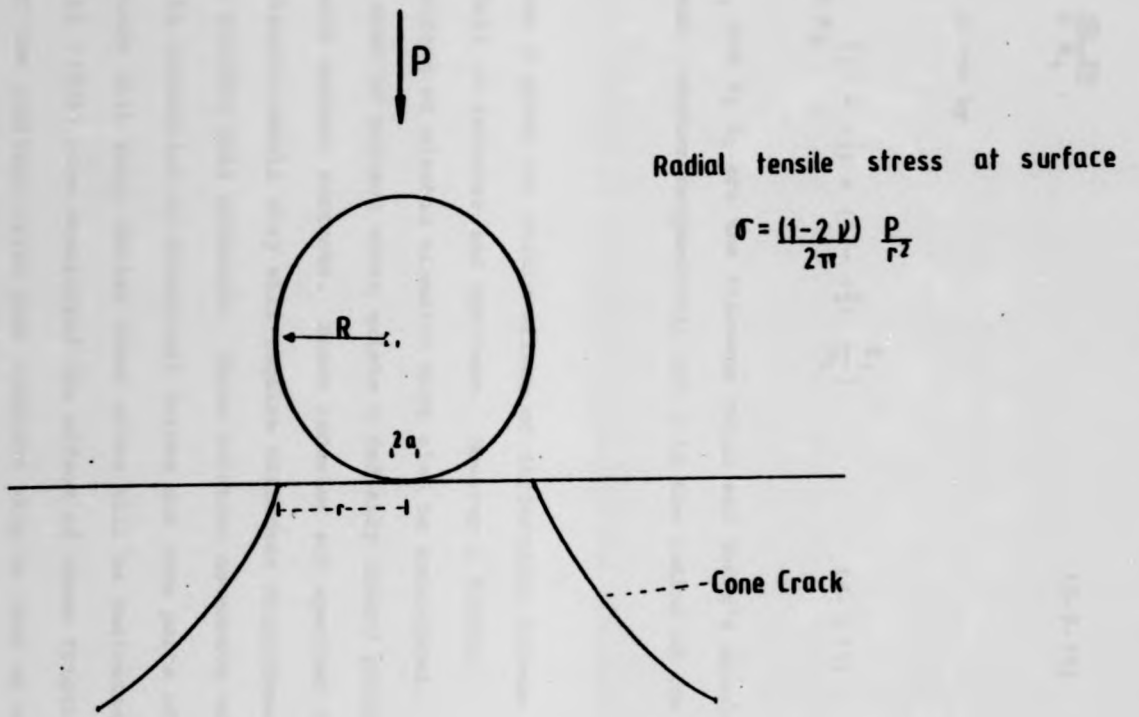

Fig. 2.2 Schematic representation of the Hertzian Cone crack and Characterising Parameters.

The radius of the area of contact is given by

$$a^3 = \frac{4k\ PR}{3\ E_1} \qquad (2.2.10)$$

where k is given by

$$k = \frac{9}{16\ E_1}\left((1 - \nu_1^2) + (1 - \nu_2^2)\ \frac{E_1}{E_2}\right) \qquad (2.2.11)$$

where ν_1 E_1 and ν_2 E_2 are the Poissons ratio and Young's modulus of the glass and indenter respectively and R is the radius of the indenter.

The parameter k gives the static effect of differences between the elastic moduli of indenter and specimen. However a further "dynamic" effect of elastic mismatch must also be considered. Within the area of contact there exists a radially inward pressure acting on both contact surfaces. Since indenter and specimen have differing elastic moduli they will require different displacements in order to relieve this pressure. These relative movements will in general be restricted by frictional forces and some parts of the area of contact will slip, whilst other areas will be restrained. Johnson et al (1973) have considered the effect of these frictional forces under the limiting cases when complete slip or when no slip occurs. Under complete slip conditions the effect of the frictional tractions on the surface stress outside the area of contact is governed by the coefficient of friction f. Fig 2.3(a)

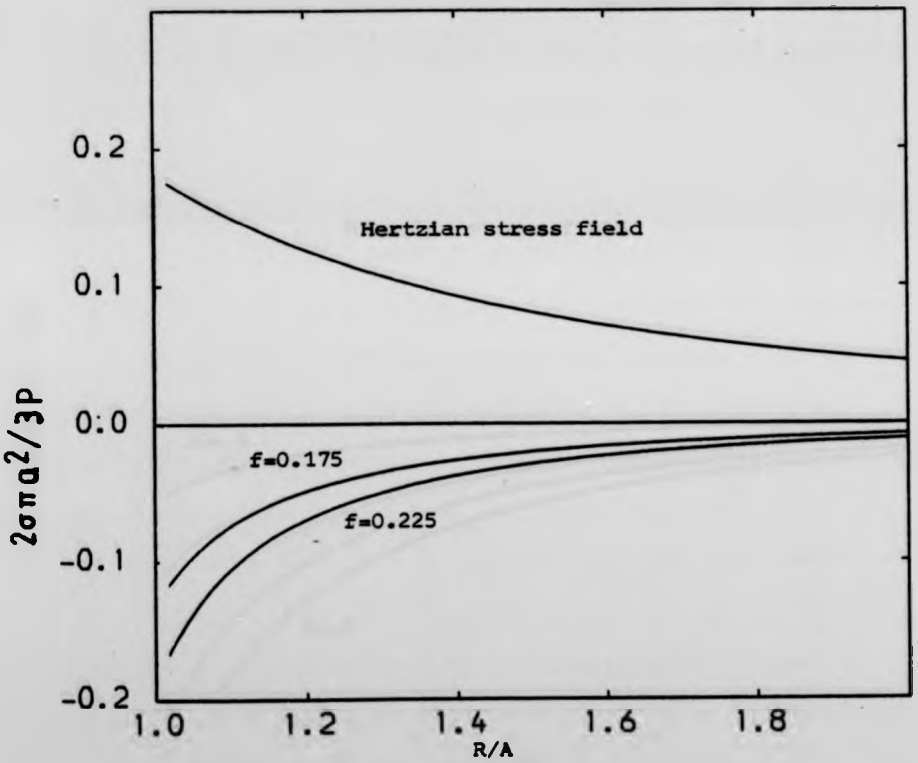

Fig. 2.3(a) Indenter stress field under COMPLETE SLIP conditions.
After JOHNSON et al(1973).

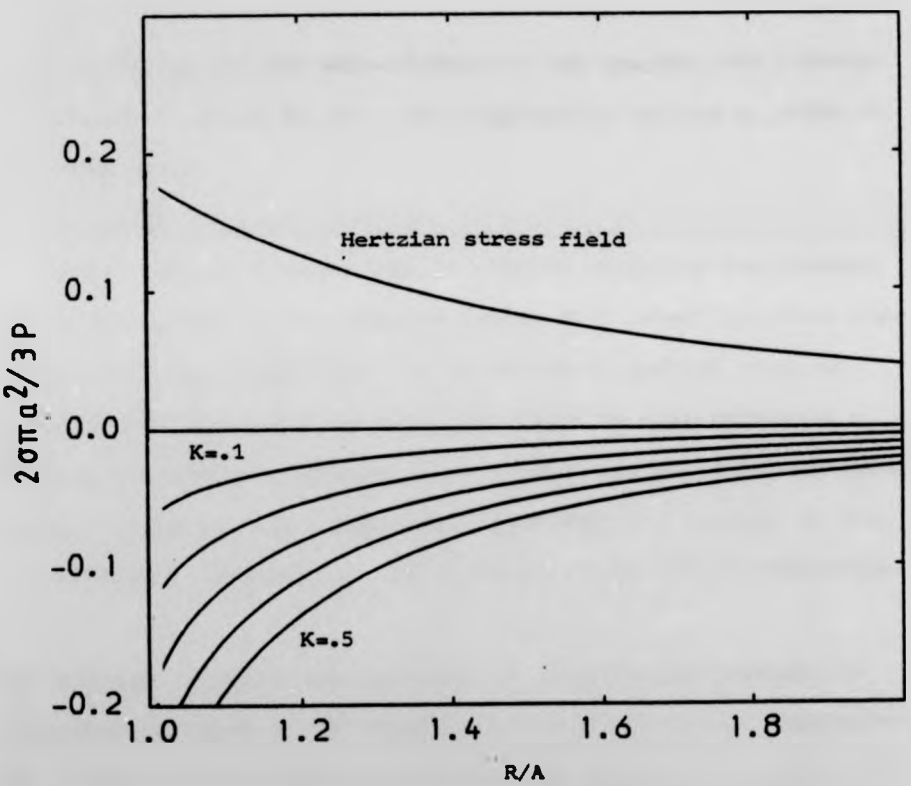

Fig. 2.3(b) Indenter stress field under NO-SLIP conditions. After JOHNSON et al(1973).

shows the compressive stress field component generated by the frictional forces together with the results of equation 2.5. Under no slip conditions the compressive components due to elastic mismatch are governed by the parameter K defined as:

$$\frac{(1-2\nu_1)/G_1 - (1-2\nu_2)/G_2}{(1-\nu_1)/G_1 + (1-\nu_2)/G_2} \qquad (2.2.12)$$

where G_1 and G_2 are the shear moduli of the specimen and indenter respectively. Fig 2.3b shows the compressive components under no slip conditions.

In general slip will occur over an annular region of the contact area. The extent of this annular region will depend on ratio f/K. Spence (1971) has considered the situation of partial slip and evaluated the radius of the area over which no slip occurs as a function of K and f. Johnson et al (1973) considered the effect of surface roughness, and showed that its effect was similar to that of interfacial friction but of relatively insignificant magnitude.

The Hertzian fracture test has been of considerable interest to researchers because of the observation of the so-called "Auerbach's Law" (1891). For a perfectly homogeneous material it is possible to show that the critical load for failure P_c is proportional to the square of the indenter radius R. However for a brittle material the characteristics described by Auerbach's law are

shows the compressive stress field component generated by the frictional forces together with the results of equation 2.5. Under no slip conditions the compressive components due to elastic mismatch are governed by the parameter K defined as:

$$\frac{(1-2\nu_1)/G_1 - (1-2\nu_2)/G_2}{(1-\nu_1)/G_1 + (1-\nu_2)/G_2} \qquad (2.2.12)$$

where G_1 and G_2 are the shear moduli of the specimen and indenter respectively. Fig 2.3b shows the compressive components under no slip conditions.

In general slip will occur over an annular region of the contact area. The extent of this annular region will depend on ratio f/K. Spence (1971) has considered the situation of partial slip and evaluated the radius of the area over which no slip occurs as a function of K and f. Johnson et al (1973) considered the effect of surface roughness, and showed that its effect was similar to that of interfacial friction but of relatively insignificant magnitude.

The Hertzian fracture test has been of considerable interest to researchers because of the observation of the so-called "Auerbach's Law" (1891). For a perfectly homogeneous material it is possible to show that the critical load for failure P_c is proportional to the square of the indenter radius R. However for a brittle material the characteristics described by Auerbach's law are

observed; namely that Pc is proportional to R. In order to explain this phenomenon, two completely different theories have been postulated, one based on fracture mechanics, and the other based on flaw statistics.

In considering a fracture mechanics analysis, the initiation and propagation stages of crack development can be considered separately. The propagation of a fully formed cone crack under steady state conditions was analysed by Roestler (1956) who considered the crack growing so as to maximise the strain energy release rate i.e. along a section normal to the maximum principal stress. Roestler (1956) was able to show that the radius of the base of the cone crack is proportional to $P^{\frac{2}{3}}$. This relationship has been confirmed by various experimental investigations e.g. Swain and Lawn (1973).

Applying the Griffith energy balance together with the fracture mechanics techniques to the initiation stage of crack formation is considerably more difficult because of the extreme stress gradients near the glass surface. In order to make the problem tractable the effect of interfacial friction has to be ignored. Frank and Lawn (1967) have carried out an analysis applying the Griffith equation in a step-wise manner as the crack grows. For such a crack growing under equilibrium conditions they obtained,

$$G = \frac{P}{kR} \left(\beta\left(\frac{c}{a}\right)\right)_{\nu, r/a} \qquad (2.2.13)$$

where $\oint$ is a dimensionless function usually evaluated numerically. For the case of crack growing at the contact circle Fig.2.4 shows the normalised strain energy release rate as a function of c/a. The sequence of events for a flaw of initial size cf forming a full cone crack is as follows. Load increases until P_2 at which point unstable growth occurs to the c_1 branch. Further stable crack growth will then occur until the load is Po and hence c = c*. At this point unstable crack growth will occur and the downward propagating cone crack appears. From equation 2.2.13 it is possible to show that P critical is proportional to R (Auerbachs law) for the range of defect sizes $c_o^* < cf \ll c^*$ and independent of cf. Langitan and Lawn (1969) have described the stable crack growth from cf to c* as the formation of a ring crack from a point flaw which then slowly propagates to c* to form the cone.

This analysis forms the first major development in the field of indentation fracture mechanics. As was described in section 2.2.3 there are basically two approaches to the study of the nature of flaws. The first, phenomenological studies were described in section 2.2.3, whilst the second aims to model macroscopically the flaws and the flaw inducing processes. Lawn and Marshall (1978) have reviewed in detail the field of indentation fracture mechanics. Briefly indentation fracture mechanics models a damage inducing contact event by characterising the indenting particle as being either sharp or blunt. For the blunt indenter the stress field and subsequent cracking is Hertzian. For the sharp indenter, however, the stress situation is markedly different in that the

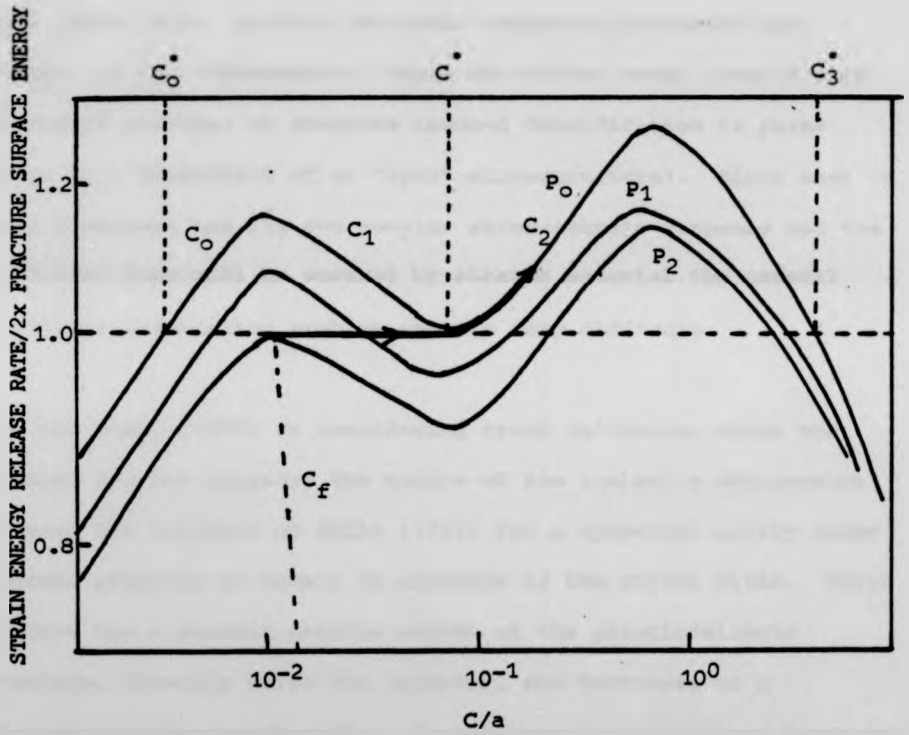

Fig. 2.4. Fracture Mechanics representation for idealised cone crack formation.After LAWN and WILSHAW(1975).Heavy arrowed lines indicate stages of crack extension.

elastic stress field has a small tensile stress at the surface and an extensive highly compressive region below the indenter where shear and compressive hydrostatic component are several times greater than the tensile stress. In addition inelastic deformations below the sharp indenter will occur. In brittle materials the nature of these inelastic deformations remains a contentious issue, in that two basic competing processes may account for the deformation. These are either shear induced flow (plastic or viscous) or pressure induced densification (a phase change or a compaction of an "open" microstructure). Since each of these processes has its own complex stress-strain response and the non-linear zone will be encased by elastic material the general non-linear indentation problem appears very difficult.

Lawn and Evans (1977) in considering crack initiation below the indenter did not consider the nature of the inelastic deformation but used the solution of Hills (1950) for a spherical cavity under internal pressure to obtain an estimate of the stress field. Their solution has a maximum tensile stress at the plastic/elastic interface, directly below the indenter, and decreases to a compressive value at the point of contact and to zero away from the point of contact.

The sequence of damage which occurs below a sharp indenter is shown schematically in Fig. 2.5: (a) the sharp indenter region produces an inelastic deformation region; (b) at some threshold a deformation-induced flaw develops into a small median crack along a

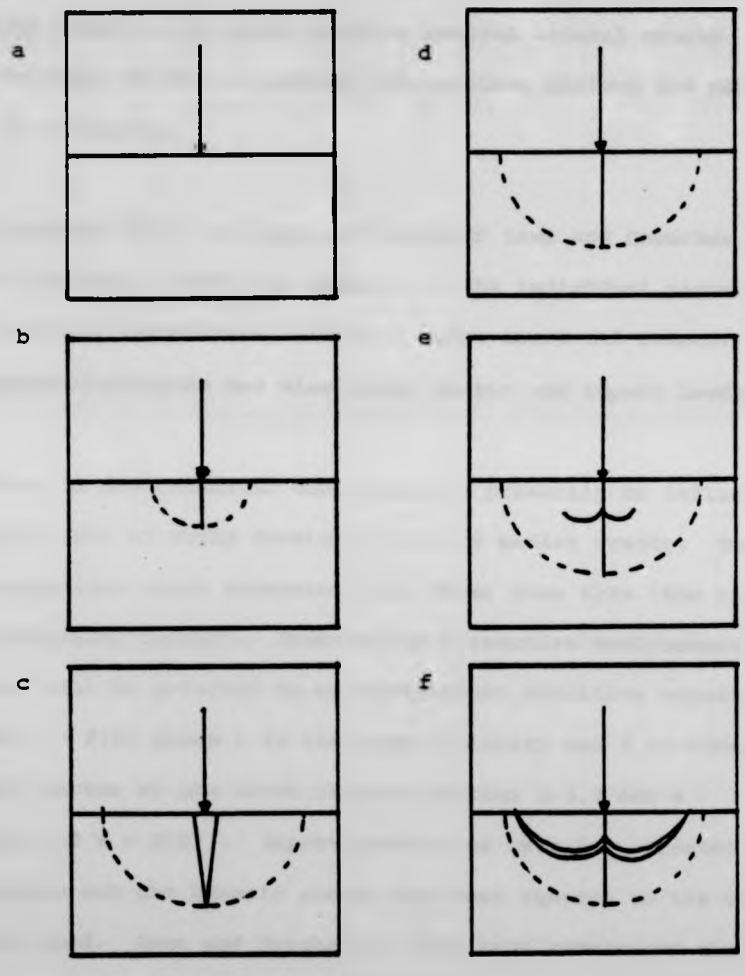

Fig. 2.5 Evolution of Median/lateral Cracks below a sharp Indenter.For a-c load increasing,for d-f load decreasing. After LAWN and MARSHALL (1978).

contact axis; (c) increasing load produces stable growth of the median crack; (d) on unloading the median crack tries to close: (e) during load reduction the build-up of residual stress due to the inelastically deformed region results in lateral vents (sideways extending cracks); (f) upon complete removal lateral cracks continue their extension towards the specimen surface and may result in chipping.

In considering these two types of indenter Lawn and Coworkers (see Lawn and Marshall (1978) for details of the individual papers) have considered the indentation situation under inert and reactive environment conditions and also under static and impact loading.

The effect of environmental conditions is primarily to influence the growth rate of fully developed cone or median cracks. Under inert conditions crack extension will occur when K>Kc (the critical stress intensity factor). However, in a reactive environment crack extension will be governed by an environment sensitive equation of the form v = f(K) where v is the crack velocity and K is stress intensity factor at the crack tip(see section 2.3.3 for a discussion of v = f(K)). Impact conditions have been treated as quasi-static and the kinetic energy has been equated to the maximum impulsive load. Lawn and Marshall (1978) have summarised the relationship between Pcritical and K_c (critical stress intensity factors) for different indenter situations

For a blunt indenter:

$$P_c = \frac{\alpha_E R K_c^2}{E} \quad \text{for initiation} \qquad (2.2.14)$$

$$P/c^{3/2} = \beta_E K_c \quad \text{for stable propagation} \qquad (2.2.15)$$

and for a sharp indenter

$$P_c = \alpha_p K_c^4/H^3 \quad \text{for initiation} \qquad (2.2.16)$$

$$P_{\sim}/c^{3/2} = \beta_p K_c \quad \text{for propagation} \qquad (2.2.17)$$

where H is the Vickers hardness of the glass and α_E, B_E, α_p, B_p are dimensionless constants dependant on the materials and indenter situation and are usually evaluated experimentally.

In order to study the macroscopic effect of these macroscopically induced flaws a number of studies have been carried out where specimens have been indented and then tested in flexure. Lawn et al (1978) gave results for specimens which have undergone static loading by blunt indenters and then tested in four point bending in an oil environment, Fig. 2.6. As predicted by the Frank and Lawn (1967) analysis, for a given c_f° no appreciable strength degradation occurs, and strength is governed by c_f° until a critical value of P is attained . At this critical value of P (which is independent of

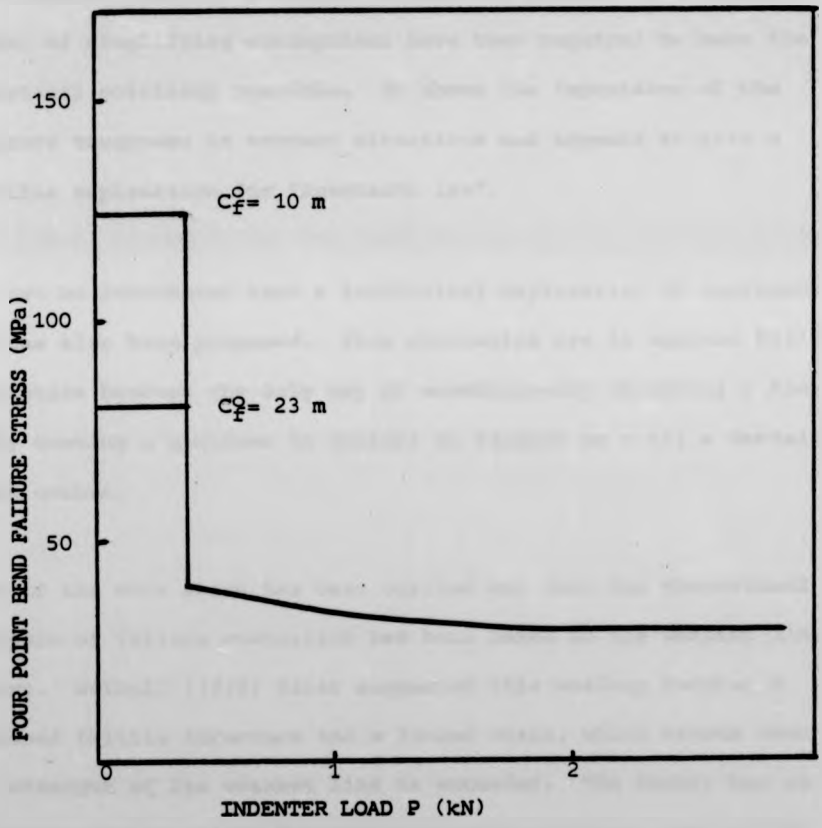

Fig. 2.6 Strengh Degradation as a function of Indenter Load. After Lawn et al (1975).

c_f^o) there is sharp decline in strength associated with the formation of a cone crack followed by a slow decline associated with developed cone crack extension. Comparable behaviour has been observed for indentation by sharp particles (Lawn, Fuller and Wiederhorn 1976) although the strength degradation occurs at much lower loads. Thus indentation fracture mechanics appears to give a good insight into the strength degradation process even though a number of simplifying assumptions have been required to make the analytical solutions possible. It shows the importance of the fracture toughness in contact situations and appears to give a credible explanation for "Auerbachs law".

It must be remembered that a statistical explanation of Auerbachs law has also been proposed. Flaw statistics are in essence failure statistics because the only way of unambiguously observing a flaw is by testing a specimen to failure in flexure or until a Hertzian crack occurs.

Most of the work which has been carried out into the theoretical analysis of failure statistics has been based on the weakest link theory. Weibull (1939) first suggested this analogy between a stressed brittle structure and a loaded chain, which breaks when the strength of its weakest link is exceeded. The theory has as its basis the so called Poisson postulates which are that if the surface is divided into small areas of size δA it is possible to consider these small areas under the conditions that:-

(1) Flaws in each area are considered to be independent of one another.

(2) Each area is considered to be independent of every other area.

(3) The probability $\delta P(\sigma)$ of a flaw of less than a given size in an area is proportional to the area for small areas

$$\delta P(\sigma) = \beta \delta A$$

(4) The probability of more than one flaw of a given size in a single area is small for small areas.

It can be shown, e.g. Batdorf 1978, that the probability of failure of a glass specimen at a stress less than σ is

$$P_f(\sigma) = 1 - \exp\left(-A\, C(\sigma)\right) \qquad (2.2.18)$$

where A is the total area stressed to a level of σ and $C(\sigma)$ is simply the number of flaws per unit area of a size less than or equal to that required to produce failure at a stress level σ. The attractiveness of such an equation is that if one can arrive at a $C(\sigma)$ by small scale testing one should in theory be able to predict the probability of failure for a large number of articles at low stresses. The Hertzian fracture test is particularly attractive for this type of study because it allows a large amount of

experimental data to be obtained from a small amount of specimen material.

Two approaches have been used to obtain $C(\sigma)$. The first, proposed by Weibull (1939), is to describe $C(\sigma)$ by an equation of the form $C(\sigma) = (\sigma/\sigma o)^m$ or $C(\sigma) = ((\sigma-\sigma n)/\sigma o)^m$ where in the two parameter equation σ can have any positive values, whilst in the three parameter equation $\sigma \geq \sigma n$, for $C(\sigma) > 0$. The parameter m is a measure of the dispersion of the distribution function, whilst σn and σo are effectively scaling parameters. Oh and Finnie (1967), (1970) and Hamilton and Rawson (1970) and others have used the Weibull parametric approach to analyse Hertzian fracture results. In these studies the authors were able to show good agreement between the fitting of the experimental data to a Weibull form and the observation that Auerbachs law was obeyed for a range of indenter sizes. Oh and Finnie (1970) showed theoretically how, if $C(\sigma)$ takes a Weibull form, then Auerbachs law can be obtained on statistical arguments alone. Hamilton and Rawson (1970) were able to show the interesting result that for surfaces having different flaw distributions, ie. after polishing or etching, Auerbachs law was still obeyed although the constant of proportionality varied with surface treatment, which is a direct contradiction of the fracture mechanics theories of Frank and Lawn (1967).

The other major approach to the evaluation of $C(\sigma)$ is to analyse the experimental results obtained, whilst making no a priori assumptions as to the form of $C(\sigma)$. A number of workers in the

field have used this approach. Tsai and Kolsky (1967) in analysing Hertzian fracture results fitted their data to a form of $P = K_1R + K_2R^2$ and used the parameters K_1 and K_2 to define $C(\sigma)$. Matthews et al (1976) were able to define complex closed form expressions relating the probability of failure at a given experimental stress level to the number density of flaws $C(\sigma)$.

Poloniecki and Wilshaw (1971) have reported a direct technique for estimating the number densities of flaw of a given size. Their approach was to carry out a series of Hertzian fracture tests and then simply divide the number of defects of a given size by the sum of all the areas having experienced a stress sufficient to initiate cracking from such a defect.

It was originally stated that one of the attractions of the Hertzian fracture test was that, in theory at least, one could obtain a flaw distribution function and hence a probability of failure for a glass surface, from a small quantity of material and in a relatively inexpensive manner. Lewis and Rawson (1976) compared the results obtained by performing a Weibull analysis on Hertzian fracture results and on plate bending data from over 100 float glass discs. They reported that the flaw distribution functions obtained from Hertzian fracture data cannot be used to predict the strength when large areas are stressed. The Weibull parameters they obtained gave a zero value of σ_n for plate bending whilst the result from Hertzian fracture gave values of greater

than 98.07 MPa. They also observed that the minimum values of fracture stress were 48.54 MPa and 143.08 MPa for bending and Hertzian fracture respectively. The work of Johnson et al (1973) on frictional forces can account for only part of this discrepancy. From Fig 2.3 it can be seen that even at high values of K and f it is only points close to the area of contact that will experience a stress reduction of 30% or more.

In an effort to resolve the differences between the theories proposed to explain 'Auerbachs Law', Harrison and Wilks (1978) carried out a computer simulation of Hertzian fracture studies whilst varying the flaw densities and flaw sizes. They concluded that for those experimental studies e.g. Tsai and Kolsky (1967), Oh and Finnie (1967) where the standard deviation of fracture load was greater than 20% then Auerbachs law could be explained by statistical methods. For those studies where heavy abrasion results in a low standard deviation for fracture load then an analysis of the form proposed by Frank and Lawn (1967) taking into account the inhomogeneity of the stress field must be carried out.

In conclusion, it must be stated that despite the considerable controversy which exists concerning the details of the explanations of Hertzian fracture, it is still a valuable comparative technique. The ease with which it is possible to obtain a considerable amount of information from a small quantity of glass makes this test particularly suitable when the quantity of test material is limited.

2.3 FATIGUE BEHAVIOUR

2.3.1 Introduction

It was stated in Chapter 1 that glass undergoes fatigue behaviour i.e. that the observed failure stress is a function of the time for which the glass has experienced that stress. Fatigue behaviour of glass has been observed for over thirty years. Over the last ten or fifteen years fatigue studies have taken the major part of the experimental and theoretical effort in the field of fracture of glass. In reviewing fatigue behaviour it is convenient to consider it in three parts: early static fatigue studies, macroscopic crack growth measurements, and dynamic fatigue studies.

2.3.2 Early Static Fatigue Studies

One of the most important and systematic early studies of static fatigue was carried out by Charles (1958). Over 3000 soda-lime-silica rods were tested under four point bend testing and under conditions of controlled temperature and relative humidity. Charles observed that static fatigue was temperature dependant, with fatigue being absent only at temperatures below -170°C. The highest fatigue susceptibility was observed at 150°C and at 100% relative humidity.

The most extensive study of the fatigue behaviour of glass was performed by Mould and Southwick (1959 a,b, 1960, 1961), when they

considered the effects of surface condition, environment, and ageing. Testing was carried out using soda-lime-silica slides in three point bending with pulse loads being applied over the duration 10^{-3} to 10^{3} secs. In considering the effect of different surface abrasions (see section 2.2.3) Mould and Southwick observed that varying the surface condition resulted in a displacement of the curves, describing strength as a function of load duration. In order meaningfully to compare the effect of different abrasion treatments, Mould and Southwick normalised the failure stress by the failure stress at liquid nitrogen temperatures , σN, and the time to failure by $t_{0.5}$ the time to failure at half the liquid nitrogen strength. The result of this normalisation was to reduce the failure time characterisatics of different abrasions to a single curve which they called the "Universal fatigue curve". This indicated that the parameter $t_{0.5}$ was heavily influenced by abrasion technique. Accordingly, they observed that by plotting $t_{0.5}$ as a function of $1/\sigma_N^2$ they were able to distinguish between linear flaws (those orientated perpendicular to the direction of stress) and point flaws (those orientated parallel to the direction of stress); specimens containing linear flaws appearing to fatigue more rapidly than those containing point flaws. In contrast Ritter and Sherburne (1971) observed that acid etched glasses did not fall on the same universal fatigue curve as abraded specimens.

The influence of the surrounding medium was also considered and tests were carried out under conditions of varying humidity, in different alcohols and under a range of acid and alkali solutions.

Under conditions of varying humidity it was found that for intermediate load durations ($>10^{-3}$ and $<$1h) a strong correlation existed between humidity and strength, an increase in the relative humidity or testing under water giving a considerable reduction in time to failure at a given stress. The influence of atmospheric water content was less marked when testing was carried out at very short ($<10^{-3}$ sec), or very long ($>$1h) durations. In the intermediate timescale range the characteristic duration time $t_{0.5}$ in 0.5% and 43% relative humidity and under water were 3500, 200 and 8 seconds respectively.

When carrying out tests in methyl and isopropyl alcohol, Mould (1961) observed that testing under isopropyl alcohol gave greater strength than in methyl alcohol over a range of load durations of 10^{-3} to 100 secs. By testing in water and alcohol mixtures, Mould suggested that the water content of the alcohol was the dominant factor in defining the fatigue behaviour.

Strength was shown to be independent of pH in the range pH 1 to 13 although for values of pH $>$ 13 a strength increase was recorded whilst for values of pH $<$ 1 a strength decrease was recorded.

In studying ageing, Mould (1960) considered the effect of storing specimens under conditions of different humidity and under high temperature vacuum conditions prior to testing. The results of storing in an atmosphere of varying water content were that the higher water content atmospheres resulted in a greater liquid

Under conditions of varying humidity it was found that for intermediate load durations ($>10^{-3}$ and $<1h$) a strong correlation existed between humidity and strength, an increase in the relative humidity or testing under water giving a considerable reduction in time to failure at a given stress. The influence of atmospheric water content was less marked when testing was carried out at very short ($<10^{-3}$ sec), or very long ($>1h$) durations. In the intermediate timescale range the characteristic duration time $t_{0.5}$ in 0.5% and 43% relative humidity and under water were 3500, 200 and 8 seconds respectively.

When carrying out tests in methyl and isopropyl alcohol, Mould (1961) observed that testing under isopropyl alcohol gave greater strength than in methyl alcohol over a range of load durations of 10^{-3} to 100 secs. By testing in water and alcohol mixtures, Mould suggested that the water content of the alcohol was the dominant factor in defining the fatigue behaviour.

Strength was shown to be independent of pH in the range pH 1 to 13 although for values of pH >13 a strength increase was recorded whilst for values of pH <1 a strength decrease was recorded.

In studying ageing, Mould (1960) considered the effect of storing specimens under conditions of different humidity and under high temperature vacuum conditions prior to testing. The results of storing in an atmosphere of varying water content were that the higher water content atmospheres resulted in a greater liquid

Under conditions of varying humidity it was found that for intermediate load durations ($>10^{-3}$ and $<1h$) a strong correlation existed between humidity and strength, an increase in the relative humidity or testing under water giving a considerable reduction in time to failure at a given stress. The influence of atmospheric water content was less marked when testing was carried out at very short ($<10^{-3}$ sec), or very long ($>1h$) durations. In the intermediate timescale range the characteristic duration time $t_{0.5}$ in 0.5% and 43% relative humidity and under water were 3500, 200 and 8 seconds respectively.

When carrying out tests in methyl and isopropyl alcohol, Mould (1961) observed that testing under isopropyl alcohol gave greater strength than in methyl alcohol over a range of load durations of 10^{-3} to 100 secs. By testing in water and alcohol mixtures, Mould suggested that the water content of the alcohol was the dominant factor in defining the fatigue behaviour.

Strength was shown to be independent of pH in the range pH 1 to 13 although for values of pH >13 a strength increase was recorded whilst for values of pH <1 a strength decrease was recorded.

In studying ageing, Mould (1960) considered the effect of storing specimens under conditions of different humidity and under high temperature vacuum conditions prior to testing. The results of storing in an atmosphere of varying water content were that the higher water content atmospheres resulted in a greater liquid

nitrogen strength, which Mould attributed to rounding at the crack tips.

In assessing the effect of storage under high temperature vacuum conditions, Mould (1960) attributed the decrease in fatigue susceptibility as being due to the dehydration of the surface water and resultant nonwettability after dehydration.

These results form the major experimental findings of the early fatigue work. In order to explain these results a number of theories have been put forward. The most important of the early theories, and those finding the greatest success have been based on the stress corrosion mechanism. Charles (1958) suggested that crack growth prior to failure can occur with the modifications in crack geometry being brought about by a stress enhanced corrosion.

In this review of the mechanical strength of glass, glass has been treated as an isotropic continuum. However, in order to have a physical model of the corrosion process it is desirable to have an insight into the glass structure. For the purpose of this section it is sufficient to consider glass as a network of Si-O-Si bonds with alkali metal ions e.g. Na^+ present in the near vicinity of these bonds. Charles (1958) postulated that the presence of the alkali ion and water results in the dissociation of the water molecule, with the resultant free hydroxyl ion capable of interacting with the silica network such that

$$Si - O - Si + OH^- \rightarrow + SiOH + SiO^-$$

and the SiO^- group being capable of further dissociation of water. It was suggested that this reaction may lead to an excess of OH^- groups and hence be autocatalytic. In analysing the effect of this reaction on a flaw Charles (1958) postulated that the crack tip radius remained constant whilst the crack length increases. By introducing an expression for crack velocity as a function of stress and including the Inglis expression, equation. 2.2.1, for the case of a crack at the conditions of failure he produced the equation

$$V = \beta \left(D^1 \left(\frac{L}{Lc}\right)^{\frac{n}{2}} + D \right) e^{-A/RT} \qquad (2.3.1)$$

where L is the instantaneous crack length, Lc is the critical crack length, D^1 and D are the stress dependant corrosion rate and the stress free corrosion rate respectively, A is an activation energy, R is universal gas constant, and B is a constant. By integrating equation 2.3.1, having neglected stress free corrosion, between the limits Lo and Lc. Charles obtained the expression

$$\log t_f = n \log \frac{1}{\sigma_c} + b \qquad (2.3.2)$$

for Lc/Lo $>$ 1.

This theory provided good agreement with experimental results except at temperatures above 200°C. A further theory of stress corrosion was developed by Charles and Hillig (1965) who considered a thermally activated and stress dependant corrosion process which results in reaction products incapable of withstanding the resultant applied stress. The velocity equation they proposed was

$$V = D \exp - (A^*(0) + YV_m\rho - \sigma_t V^*)/RT \qquad (2.3.3)$$

where V^* is an activation volume, σ_t is the critical stress at the crack tip, ρ is the radius of curvature of the crack tip, Vm is the molar volume and $A^*(0)$ is the activation energy for the corrosion process under stress free conditions. Applying this velocity equation to the Inglis (1913) expression for the stress concentration at a crack tip, Charles and Hillig (1965) arrived at an expression for the effective change in crack length $\partial u/\partial T$ in terms of a reduced crack length $2 (L/\rho)^{\frac{1}{2}}$ and a reduced time T. Using this expression Charles and Hillig postulated that when $\partial u/\partial T$ was negative then ρ, the crack tip radius, was increasing as the crack extended, when $\partial u/\partial T$ was positive then ρ decreased as the crack extended, and finally when $\partial u/\partial T$ is zero then the increase in ρ just balances the increase in crack length to produce a constant stress concentration factor. By applying their analysis to the results of Mould and Southwick (1958), they obtain an activation volume of the same order as that for alkali ion diffusion in

soda-lime-silica glass, and are able to predict the static fatigue limit which Mould and Southwick had observed.

2.3.3 Dynamic Fatigue Studies

Dynamic fatigue effects are observed if mechanical testing is carried out at a number of different loading rates, the failure stress increasing as the loading rate increases. The attraction of dynamic fatigue studies in investigations of fatigue behaviour is that there are considerably less time consuming than static studies. On most commercial tensile testing machines it is possible to obtain 4 or 5 orders of magnitude change in loading rate easily, however, to obtain 4 or 5 orders of magnitude variation in time for times greater than 1 sec is very time consuming.

Charles (1958) extended his experimental work and theories of fatigue behaviour to include dynamic fatigue. He obtained an equation of the form

$$\sigma_f = D\,\dot{\sigma}^{\frac{1}{n+1}} \qquad (2.3.4)$$

where D is a constant, $\dot{\sigma}$ is loading rate, and σ_f is the failure stress. For soda-lime-silica glass Charles obtained a value for n of 16 which agreed with the value obtained from static fatigue.

There have been a number of other significant dynamic fatigue studies, notably by Ritter and Sherburne (1971) and by Ritter and LaPorte (1975). However, since these studies have comprised an investigation into the comparability between dynamic fatigue and macroscopic crack growth studies, it is necessary to describe some of the macroscopic crack growth studies before discussing these works.

2.3.4 Macroscopic Crack Growth Studies

In an effort to observe fatigue behaviour at a more fundamental level, techniques have been developed for the study of macroscopic crack growth which are in general based on fracture mechanics.

The experimental methods available will be discussed in Chapter 5, but briefly all the techniques are based on observing optically or by compliance methods the change in crack length in a specimen for which the mode I stress intensity factor K_I is known as a function of geometry, crack length and load.

One of the earliest and most important studies was performed by Wiederhorn (1967) when he examined the influence of atmospheric humidity on crack growth rates as a function of stress intensity factor and observed three regions of crack propagation, Fig. 2.7. In the first region, Region I, it was postulated that the crack growth rate was limited by the rate of the chemical reactions at the crack tip. In Region II Wiederhorn ascribed this behaviour to

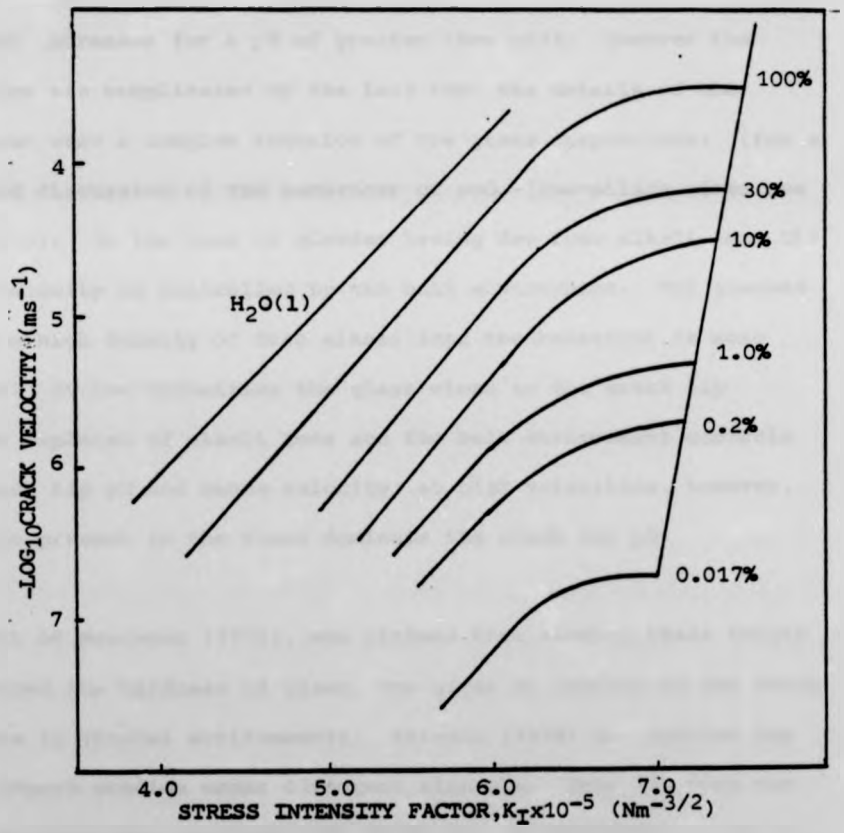

Fig. 2.7 The Influence of Humidity on Crack Propagation rate in a Soda-lime Silica glass. After WIEDERHORN(1967).

the crack growth rate being limited by the rate of transportation of the atmospheric water to the crack tip. Region III was described as being independent of environmental humidity.

Wiederhorn and Johnson (1973) studied the effect of various pH solutions of different concentrations on the crack growth characteristics of a range of different glasses. The results obtained supported the observations of Mould (1960), ie. that strength increases for a pH of greater than pH13. However the situation was complicated by the fact that the details of the behaviour were a complex function of the glass composition. (For a detailed discussion of the behaviour of soda-lime-silica glass see chapter 3). In the case of glasses having few free alkali ions the crack velocity is controlled by the bulk environment. For glasses having a high density of free alkali ions the behaviour is more complex. At low velocities the glass close to the crack tip becomes depleted of alkali ions and the bulk environment controls the crack tip pH and hence velocity; at high velocities, however, the ions present in the glass dominate the crack tip pH.

The work of Westwood (1972), who claimed that alcohol chain length influenced the hardness of glass, has given an impetus to the study of glass in alcohol environments. Frieman (1974) has carried out crack growth studies under different alcohols. From his work two theories have been proposed: the first is that alcohols act as an inert medium and it is only the water content of the alcohols that matters; the second theory suggests that the alcohol chain lengths

exert some fundamental influence based on electrostatic potential. Since the arguments for and against both theories are complex and the experimental work inconclusive, this topic will not be discussed further in this review.

One of the most intriguing aspects of macroscopic crack growth studies is the presence of crack growth under vacuum conditions first reported by Schoenart et al (1969) and by Pukh et al (1970). Wiederhorn et al (1974) investigated the effect of temperature over a range of 25°C to 500°C and for a number of different glasses under vacuum conditions. They observed that two glasses, silica and low alkali borosilicate, experienced no subcritical crack growth prior to catastrophic failure whilst for a number of other glasses, including soda-lime-silicates, subcritical crack growth did occur and they were able to evaluate an activation energy with a value of 605 kJ/mol.

A number of theories have been presented to explain the fatigue and subcritical crack growth behaviour of glass. Wiederhorn (1978) has produced an excellent review of the subject, where he considered both the experimental results available and the theories to explain these results. He considered the postulated mechanisms to fall into two categories dependant upon whether they occur close to or remote from the crack tip. In the first category Wiederhorn considered such effects as chemical reactions at the crack tip and plastic flow. In the second group he placed such mechanisms as the transport of a reactive agent to the crack tip and any mechanisms

which influence the composition of the reactive environment at the crack tip.

The theory which Wiederhorn (1978) favoured as providing the best explanation of the experimental evidence was that originally proposed by Charles and Hillig (1965), equation 2.3.3. This equation, based on the reaction rate theory analysis of the corrosion at the tip, basically consists of an activation energy type term made up in three parts. The first part is simply the stress free activation energy, the second part is a stress dependant term, and the third part considers surface tension effects due to the radius of curvature at the crack tip. The stress-corrosion based theory provides good quantitative and qualitative agreement with most of the experimental results. It predicts a static fatigue limit which has been observed at approximately $.15\sigma_N$ the liquid nitrogen failure stress. This theory also predicts however that a crack can sharpen indefinitely which is clearly not a tenable view.

The stress-corrosion based explanation for the first two regions in the slow crack growth curves, fig. 2.7, is a reasonable one. The proposition that crack tip pH influences the reactions taking place there has been proved by the work of Wiederhorn and Johnson (1973), and has been corroborated by the work of Wiederhorn (1973) on the pH of ground glass slurries in water where he recorded a pH of 11.5 to 12.3 for a soda-lime-silica glass. An additional result of interest is that for a soda-lime-silicate Wiederhorn and Bolz

(1970) evaluated an activation energy for crack growth in water of 105kJ/mol which is comparable to that recorded for sodium ion diffusion in a soda-lime-silica glass. Thus the stress corrosion theory of Charles and Hillig (1965) produces a credible explanation for many of the experimental results available. It is not the only theory available, however, and it is clearly not applicable to subcritical crack growth under vacuum conditions.

Lawn (1975) has proposed an atomistic model to explain subcritical crack growth in brittle solids. This model, based on the work of Hsieh and Thomson (1973), considers a brittle solid as a regular arrangement of atoms where subcritical crack growth can occur by a sequential rupture of bonds. This sequential rupture and the energy barrier associated with each rupture results in "lattice trapping" of the advancing crack. Crack advance occurs by the lateral motion of atomic kinks along the crack front. These kinks have been treated using statistical mechanics to define kink formation, motion and annihilation. As part of this theory the interatomic distance enters the equations at the spatial scaling parameter. For a glass however the spatial scaling parameter is the average area occupied by an interatomic bond. The strain energy release rate (αK_I^2) enters this theory as part of the activation energy. Thus a fundamental difference between this theory and that of Charles and Hillig (1965) is that in the log velocity/stress intensity factor K_I relationship, K_I enters this theory as K_I^2 whilst for the stress-corrosion theory the energy term contains only K_I.

Another theory has been produced by Weidmann and Holloway (1974) based on limited plastic flow at the crack tip. Evaluating a flow stress based on the work of Marsh (1967), and predicting a plastic zone size, Wiedmann and Holloway argued that slow crack growth occurred by a continuing extension of the plastic zone. Weidmann and Holloway have calculated that this plastic zone would be about 5nm in a soda-lime-silica glass. A consequence of this theory is that the natural logarithm of velocity is inversly related to K_I.

Cox (1969) produced a theory based on thermally activated ionic migration which generated a flaw by the simultaneous local rupturing of bonds. However Ritter and Munthuruthil (1973) in testing this theory found considerable lack of agreement between theory and experiment.

Nevertheless, although there have been a number of different theories of fatigue behaviour, the stress-corrosion concept must remain most favoured, particularly in the presence of water. However it is possible that the more general "lattice trapping" concept may ultimately show more promise.

2.4 CONCLUSIONS

This chapter has reviewed the previous major studies of mechanical strength. The purpose of such a review is partly to place the current work within a historical context, and partly to provide guidance as to the experimental studies that would be necessary in

order to define the mechanical strength of glass coherently such that a meaningful comparison between glasses of different composition could be made.

The most important parameter in defining the mechanical strength of a glass is the critical stress intensity factor K_{IC}. Experimentally less ambiguous results can be obtained by measuring K_{IC} on macroscopic rather than microscopic or sub-microscopic cracks. In chapter 5 the techniques available for macroscopic crack growth studies are discussed.

The abrasion resistance of a glass will be part of any definition of mechanical strength. Defining precisely how to characterise abrasion resistance is more difficult. Lawn and coworkers, in their various indentation fracture mechanics studies, claimed to have examined fundamentally the abrasion damage process. However all their various theoretical studies contained complex constants which were a function of the indenter/material system and usually evaluated experimentally. A simpler approach would be to characterise the abrasion resistance of a glass by the average flaw size which is produced by a standard abrasion treatment. This flaw size can be evaluated by conducting conventional strength studies at liquid nitrogen temperatures (where fatigue is absent) and then combining the failure stress obtained with the results of K_{IC} studies in equation 2.2.5.

The characterisation of the fatigue behaviour of a glass can be undertaken by either macroscopic or by microscopic studies. In macroscopic studies the slow crack growth is observed for a given glass at a given temperature and environmental water content and as a function of applied stress intensity factor. The results obtained have been fitted in numerous studies by an empirical equation of the form;

$$V = AK_I^n \qquad (2.4.1)$$

where A and n are constants for the given glass/environment system.

The term microscopic studies encompasses the fields of static and dynamic fatigue studies which were described in sections 2.3.2 and 2.3.3. In these types of studies the experimental results obtained are usually fitted to the Charles (1958) equations (2.3.2 and 2.3.4) relating the time parameter to failure stress in order to evaluate the proportionality constant n or $\frac{1}{n+1}$ for equations 2.3.2 and 2.3.4 respectively.

Evans and Johnson (1975) have carried out a fracture mechanics based assessment of the dynamic fatigue process where they included the empirical equation 2.4.1 and were able to show that n in equation 2.4.1 should be equivalent to that in equation 2.3.4 for the case when crack growth was reaction rate limited (Region 1).

This prediction has been confirmed by Ritter and La Porte (1975) for soda-lime-silica glass in alkali and water environments. However, it was observed that in acid solutions there is considerable discrepancy between the value of n recorded for soda-lime-silica glass in slow crack growth studies as compared to dynamic fatigue results. Accordingly it is proposed to carry out the major fatigue studies using slow crack growth studies, but also to conduct some dynamic fatigue studies in order to confirm the results of the slow crack growth experiments.

In this chapter the mechanical strength of glass has been reviewed from a continuum viewpoint. In the subsequent chapter it is proposed to consider the structure of glass and any detailed studies which have been carried out investigating the mechanical strength/composition relationship for soda-lime-silica glasses.

CHAPTER 3

STRUCTURAL ASPECTS OF HYDROXYL IONS IN GLASS

3.1 INTRODUCTION

It was described in Chapter 2 how mechanical strength studies of glass have been carried out in what were termed "quasi-continuum" studies with little regard for glass composition. Indeed complex commercial glasses were often used because of the ease of obtaining specimens. In order to review those studies which have been reported where compositional effects were considered it is necessary first to consider the models which have been presented to describe the structure of soda-lime-silica glass and then to consider how "water" is incorporated into that model.

3.2 THE STRUCTURE OF SODA-LIME-SILICA GLASS

There have been a number of attempts to describe the structure of glass. The most widely accepted theory is the "Random network" model proposed by Zachariasen (1932). Zachariasen proposed that the bonding and coordination of atoms and molecular groups in glasses should be similar to that in crystals. He suggested that the difference between a crystal and a glass was essentially one of geometrial arrangement of the same basic structural groups. Zachariasen postulated a set of rules which an inorganic oxide MxOy

must satisfy if it is to form a glass.

He postulated that:

(1) No more than two M atoms may be attached to any one oxygen.

(2) M must be surrounded by a small number of oxygen atoms.

(3) The oxygen polyhedra produced around the M atoms can share corners only and not edges of faces.

It was also proposed that at least three oxygens of any polyhedra must be shared. However, this final condition is of lesser importance because a number of glasses are known in which this criterion is not satisfied. According to these rules silica should form a glass. It does so, using the same basic network unit as crystalline forms i.e. the SiO_4^{4-} tetrahedron which has a silicon at its centre and four shared oxygens at the corners. For the structure of silica, Zachariasen proposed that this consisted of a random arrangement of the SiO_4^{4-} tetrahedra where the O-Si-O bond angles within the tetrahedra are rigid, and the randomness of the structure is generated by variation of the Si-O-Si bond angles between tetrahedra. Considerable support for this model has been given by the X-ray diffraction studies of Warren and Co-workers. In their latest analysis of the silica structure, Mozzi and Warren (1969) concluded that the Si-O-Si bond angles had a skewed Gaussian distribution about 144° and a half breadth of the distribution of 35°.

Oxides which are themselves capable of forming a glass are known as network formers. The oxides of sodium and calcium, however, are not network formers according to the Zachariasen rules but they do take part in glass formation. These oxides when melted with network formers form glasses by modifying the random network. The addition of one mole of Na_2O to silica will result in the formation of two moles of non-bridging oxygens by a reaction of the form

$$\equiv Si - O - Si \equiv + Na_2O \rightarrow \equiv Si - O^{-Na^+} \quad O - Si \equiv \qquad (3.2.1)$$
$$\qquad\qquad\qquad\qquad\qquad\qquad\qquad\qquad\qquad\quad Na^+$$

The result of this addition is that the network is less rigid, however sodium ions must now be accommodated within interstitial positions. The addition of CaO has a comparable effect, except that charge neutrality is maintained by one calcium ion being associated with two non-bridging oxygens.

In addition a third class of oxides exists apart from the modifiers and network formers. The so called intermediates cannot form a glass in isolation but they will form a glass with a network former. The difference between modifiers and intermediates is that the intermediate become part of the network structure. An example of an intermediate is alumina which enters the structure as AlO_4 tetrahedra, charge neutrality being maintained by an alkali ion in close proximity to the AlO_4 tetrahedra.

The glass which will be studied in this work is a soda-lime-silica glass. According to the Zachariesen model this glass contains a random network of SiO_4 tetrahedra with non-bridging oxygens and sodium and calcium ions in interstitial positions. In the following section the introduction of hydroxyl ions will be considered.

3.3 HYDROXYL IONS IN GLASS

It is well known that the majority of oxide glasses contain hydroxyl ions as an impurity. Commercial silicate glasses contain approximately 0.01 to 0.03% wt, and natural glasses can contain as much as 1% wt. In commercial glasses, prepared in gas or oil fired furnaces, water is introduced into the melt from the furnace atmosphere. The low hydroxyl ion contents so introduced are known to have a significant influence on many of the properties of a glass including density, viscosity, conductivity and dielectric measurements.

The incorporation of "water" into glass has been studied by a number of techniques. The most extensively used technique has been infra-red spectroscopy.

Infra-red spectroscopy is the study of the absorption of infra-red radiation by the glass structure. The absorption is due to the coupling which occurs when electromagnetic radiation interacts with a molecular group whose frequency of vibration in a particular mode

is identical to, or a harmonic of that of, the incident radiation. The frequencies of the vibrational modes observed in glasses are determined by the masses of the constituent atoms, the geometry of the atomic arrangement, and the interatomic forces within a molecular group.

Fig. 3.1 shows a typical infra-red absorption spectrum of a soda-lime-silica glass. Three features can be noted: an absorption band at around 2.85μm, another absorption band centred at 3.5μm, and a "cut off" in transmission above 4μm. The "cut off" at wavelengths greater than 4μm is due to absorption by the silica network itself. The other two absorption bands are due to "water" in the glass. Harrison (1947) was the first to investigate systematically the spectrum of silica which is similar to that shown in fig 3.1 except that the 3.5μm absorption band is not present. Harrison proposed that the 2.85μm band was due to an O-H vibration. However, she suggested that this was due to molecular water present in interstitial positions.

A number of other workers have considered the role of "water" in infra-red spectroscopy of glasses. The most extensive analysis was produced by Scholze in 1959 (a,b) where he considered the "water" bands in a wide range of glasses. Working on soda-lime-silica compositions Scholze (1959a) prepared glasses with a wide range of "water" contents by bubbling nitrogen through the melt to remove water and the bubbled stream through the melt in order to introduce "water". He then performed infra-red measurements on these

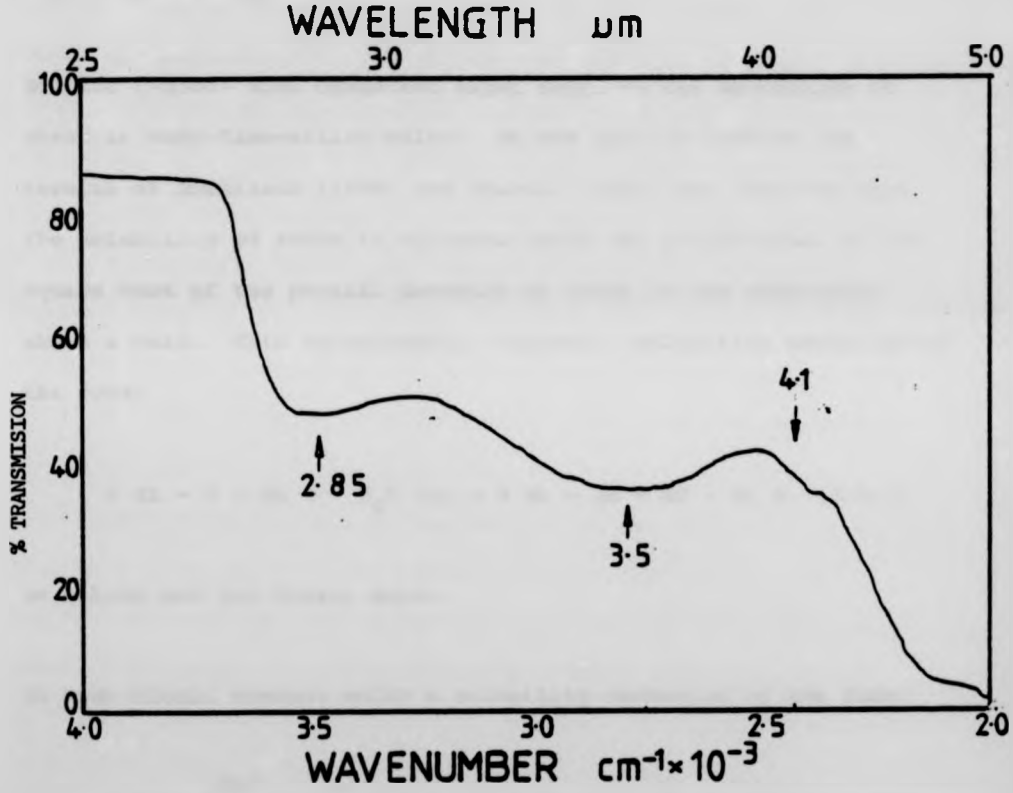

Fig. 3.1 Typical Infra-Red Transmission Spectrum for a "Water" containing glass.

glasses of differing "water" contents and claimed to observe a third absorption band at around 4.25μm. This band was discovered by obtaining a differential spectrum between glasses of differing "water" contents. Adams (1961) however, claimed that this third band was due to CO_2 because its intensity increased after bubbling CO_2 through the melt.

Scholze (1959b) also conducted experiments on the solubility of steam in soda-lime-silica melts. He was able to confirm the results of Tomlinson (1956) and Russell (1957) who observed that the solubility of steam in silicate melts was proportional to the square root of the partial pressure of water in the atmosphere above a melt. This relationship suggests a solubility mechanism of the form;

$$\equiv Si - O - Si \equiv + H_2O\ (g) \rightarrow \equiv Si - OH + HO - Si \equiv \quad (3.3.1)$$

in silica and low alkali melts.

In high alkali content melts a solubility mechanism of the form;

$$\equiv Si - O\overset{Na^+}{\underset{Na^+}{}}O - Si \equiv + H_2O \rightarrow \equiv Si - O - Si \equiv + 2\ Na^+ + 2OH^- \quad (3.3.2)$$

was proposed by Kurkjian and Russell (1958) in order to explain the minimum solubility they observed at 25 mol% Na_2O in sodium

silicates. Scholze (1969) however found no evidence of this solubility minimum. This observed solubility relationship lends weight to the suggestion that hydroxyl ions are present rather than water molecules.

Scholze (1959) considered the absorption bands to be due to hydroxyl ions rather than molecular water. He accounted for the three different bands by the presence of hydrogen bonding. Fig 3.2 shows the proposed structural incorporation of hydroxyl ions into a sodium silicate glass. The stretching mode vibrations of the free Si-OH groups were assigned to the band around 2.85μm. The 3.5μm band was accounted for by the vibration of an Si-OH group with hydrogen bonding to a non-bridging oxygen. The 4.25μm band was ascribed to an Si-OH group with strong hydrogen bonding to a non-bridging oxygen, where the silica tetrahedra to which the hydroxyl ion is attached itself has more than one non-bridging oxygen. Adams (1961) assigned the 2.88μm band in sodium silicates to an Si-OH band with weak hydrogen bonding to a bridging oxygen. The evidence he gave for this assignment was that the band occurred at higher wavelengths in sodium silicates (2.88μm) than in silica (2.73μm). Boulos and Kreidl (1972) however, favoured the analysis of Scholze (1966) which will also be used in this work.

The band centred around 3.5μm was shown conclusively by Scholze (1959b) to be associated with hydrogen bonding to a non-bridging oxygen. In a series of soda-alumina-silicates he observed that as the sodium/aluminium ratio approched one, i.e. the situation

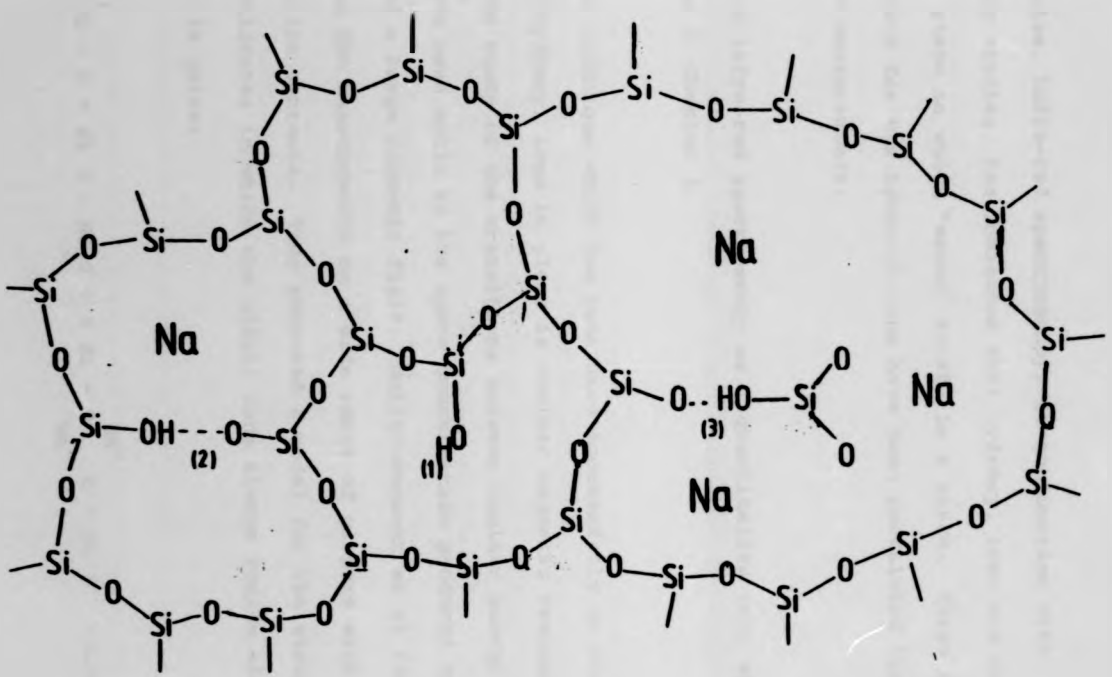

Fig. 3.2 The Sructural Incorporation Of Hydroxyl Ions into a Sodium Silicate Glass.After SCHOLZE(1959).

where no non-bridging oxygens would be present, the 3.5μm band decreased while the 2.85μm band increased. It was also observed in sodium silicates that, as the sodium content increased, so the 3.5μm band also increased.

To summarise, infra-red spectroscopy, in conjunction with solubility studies, has indicated that hydroxyl ions are the most probable state in which "water" exists in a glass. Three distinct environments for the hydroxyl ions have been postulated based on infra-red measurements.

The use of infra-red spectroscopy as a quantitative tool will be discussed in Chapter 4.

The other technique which has been used successfully to study the state of hydroxyl ions in glass is nuclear magnetic resonance (NMR). NMR is the study of the transitions between nuclear energy levels which have been split by the space quantization produced by the action of a large magnetic field. Muller-Warmuth et al (1965) performed NMR measurements on a wide range of glasses with varying hydroxyl ion contents. They proposed a model for the structure of alkali silicates in which the alkali ions always reside close together in pairs.

$$\equiv Si - O - Si \equiv + Na_2O \rightarrow \equiv Si - O\overset{Na^+}{\underset{Na^+}{}}O - Si \equiv \qquad (3.3.3)$$

They also suggested that in hydroxyl ion containing glasses the proton substitutes for an alkali ion to give a structure of the form:

$$\equiv Si - \underset{Na}{O}\overset{H}{} \quad O - Si \equiv \qquad (3.3.4)$$

with a distribution of H - Na distances with a maximum at 2.0A°.

Thus they suggest that the proton of the hydroxyl ion behaves very much like an alkali ion.

These two techniques, infra-red spectroscopy and NMR, seem to produce differing structural models for the hydroxyl ions in a glass. These differences may be artifacts of the techniques themselves in that NMR essentially considers the state of a nucleus with reference to its local nuclear environment, whilst infra-red spectroscopy is very much more dependent upon bonding. The structural dependence of the mechanical strength of glass will be discussed in the following section.

3.4 Structural Aspects of Strength Studies

Chapter 2 discussed how the mechanical strength of glass can be described by two major phenomena, brittle fracture and fatigue behaviour. Brittle fracture was itself described by two important

characteristics: the fracture toughness and the abrasion resistance of a glass.

The fracture toughness of a glass is the critical stress intensity factor K_{IC} and is most unambiguously evaluated by fracture mechanics studies of macroscopic cracks. Weiderhorn et al (1974b) reported values of K_{IC} for four glasses, a lead silicate, an alumino-silicate, a soda-lime-silicate glass and a borosilicate crown glass which give K_{IC} values at 25°C of 0.65, 0.86, 0.7 and 0.973 $MNm^{-3/2}$ respectively. These four glasses exhibited slow crack growth in an inert atmosphere, hence K_{IC} cannot be so easily characterised by abrupt fracture and thus Wiederhorn et al (1974b) took K_{IC} to be that value of K_I which results in a crack velocity of greater than $10^{-1}ms^{-1}$. A value of K_{IC} of $0.73MNm^{-3/2}$ was recorded for both silica and for a low alkali borosilicate at 25°C by Wiederhorn at al (1974). However these two glasses did not exhibit sub-critical crack growth in an inert atmosphere.

Frieman (1974) in his study of the effect of alcohols on subcritical crack growth used four different soda-lime-silicate glasses. He observed that the Region III behaviour in octanol was influenced by glass composition, thus using Wiederhorn's definition of K_{IC} it can be said that as the alkali content of the glass increases then there is a small decrease in K_{IC}. However these results are complicated by the fact that Frieman observed that the

Region III behaviour was influenced by alcohol chain length. An important study was performed by Kennedy et al (1974) who investigated the mechanical properties of sodium silicate glasses and observed that K_{IC} increased with increasing alkali content, whilst hardness decreased with increasing alkali content. However, they were unable to offer any structural model to account for this behaviour.

Thus there exists some fundamental information concerning the fracture toughness of glass. However the studies that have been carried out were in general incomplete and hence little can be said as to the general compositional effects on toughness.

The other parameter important in defining the brittle fracture characteristics of a glass is its abrasion resistance. The more common type of study undertaken however, is to carry out a standard abrasion treatment and then observe the failure stress at liquid nitrogen temperature. Watanabe et al (1961) have carried out the most extensive study of this type using glasses of the soda-lime-silica system. They observed that, for glasses in the range Na_2O 10-37%, CaO 5-30% tested at liquid nitrogen temperature immediately after abrasion, strength increases with decreasing Na_2O content reaching a maximum at 10% Na_2O the lowest amount studied. At 10% Na_2O strength is independant of CaO content over a wide range. For total alkali content of greater than 40% strength decreases rapidly with increasing alkali content. For aged abrasions similar trends were observed, however the overall strength decrease as a

result of increasing Na_2O was smaller, and at a constant 10% Na_2O strength decreased with increasing silica content.

The fatigue studies which have been carried out in which composition has been considered can again be divided into types ie. macroscopic and microscopic studies. Wiederhorn and Bolz (1970) studies the subcritical crack growth of macroscopic cracks under Region I behaviour of the 3 stage slow-crack-curve observed for glasses in water containing environments. Figure 3.3 shows the results obtained for the various glasses considered in water. Again it can be seen that the presence of sodium in the soda-lime-silicate produces the greatest crack growth rate at low values of K_I. Wiederhorn and Bolz (1970) also considered the effect of temperature and, as described earlier, evaluated an activation energy for the various glasses with soda-lime-silica having an activation energy of 109 kJ/mol. Wiederhorn et al (1974) also observed Region III behaviour under vacuum condition for similar compositions to those used in the water environment studies. The activation energy evaluated for the Region III behaviour of a soda-lime-silicate was 605 kJ/mol. They proposed that the "lattice trapping" theories could be used to explain qualitatively the behaviour of the glasses, but they could offer no real insight into how the structure of glass affects this behaviour other than in terms of the bulk modulus behaviour of the glass.

The other type of fatigue study which has been conducted is that using microscopic flaws, ie. conventional strength test. By far

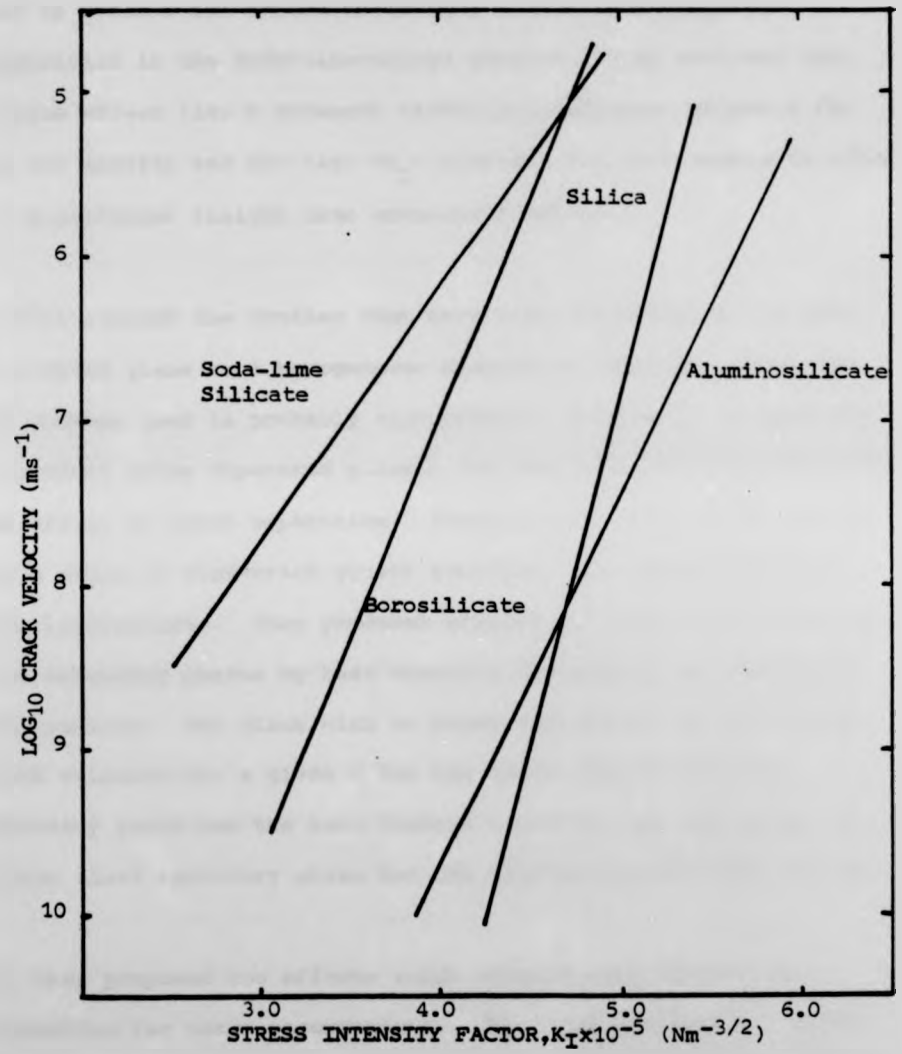

Fig. 3.3 Effect of Glass Composition on Crack Propagation Rate. Tested in Water at 25 C.After WIEDERHORN and BOLZ(1970).

the most extensive study of relevance to this investigation was carried out by Watanabe et al (1961), who by carrying out bend tests at room temperature and at liquid nitrogen temperature were able to isolate the effect of fatigue over a wide range of composition in the soda-lime-silica glasses. They observed that fatigue effect (ie. % strength reduction) decreased slightly for low CaO glasses and for high Na_2O glasses, but were unable to offer any significant insight into structural effects.

In this section the studies that have been described so far have considered glass as a homogeneous disordered material, which for the glasses used is probably appropriate. However it is possible to produce phase separated glasses and some studies have considered the effect of phase separation. Ismail et al (1976) have carried out a study of slow-crack growth behaviour in a phase separated soda-lime-siliate. They produced samples of glass with different size secondary phases by heat treating the samples for different time periods. The glass with no phase separation had the lowest crack velocity for a given K but the glass with 0.09μm size secondary phase had the next highest velocity, and the glass with 0.04μm sized secondary phase had the highest velocity for a given

K. They proposed two effects which could be significant in accounting for these observations. The first was that an alkali rich phase was produced in which crack growth would be enhanced by the increased alkali. The second effect suggested was that two phases will have different rates of thermal expansion (alkali rich

generally higher) and could thus give locally tensile stress around particles.

Sproull and Rindone (1974) examined the effect of bubbling various gasses, with and without water, through a $0.5Li_2O - 0.5K_2O - 2SiO_2$ glass for extended periods. They observed considerable variation of strength which they associated with phase separation in the presence of considerable platinum contamination. The mean particle size of the secondary phase correlated well with strength according to the Griffith relationship.

A mechanical property which is not strictly part of mechanical strength in hardness. However hardness forms a parameter of the indentation fracture mechanics studies of Lawn and co-workers. Ernsberger (1977) has reviewed the hardness studies of glass. However he concluded that whilst the ready availability of the apparatus encouraged researchers to undertake the studies, the many difficulties associated with obtaining accurate measurements makes it very difficult to compare results from different laboratories. A study of interest to the current work is the study by Georoff and Babcock (1973), who examined the hardness of soda-lime-silica glasses over a wide range of compositions. They observed that hardness was linearly related to oxide molar fraction with unique relationships for each of the primary crystalization phase fields.

3.5 OTHER PROPERTY/COMPOSITION EFFECTS AND THE OBSERVED EFFECTS OF WATER IN GLASS

The previous section described the studies which have been carried out where strength/composition relationships have been considered. It is clear that these studies have not been extensive and the results obtained are difficult to interpret. In order to further an understanding of composition/property relationship, it is proposed to describe those properties where compositional effects (particularly of water) are more fully understood. Boulos and Kreidl (1972) have reviewed the effect of hydroxyl ions in glass on the viscosity, internal friction, elastic modulus, density and electrical conductivity.

Viscous flow in glass can be treated as a rate process limited by potential energy barriers. The coefficient of viscosity therefore might be expected to vary with temperature according to an equation of the form:

$$\eta = \eta_o \exp \frac{Ev}{RT} \qquad (3.5.1)$$

where η_o represents a collision factor, that is the number of opportunities for migratory processes to occur, and Ev is the activation energy for viscous flow. Ev is usually fairly constant in liquids, however in multicomponent silicate glasses the activation energy for viscous flow decreases with increasing temperature. Meiling and Uhlmann (1967) observed that for sodium silicates at low temperatures when the viscosity is 10^{12}P, the activation energy for flow is ~ 400 KJ/mol, and decreases to 200

kJ/mol at high temperatures when the viscosity is 100P. However over a small viscosity range the activation energy can be assumed to be constant. The viscosity of a glass will clearly be dependent on the extent of the de-polymerisation introduced by the presence of alkali or hydroxyl ions. Heatherington et al (1964) have shown that in silica the addition of 0.1 wt% hydroxyl ions lowers the activation energy at temperatures greater than 1000°C from 713 kJ/mol to 512 kJ/mol, the actual viscosity being lowered by three orders of magnitude. This reduction was attributed to the depolymerisation of the silica network which occurs with the addition of hydroxyl ions.

In multi-component glasses the addition of excess alkali ions and the influence of hydroxyl ions leads to more complex behaviour. An extensive study of various modifications to the composition of a sodium trisilicate, and their subsequent effects on viscosity, has been carried out by Shelby and McVay (1976), who observed that the introduction of hydroxyl ions produced a reduction in viscosity at a given temperature and also a reduction in the activation energy for viscous flow. Comparable effects, if of smaller magnitude, were observed with the addition of less than 1% mol of other alkali oxides. Shelby and McVay argue that these reductions in viscosity could not be attributed to the increase in non-bridging oxygen density because the glass used, ie. a sodium trisilicate, already contains two non-bridging oxygens for every three silica tetrahedra. Instead, they proposed that hydroxyl ions played a

role similar to alkali ions and exhibited a "mixed alkali" effect similar to that observed for alkali ions.

The effect of compositional changes on the internal friction behaviour of glass has been reviewed by Zdaniewski et al (1979). Internal friction is the measurement of the anelastic behaviour of materials and is usually given as the tangent of the angle by which strain lags behind an applied sinusoidal stress. In glasses the internal friction varies with both frequency and temperature. However, in any particular study results are usually obtained at a given frequency ~1 Hz as a function of temperature. Typical results obtained from such a study are shown in figure 3.4 for a sodium silicate with two different water contents (after Maklad and Kriedl, 1971). The low temperature peak is considered to be caused by the stress-induced diffusion of sodium ions. The second peak has been ascribed to the involvement of protons or hydroxyl ions in a mechanism similar to that found in mixed alkali glasses. Coenen (1961) has observed that increasing sodium content increases the height of the "alkali" peak and decreases the temperature at which the peak occurs. In soda-lime-silicate glasses, Ryder and Rindone (1961) observed that the addition of CaO increased the temperature at which the "alkali" peak occurred and decreased its magnitude. Similarly the presence of additional CaO broadens the second peak which also goes to higher temperatures. Forry (1957) has also shown that the second peak increases in height with increasing alkali content.

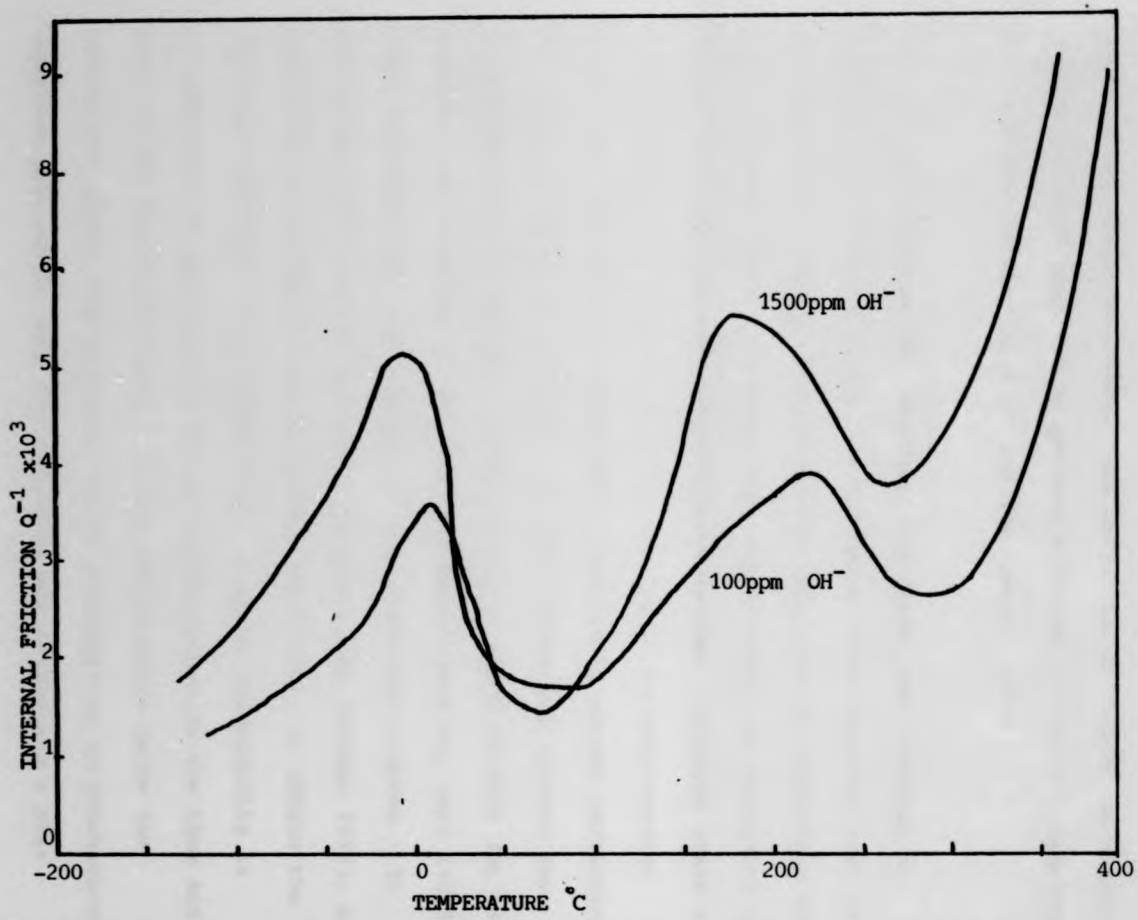

Fig. 3.4 The effect of Hydroxyl ion content on the Internal Friction of an 18mol% Sodium Silicate, Freq=0.4Hz. After MAKLAD and KREIDL (1971) .

Thus the behaviour of the hydroxyl ions in internal friction is broadly in accord with the other similarities between the influence of alkali and hydroxyl additions, although some anomalies do exist.The mixed alkali effect is observed when a second alkali is added to an alkali silicate. The effect is to reduce the magnitude of the "alkali" peak and to produce a second peak at a temperature intermediate to the "alkali" and the "water" peaks.

Much of the evidence for ascribing the first peak observed in internal friction to alkali ion diffusion comes from the fact that the activation energy associated with this peak is comparable to that obtained for D.C. conductivity where alkali ion diffusion is known to be the dominant conduction mechanism. Although glass is conventionally considered to be an insulator, at temperatures above room temperature, measurable conductivity exists particularly in alkali containing glasses. In most commercial glasses the conducting ion is Sodium. Faraday's law is found to hold for these glasses, and a number of electrolysis experiments eg. Burt (1925) have confirmed the ionic nature of the conduction process. In analysing ionic conduction, it is possible (see Doremus 1973), by equating the diffusive and electrical mobilities, to obtain the Einstein equation, which gives that the ionic conductivity is proportional to the product of the concentration of the ions and their diffusion coefficient. At low temperatures below the transition point, conductivity can be described by an Arhenius-type equation similar to that for viscosity and containing a pre-

exponential factor and an activation energy which is independent of temperature.

Considering the effect of composition on the D.C. conductivity of sodium silicate glasses, Johnson et al (1951) showed that the diffusion coefficient increases and the activation energy for conduction decreases with increasing alkali content. Qualitatively this can be understood as the silica lattice becoming more open as the alkali concentration increases. The addition of CaO to sodium silicate results in a decrease in the alkali ions' mobility (Mazurin and Borisovski 1957). The most remarkable effect of composition on D.C. conductivity observed is the decrease in conductivity which occurs when a second different alkali is added to an alkali silicate, ie. the so called "mixed alkali" effect. This effect is most obvious in the properties dependant on alkali mobility. The effect in electrical conductivity has been widely studied and it has been found that the minimum conductivity occurs for a given alkali ratio, when the alkali mobilities are equal. Similar effects have been observed in studies of internal friction and Day (1976) in studying Na-K silicates showed that the critical composition was a function of the glass former, alkali concentration, and in some glass systems was also temperature dependant. It can be concluded that for internal friction the mixed alkali peak is due to the cooperative reorientation of dissimilar alkali ions, which is controlled by the slower moving alkali ion.

There is very little information available as to the effect of hydroxyl ions on the D.C conductivity of soda-lime-silicates. Milnes and Isard (1962), however, have considered the effect of hydroxyl ion content on the conduction process in lead-silicate glasses. They observed experimentally that the conductivity increased with increasing OH content. They attributed this behaviour to the presence of hydrogen bonding between the OH and an oxygen bonded to a lead ion, which results in the lead ion being able to move more freely.

The density of a silica based glass is clearly a function of the alkali and the alkaline earth content, and hence of the extent to which the silica network is depolymerised. The effect of hydroxyl ions on the density of silica is to increase it by increasing the degree of depolymerisation of the silica network. Bruckner (1971) reported that in multi-component glasses the presence of hydrogen bonding results in an increase in density with increasing hydroxyl ion content.

To summarise, the effect of hydroxyl ions, particularly in alkali containing glasses can be considerable and much of the observed behaviour has been interpreted in terms of the mixed alkali effect.

In the following chapter the methods used to produce glasses of different hydroxyl ion contents will be described.

CHAPTER 4

GLASS PREPARATION AND HYDROXYL ION DETERMINATION

4.1 INTRODUCTION

In this chapter the methods available for preparing a soda-lime-silica glass of varying hydroxyl ion content are described. The techniques for evaluating the hydroxyl ion content of a glass are briefly reviewed and the technique used is described. Results for the hydroxyl ion contents of the glasses prepared are tabulated together with the methods used to prepare them.

4.2 GLASS PREPARATION

The composition chosen for study was 16% wt Na_2O, 10% wt CaO and 74% wt SiO_2 (equivalent molar percentages are 15.47%, 10.69% and 73.83% respectively). The composition was chosen for a number of reasons; one of which was that this composition had been used by Scholze (1959a) for infra-red studies and hence quantitative infra-red spectroscopy (Section 4.3) could be carried out. Also this composition appeared to offer a reasonable melting temperature (1400-1450°C) and there was no record in the literature that this glass exhibited any tendency to phase separate or crystallize. In addition it was felt that the composition chosen should reflect the composition of commercial glasses, so that comparisons could be made with the majority of published mechanical strength data which

has been obtained on commercial glasses. This composition is comparable with that of Pilkington Bros. "float" glass, which has a nominal composition of 72.7% wt SiO_2, 9.3% CaO, 13.0% Na_2O with the final 5% made up of Al_2O_3, MgO, K_2O, Fe_2O_3.

The different methods available for the introduction and removal of hydroxyl ions have been reviewed by Boulos and Kreidl (1972). The techniques they considered for the introduction of hydroxyl ions into the glass included:

(a) melting in a steam atmosphere:

(b) heating the glass to 500°C in the presence of hydrogen;

(c) neutron or gamma irradiation in the presence of hydrogen;

(d) heating samples of the glass in an autoclave containing a steam atmosphere.

Techniques (b) and (c) were discounted because it has been shown by the results of Faile and Roy (1972) that the techniques involve the production of Si-H bonds as well as Si-OH bonds.

Technique (d) was used successfully by Ernsberger (1977) for thin films. The technique as described by Ernsberger consisted of treating a 30μm film in a steam atmosphere at 360°C and a pressure of 360 psi for 64 hours. A similar technique was patented by Stookey (1970), however; he considered it suitable for glasses of CaO content of less than 5% only. This type of steam treatment affects only the surface of a glass sample or a thin film, whereas for mechanical strength measurements it is necessary to have bulk

samples homogeneous with regard to hydroxyl ion content. In view of this, the technique adopted in the present programme was to bubble steam through the molten glass.

The two major methods available for the removal of hydroxyl ions from the melt consisted of:

(a) vacuum melting;

(b) melting in a dry atmosphere or bubbling dry gases through the melt.

At the start of this work there were no vacuum or contained atmosphere melting facilities readily available. Thus, the only technique which could be used to produce a low hydroxyl ion content glass was to bubble a dry gas through the melt. The two gases readily available with low water contents were nitrogen and oxygen. Oxygen was felt to be undesirable because it was shown by Greene and Kitano (1960) that oxygen can be chemically dissolved in soda-lime-silica glass. It was proposed, therefore, to use nitrogen which had a water content of less than 5ppm by wt.

Preliminary melting was carried out at the University using Analar grade sodium and calcium carbonates and Angolan quartz as the base materials. Prior to melting, the batch materials were ball milled for 3 hours to ensure homogeneity of the batch. The batch was then melted for 6 hours at 1430 ±2°C in a Pt-5%Rh crucible in an electric furnace and then transferred to the bubbling furnace.

Bubbling was carried out in a top-loading electric furnace with silicon-carbide elements and temperature control of ±5°C by means of a Pt-Pt/13%Rh thermocouple and Eurotherm controller. The furnace had been modified by producing two bricks from alumina cement which could be used to replace the lid of the furnace and through which a bubbling tube could be inserted.

The bubbling tube which was inserted into the melt was a 6mm bore platinum tube of 150mm length which was cemented with alumina cement into an 8mm bore alumina tube. This in turn was cemented into a stainless steel tube which was connected to a steam generator by glass fibre reinforced plastic tubing.

A serious problem was encountered using this bubbling system, and this was that bubbling resulted in the formation of a stable foam which rapidly overflowed the crucible. Attempts were made to reduce this foaming by varying the temperature of the melt, and the pressure and flow rate of the steam. However, these adjustments appeared to have very little effect on the production of the foam. It was felt that the primary cause of the stability of the foam was the small size of the cricible (approximately 7cm diameter) which allowed the foam to adhere to all sides of the crucible and the platinum tube. In addition the maximum temperature of this furnace was 1430°C and at this temperature the viscosity of the glass was such that it encouraged stability of the foam.

Exactly the same problems were encountered with trying to bubble nitrogen in the melt.

The facilities for bubbling into larger melts (greater than 1 litre) and at higher temperatures (greater than 1500°C) were made available by Pilkington Brothers Lathom Laboratories. After preliminary experiments had proved successful, all the glass preparation work was carried out at the Lathom Laboratories.

Glasses were prepared using Limoges quartz and commercial grade sodium and calcium carbonates, with 0.73% wt of the soda being added as sodium sulphate in order to aid refining. After a preliminary melt of 1 hr the glasses were cast and then crushed to 30 mesh sieve size (180 μm mean particle diameter), using a hydraulic press. The crushed glass was passed between the poles of a powerful electromagnet to remove any possible iron contamination from the crushing process. The crushed glass was next weighed out into 1 kg batches and put back into the appropriate furnaces in Pt-3%Rh crucibles. The majority of glasses for which a high hydroxyl ion content was aimed for were remelted in gas furnaces at 1400°C, overnight, and then bubbling of steam at 1500°C ±10°C (melt temperature) was carried out the next day. The use of a gas furnace with its inherently high water content atmosphere had obvious advantages in that it would reduce hydroxyl ion loss from the surface of the melt. Steam was provided by a commercial steam generator manufactured by Them-Vac Ltd. which produced steam at a pressure of 0.275 MPa. Flow rate was controlled by an uncalibrated

needle valve. The time of bubbling was varied from 2 to 5½ hrs in order to see whether prolonged bubbling was required for the melt to reach an equilibrium with its surrounding atmosphere. In addition, it was hoped to observe whether bubbling and hence extra mixing of the melt had any effect on the mechanical strength. It was also attempted to produce a glass of high hydroxyl ion content by pouring the melt into distilled water after preliminary melting and then remelting with steam playing on the top surface of the melt. However, this glass 5/6 did not exhibit an exceptionally high water content as shown in Table 4.2.

Glasses for which a low hydroxyl ion content was desired were remelted in an electric furnace at 1400°C, overnight, and then either cast the next day or bubbled with nitrogen. Bubbling with nitrogen was carried out at 1430°C ±3°C and although this lower maximum temperature meant that bubbling was more difficult this was compensated for by the fact that nitrogen supply was more controllable than the steam supply. It was also found that drying the batch material at 700°C prior to melting gave glasses of a low hydroxyl ion content.

After bubbling, the glasses were allowed to refine for 2 hrs with steam or nitrogen being played on the top of the melt. The glasses were then cast into blocks and annealed for 4 hrs at 565° ±1°C. The blocks were then allowed to cool to room temperature over a period of 48 hrs. In addition some rods and fibres were pulled from the first series of glasses prepared. Tables 4.1, 4.2 and 4.3

give a list of all the glasses prepared, their preparation technique and their hydroxyl ion content.

Bubbling was carried out using silica tubes for both the steam and nitrogen bubbling. These tubes partly dissolved into the glass melt during the course of bubbling. It was estimated that approximately 6 gms of silica were dissolved into each 1 kg melt, giving a compositional change of approximately 0.8% excess silica. In order to verify this estimate and to check for any other impurities, chemical analysis was carried out on some of the glasss by the Eccleston Grange Laboratories. Table 4.4 and 4.5 show the results obtained from this analysis and indicate that glasses which have undergone prolonged bubbling (4/4, 4/5, 5/3) do show some indications of excess silica. It can also be seen from Tables 4.4 and 4.5 that bubbling for over 5 hrs results in some alkali loss, e.g. glass 4/5 contains 15.7% wt Na_2O and glass 5/3 contains only 15.5% wt Na_2O.

A vacuum melt was prepared, towards the end of the work, by Barr and Stroud Ltd, of Glasgow. However, this glass was contaminated with particles of refractory material and a considerable quantity of bubbles and therefore was not suitable for mechanical strength measurements.

4.3 HYDROXYL ION CONTENT DETERMINATION

Boulos and Kreidl (1972) have reviewed the techniques available for the determination of hydroxyl ion content. The three major techniques they listed were:

(1) Chemical analysis;

(2) Nuclear magnetic resonance;

(3) Infra-red spectroscopy.

Chemical analysis can take a number of forms, but essentially it consists of remelting the glass and then using either a vacuum or a dry gas flow to remove the hydroxyl ions from the melt as water vapour which is then carried away to a detection system. The detection system will consist of some form of water sensitive device, e.g. an electrolytic cell as used by Williams et al. (1976) or a mass spectrometer may be used.

The major disadvantage of this form of analysis is that in soda-lime-silica glasses considerable alkali volatilisation will occur. The sodium vapour evolved condenses in cooler parts of the system and reacts with the evolved water to produce sodium hydroxide. This prevents the water vapour from reaching the detection system and hence can introduce considerable errors. In addition, the need to obtain accurate background calibrations for the apparatus also detracts from the ease of use of this technique.

Extensive nuclear magnetic resonance (NMR) studies have been carried out by Muller-Warmuth et al. (1965). By measuring the intensity of the proton resonance from a known standard and comparing it with that due to a known volume of glass, they were able to evaluate the number of protons per unit volume of glass. However, they concluded that NMR had a maximum sensitivity of 30 ppm by weight, while infra-red spectroscopy was found to be an order of magnitude more sensitive.

Fig.4.1 shows the infra-red transmission characteristics of a range of the glasses prepared. Absorption bands due to hydroxyl ions are centred at 2.87 μm, 3.5 μm and 4.25 μm. Quantitative infra-red measurements are made by assuming that the absorption at a particular band is governed by the Beer-Lambert Law.

$$c = \frac{1}{\varepsilon d} \log_{10} \frac{I_o}{I} \qquad \ldots (4.1)$$

where c = concentration of the absorbing species in units of mol/litr

I_o = the % transmission without the absorbing species

I = the % transmission with the absorbing species

d = the thickness in cm

ε = the molar decadic extinction coefficient at the main frequency of absorption.

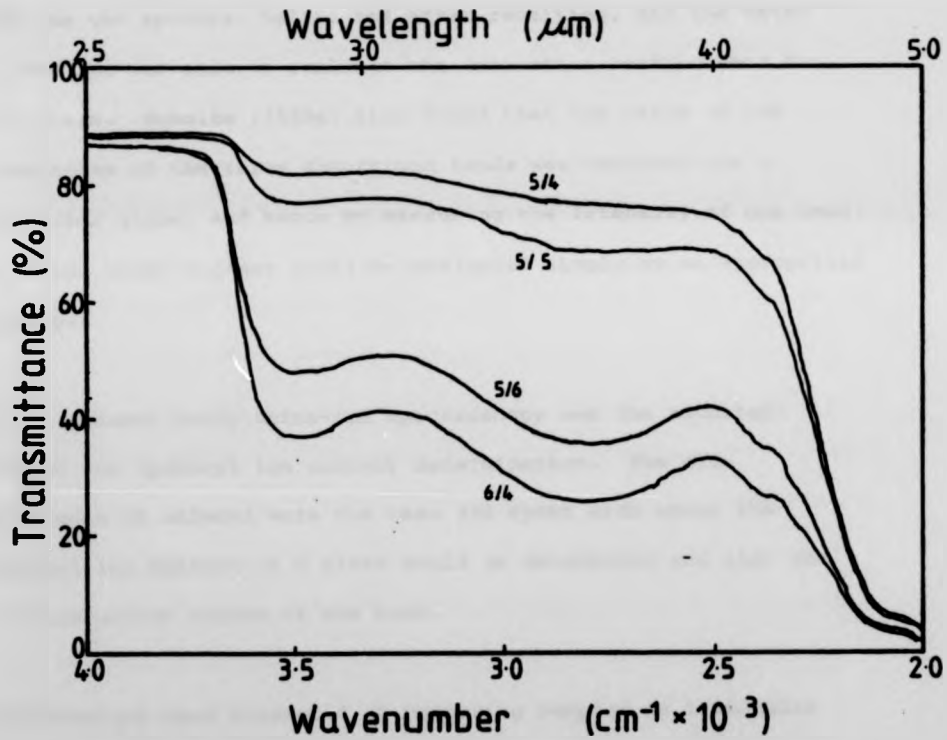

Fig. 4.1 Infra-Red Transmission Spectra for glasses from this study .

Scholze (1959a) evaluated the extinction coefficients for the various hydroxyl ion bands in a wide range of glass compositions, including the glass used in this study. The technique he used was to perform infra-red spectroscopy on a sample of glass and then remelt the glass under a stream of dry nitrogen and condense the evolved water in a dry ice trap. He measured the amount of water present and then reperformed infra-red spectroscopy on the sample. From the two spectra, before and after remelting, and the water evolved, he was able to evaluate the extinction coefficients for each glass. Scholze (1959a) also found that the ratio of the intensities of the three absorption bands was constant for a particular glass, and hence by measuring the intensity of one band the total water content could be evaluated simply by an appropriate scaling.

In the present study infra-red spectroscopy was the technique adopted for hydroxyl ion content determination. The main advantages it offered were the ease and speed with which the hydroxyl ion content of a glass could be determined and also the non-destructive nature of the test.

The technique used consisted of preparing samples as 1 mm thick plates by first grinding the samples flat with a diamond wheel. The samples were ground with 150 silicon carbide and finally

polished with cerium oxide on a felt pad. The infra-red spectroscopy was carried out using a Perkin Ellmer 577 grating spectrometer and spectra were obtained over a range of 4000-2000 cm^{-1} wave numbers (2.5μm - 5μm). Immediately prior to placing the spectrometer the samples were washed with acetone to remove absorbed water form the surface of the glass. To evaluate the hydroxyl ion content using the Beer-Lambert law (Eqn. 4.1), the intensity of transmission without hydroxyl ions, I_o, was taken as the percentage transmission at 2.5 μm. The percentage transmission at the centre of the 2.85 μm band was taken for I.

Scholze when evaluating the hydroxyl ion content of glasses accounted for reflection and overlap effects. In the present work reflection losses were not considered because they are a small and constant percentage of both I and I_o. Correction for overlap effects was not carried out because it as felt that they were not significantly in view of the accuracy of the evaluated extinction coefficients. Scholze (1959a) evaluated an extinction coefficient of 41cm^2/molwhen considering the 2.85 μm band with the listed correction. However, Williams et al (1978) evaluated extinction coefficients of between 37 and 43 cm^2/mol for soda-lime-silica glasses at the 2.85 μm band without any reported overlap or reflection corrections.

4.4 DISCUSSION

From the hydroxyl ion contents listed in Tables 4.1, 4.2, 4.3, it can be seen that the total range of hydroxyl ion contents was 59 to 780 ppm by wt. It would have been desirable to obtain a very low hydroxyl ion content by nitrogen bubbling but the nitrogen bubbling glass 6/3 (OH content 59 ppm) does not result in a very significant improvement on the presintered melt 5/4 (OH content 72 ppm). A possible explanation that can be offered is that the removal of hydroxyl ions by bubbling with nitrogen must take a considerably longer time than 4½ hours to be effective in a 1 kg melt.

The maximum hydroxyl ion content obtained was in glass 6/4 (779 ppm). The maximum hydroxyl ion content is limited by the partial pressure of steam above the melt. It would be possible to achieve a higher OH content by having a sealed atmospheric chamber in which the glass could be melted. However the problems associated with a pressure vessel capable of sustaining 1400°C are so formidable that such an approach was not attempted. In order to obtain a homogeneous glass in an eight hour day at the Lathom laboratories steam must be bubbled through the melt. Thus the characteristics of the melt under the action of bubbling will limit the maximum hydroxyl ion content that can be obtained. A number of attempts were made to increase the hydroxyl ion content of the glass by varying the temperature, pressure and flow rate of steam, and position of the tube in the melt. However, the process of bubbling steam was found to be particularly unstable and only one set of conditions gave satisfactory bubbling and a hydroxyl ion content of between 740-780 ppm.

TABLE 4.1

Table of Glasses Prepared in Series 4

Glass	Preparation Technique	Hydroxyl Ion Content in ppm
4/1	The batch was presintered at 700°C in electric furnace overnight and then melted at 1430 for 1 hr, cast, crushed, and then remelted overnight and cast after rods and fibres had been pulled.	110
4/2	The batch was melted for 1 hr in an electric furnace, cast, and then crushed and remelted overnight and cast the next day.	152
4/3	Melted for 1 hr in a gas furnace, cast, then crushed and remelted overnight at 1500°C, then cast the following day.	356
4/4	Same technique as 4/3 but in addition steam bubbled through the melt for 2 hrs and then the glass refined for 2 hrs and then cast.	779
4/5	Same technique as 4/4 but bubbling carried out for 5¼ hrs.	763

TABLE 4.2

Table of Glasses Prepared in Series 5

Glass	Preparation Technique	Hydroxyl Ion Content in ppm
5/1	Same technique as 4/4.	762.9
5/2	Same technique as 4/3.	469
5/3	Same technique as 4/5.	734
5/4	Same technique as 4/1.	72
5/5	Same technique as 4/2.	134
5/6	The batch was melted for 1 hr in a furnace and then poured into water, crushed, and then remelted for 4 hrs with steam being played on the top surface of the melt.	513
5/7	Same technique as 4/2, but steam passed through the melt for 1½ hrs, and the glass refined for 2 hrs with steam being played on the top surface of the melt.	754

TABLE 4.3

Table of Glasses Prepared in Series 6 and 7

Glass	Preparation Technique	Hydroxyl Ion Content in ppm
6/1	The batch was melted for 1 hr in a gas furnace and then cast, crushed and remelted overnight. Then nitrogen bubbled for 4½ hrs and then the melt was allowed to refine overnight.	394
6/2	Same as 4/4	774
6/3	Batch melted for 1 hr in an electric furnace and then cast, crushed, and remelted overnight, and then nitrogen bubbled for 4½ hrs and the glass refined overnight.	59
6/4	Same as 4/5 and 5/3.	778
7/1	Same as 4/2.	137
7/2	Same as 4/3.	358

TABLE 4.4 CHEMICAL ANALYSIS OF 4 SERIES GLASSES

Glass	4/1	4/2	4/3	4/4	4/5	
SiO_2	73.1	73.5	73.0	73.5	73.4	wt%
CaO	10.6	9.8	10.5	10.6	10.6	
Na_2O	15.8	16.1	15.9	16.0	15.7	
K_2O	TR	TR	TR	TR	TR	
MgO	0.4	0.4	0.4	0.2	0.2	
Al_2O_3	0.05	0.05	0.05	0.05	0.05	
Fe_2O_3	53 ppm	56 ppm	42 ppm	41 ppm	39 ppm	
SO_3	0.014	0.12	0.15	0.08	0.08	

TABLE 4.5 CHEMICAL ANALYSIS OF 5 SERIES GLASSES

	5/3	5/6	5/7	7/2
SiO_2	74.6	73.9	73.8	73.8
CaO	9.7	9.8	9.8	9.8
Na_2O	15.5	16.1	16.1	16.1
K_2O	0.01	0.01	0.01	0.01
MgO	0.1	0.1	0.1	0.1
M_2O_3	0.1	0.1	0.1	0.1
SO_3	0.06	0.18	0.15	0.13

CHAPTER 5

MECHANICAL STRENGTH EXPERIMENTATION

5.1 INTRODUCTION

The aim of this work, as already stated, is an attempt to investigate the compositional dependence of mechanical strength. In order to carry out such an investigation it is clearly necessary to define a set of parameters which can fully describe mechanical strength. In Chapter 2 the theories of mechanical strength were reviewed and the experimental parameters relevant to these theories were described.

Briefly the conventional parametric approach to mechanical strength is one where brittle fracture occurs when an initial value of stress intensity factor (K_{IC}) is reached and fast fracture ensues The stress intensity factor K_I which is a function of crack length and stress, can be increased by the crack length increasing by the stress corrosion/static fatigue model of strength degradation proposed by Hillig and Charles (1965). The model of Hillig and Charles was a microscopic one, later work however, on macroscopic cracks has lead to theories of fatigue where the behaviour of these macroscopic cracks is assumed identical to microscopic defects, Evans and Johnson (1975) were foremost in expounding this view. The parameters necessary then to define mechanical strength of various glasses after a standard abrasion technique are:-

(1) The critical stress intensity factor K_{IC}.

(2) The mean initial flaw size which results from a standard abrasion technique.

(3) The distribution of flaws present in a surface after abrasion.

(4) The stress corrosion parameters A and n.

The critical stress intensity factor can most unambiguously be obtained from fracture mechanics studies. Similarly the stress corrosion parameters A and n can be evaluated by macroscopic flaw crack growth studies. However, because of the doubts expressed as to whether macroscopic crack growth is equivalent to static and dynamic fatigue, it would also be desirable to evaluate fatigue by more conventional methods.

The initial flaw size introduced by standard abrasion can be evaluated by performing four point bend studies under liquid nitrogen when fatigue is absent and then combining these results with the K_{IC} measurements to obtain a flaw size. In order to obtain more detailed information on the distribution of flaws present after a standard abrasion it is clearly necessary to perform a large number of fracture tests. Hertzian fracture is the only test which is suitable because of the small amount of material required. However, the Hertzian indentation test is not one which can easily be performed under liquid nitrogen conditions and in the present work it will be performed at room temperature and 60% relative humidity. The results obtained from the Hertzian fracture tests will therefore have to be corrected for fatigue behaviour and the differences in critical stress intensity factor.

It is also proposed to carry out some room-temperature four point bend studies for comparison with the Hertzian fracture results.

5.2 FRACTURE MECHANICS STUDIES

5.2.1 Introduction

As previously described the aims of the fracture mechanics studies were twofold. Firstly the slow crack growth experiments were to be used to study macroscopically the fatigue behaviour. Secondly the fast fracture studies were aimed at evaluating K_{IC} the critical stress intensity factor.

With these two aims in mind the type of testing system and the environmental control were then considered. Slow crack growth studies have been reported in a wide range of differing environments. However since the data which was to be obtained was to be considered in conjunction with four point bend studies and Hertzian facture measurements it would obviously have to be performed in comparable environmental conditions. Accordingly it was proposed to carry out the stage I slow crack growth studies at a relative humidity of 60% and at room temperature and these would then be used for the other environmental sensitive experiments.

In order to evaluate K_{IC} accurately, it was necessary to evaluate as much of the stage III region as possible. Hence, low humidity measurements, (where the transition to stage III behaviour occurs at a low velocity), were felt to be most suitable.

Two fracture mechanics testing systems were considered for use in this work. These were the double torsion test and the double cantilever beam test. The double torsion test was described by Evans (1972) and by Evans and Williams (1973). This technique has three advantages. The first of these is that K_I is independent of crack length. The second advantage is that the load is applied compressively to the specimen and so there is no need for any rigid attachment to the specimen. In addition, by use of the load relaxation method, the crack velocity can be obtained without the need for the optical measurement of crack length changes. The disadvantages of the double torsion technique were twofold. Firstly, because this technique requires that constant displacements be maintained for a long time, it is necessary to use a commercial testing machine of low compliance. The second disadvantage of the double torsion technique was that it had been analysed by Evans (1972) only for the case of a straight crack front. However, it was known that the crack front is curved, being more advanced on the tensile side of the specimen. The effect of crack front curvature was only analysed in 1977 by Trantina, who proved that for curvatures with angles between 30°- 40° and for specific width to thickness ratio's the configuration did in fact give a constant K_I.

The other specimen configuration which was considered was the double cantilever beam arangement as shown in fig 5.1. Two alternative loading arrangements are available, namely the application of a tensile load P_1 or the application of a moment M_1.

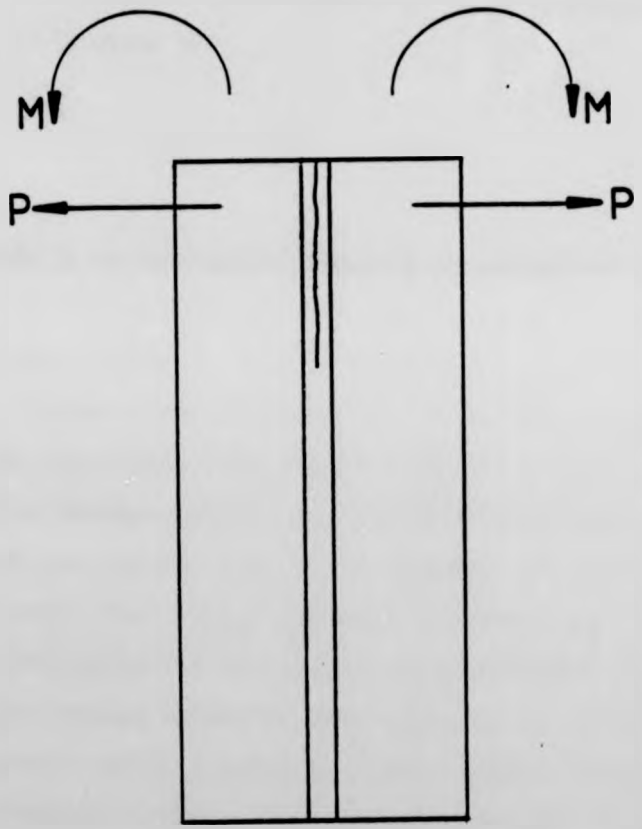

Fig 5.1 Constant Moment and Constant Load modes for the Double Cantilever Beam Fracture Mechanics Specimen.

Tension loading has two disadvantages. In this mode K_I is dependant on crack length and also for pure tension a pin loading arrangement should be used with holes drilled through the specimen.

The constant moment test technique was proposed by Frieman et al (1973) and has the advantage that K_I is independant of crack length and is given by:-

$$K_I = \frac{M}{\sqrt{It}} \qquad (5.2.1)$$

Here, M is the applied moment, I is the moment of inertia of one half of the specimen about its centre of cross-section and t is the thickness through which the crack passes. Since K_I is independent of crack length a constant stable crack velocity can be achieved by the simple application of a constant moment. A constant moment is obtained by the application of a constant load to the ends of loading arms which are rigidly fixed to the specimen and pivoted at a fixed distance along their length. Because a constant load is required this is best obtained by the use of dead weight loading. The use of dead weight loading allows the test apparatus to be easily incorporated into a totally enclosed humidity control system. During this constant moment technique a rigid joint to the specimen must be used. It was felt that this requirement could be achieved by the use of an epoxy resin.

5.2.2 Experimental

The constant moment apparatus in a glove box with a nitrogen atmosphere of controllable humidity and optical measurement of crack velocity was

adopted as the most suitable apparatus for the aims of this study. The apparatus was constructed by the Physics department workshop, Fig 5.2 is a photograph of the complete apparatus, the details of the loading arrangement are shown in Fig, 5.3 and the atmospheric control system is shown schematically in Fig, 5.4.

All the low humidity measurements were carried out first because it was found that a constant low humidity was achieved only after dried nitrogen had been passed continuously for 30 to 40 days through the glove box. This length of time necessary to achieve a constant value was thought to be due to water diffusing out of the perspex windows of the box. The lowest humidity which could be obtained was 1% Relative humidity at 25°C and was achieved by closing valves A and C (Fig, 5.4) and passing nitrogen through the system at 4 litres/min. The relative humidity measurements for low humidities were made using a silvered cup, dew point hygrometer shown in Fig, 5.5 which was attached to the outlet from the glove box. Cooling of the cup was achieved by means of acetone/dry ice mixtures, and the temperature at which ice just dissapeared from the outside of the cup was measured using an insulated T_1/T_2 thermocouple attached to the inside of the polished nickel cup.

Initial testing of the apparatus was carried out using 2.4mm thick "Float" glass supplied by Pilkington Bros. Considerable care was taken to produce uniformly rectangular specimens. Specimens were approximately 25mm wide by 90mm long by 2.4mm thick and were ground flat to less than 25 μm variation in thickness over their entire length and less than 12μm variation in width. A central grinding

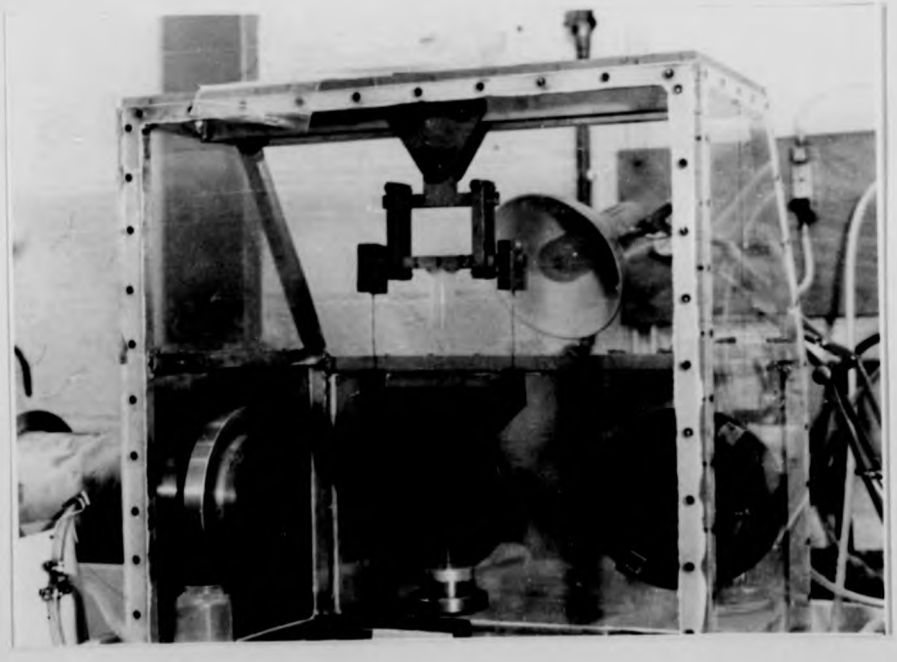

Fig. 5.2. Photograph of Fracture Mechanics Equipment.

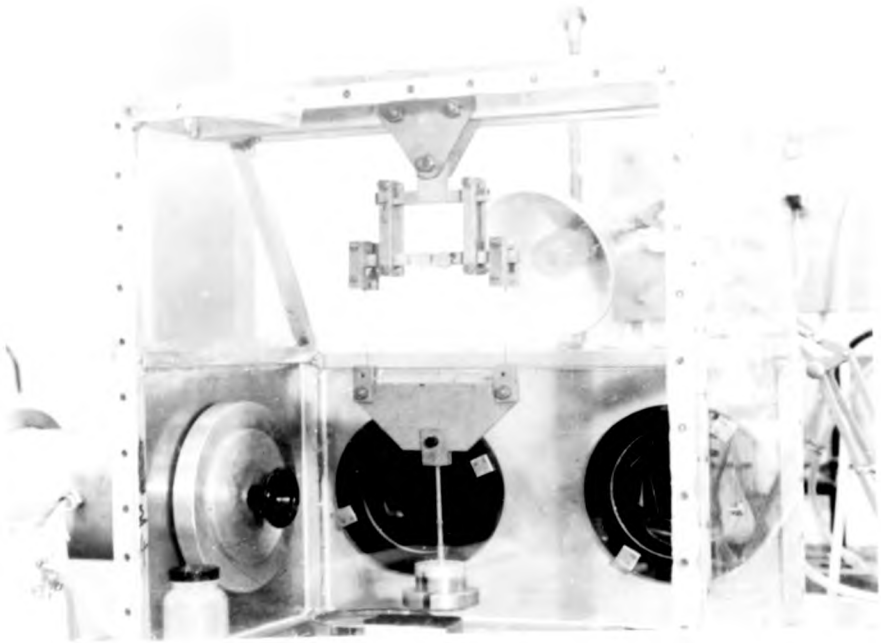

Fig. 5.2. Photograph of Fracture Mechanics Equipment.

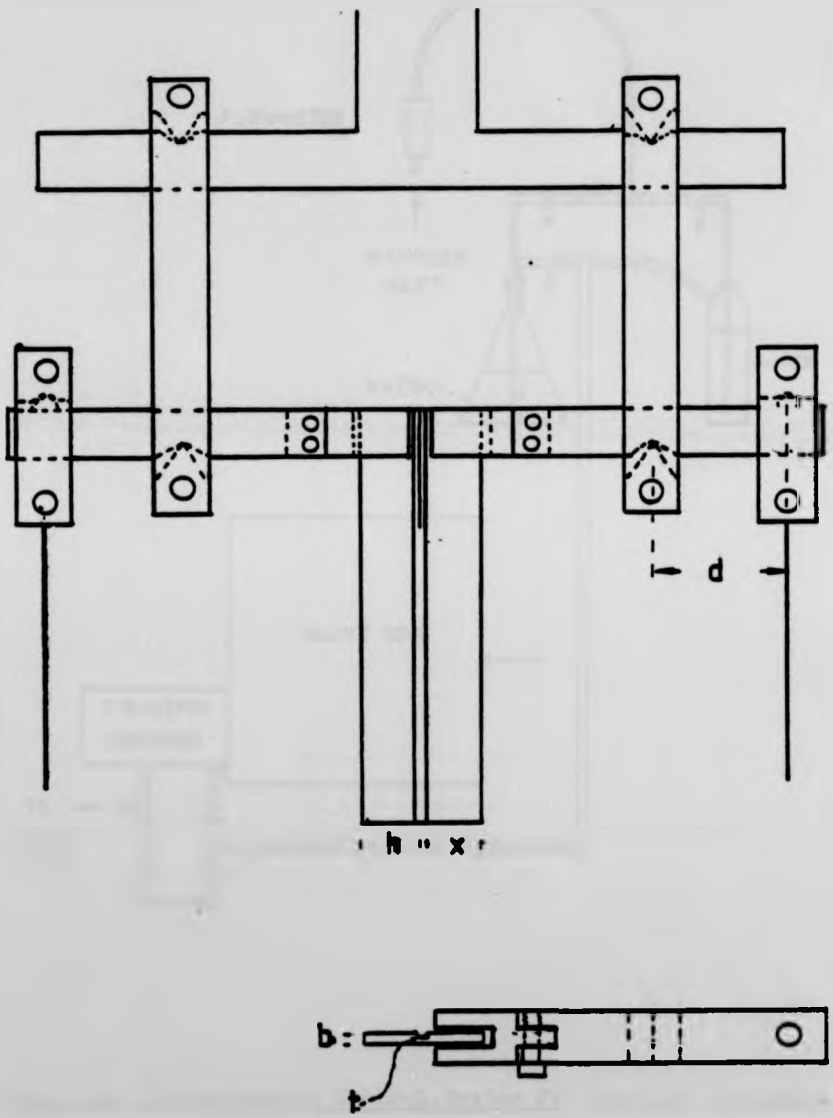

Fig. 5.3 Details of Constant Moment, Double Cantilever Beam, Arrangement for Fracture Mechanics Studies.

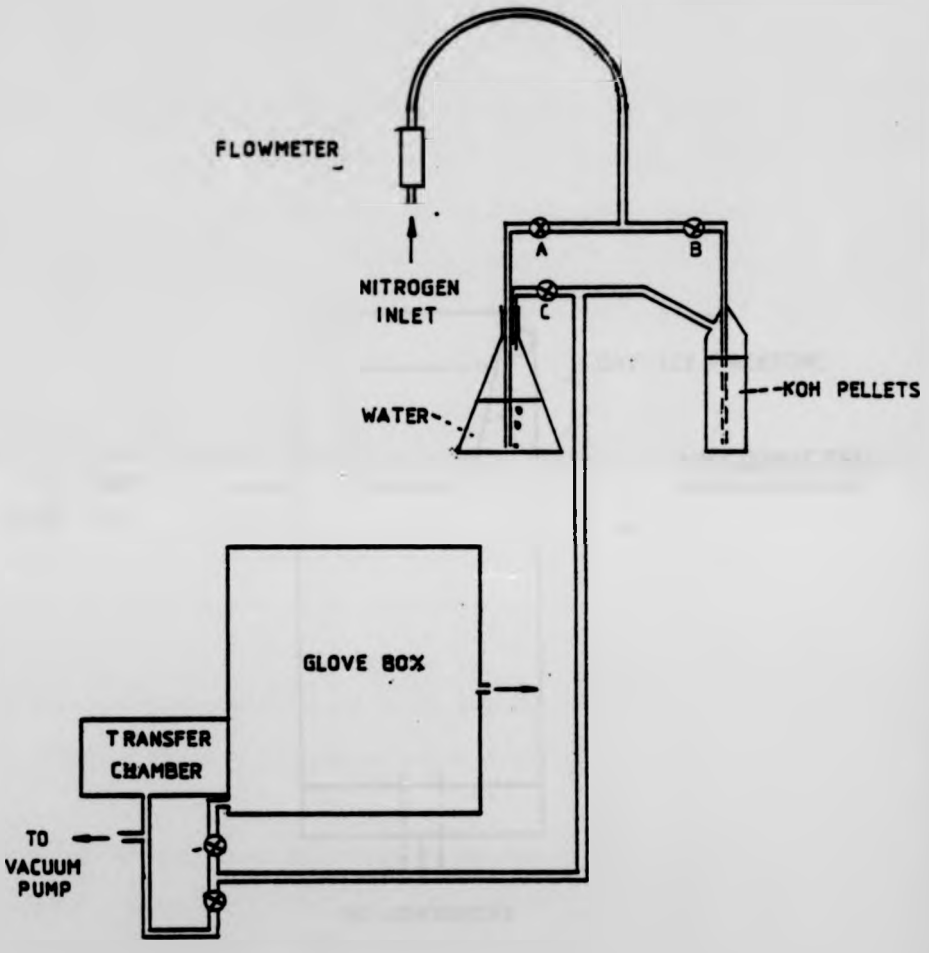

Fig. 5.4 Environmental Control System For Fracture Mechanics Studies.

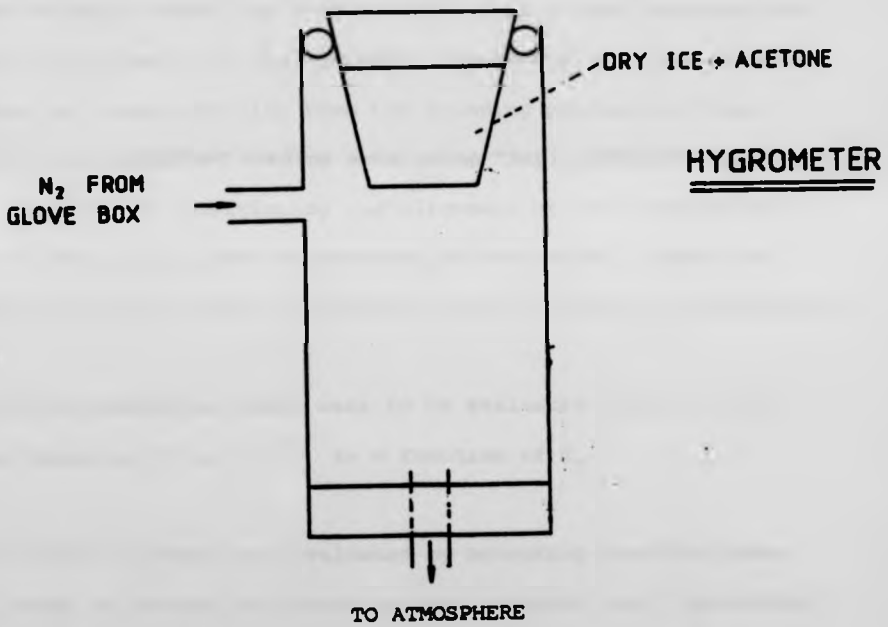

Fig. 5.5 Hygometer used to Measure The Humidity of the Nitrogen leaving the Glove Box.

groove of width 1.75m and depth equal to half the thickness was introduced.

A crack was introduced into the grinding groove by first scribing a line of length 12mm from one end inside the groove using a Tungsten carbide tipped knife. The specimen was then inverted and placed in the sharpened screw device shown in Fig 5.6 and the screw tightened directly above the scribed line until a crack appeared and propagated a few mm along the specimen. Specimens were then washed in acetone to remove any oils from the grinding process and then glued into the assembled loading arms using "Rapid Araldite" epoxy resin. Reproducable positioning and alignment of the specimen with respect to the loading arm was achieved by the use of a specially scribed ruler and set square which were used to position the specimens.

The two quantities which were to be evaluated from this test were crack velocity (V in m s^{-1}) as a function of K_I.

The crack velocity was evaluated by measuring the time taken for the crack to change its length by approximately 1mm. Measurement of crack length was achieved by a cathetometer with a 10x magnification and a vernier accuracy of .01mm. Timing was carried out using a stop watch accurate to 0.2 secs for times less than 15 mins and an electric clock accurate to 1 sec in 24 hours for the longer time periods.

For the evaluation of K_I from equation 5.2.1 the three quantities required are M the applied moment, I the moment of inertia and t the thickness. Considering these three quantities in turn, M the applied

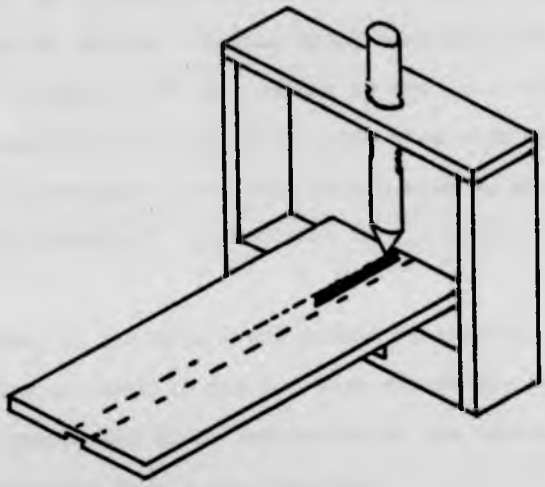

Fig. 5.6 Sharpened Screw Device for Pre-Cracking Fracture Mechanics Specimens.

moment is the product of half the total applied load multiplied by d the distance from the centre of the ball bearing to the knife edge (see Fig,5.3). To this corrections must be made for the moments about the knife edge due to the weight of the loading arms and the specimens. These corrections were evaluated by balancing, on the knife edges, the loading arms and half the specimen and then measuring the upthrust at the ball bearing using a chemical balance. These corrections together with the weight of the lower half of the apparatus gave an effective applied load of 1.059 k gm with no external weights applied. The distance d was 30mm to ± 0.01mm as measured using a travelling microscope.

In order to evaluate I the moment of inertia, dimensions b, h, t and x as shown in Fig 5.3 were accurately measured using a travelling microscope after completion of the testing of a specimen. For a rectuangular beam I is given by:-

$$I = \frac{b\,h^3}{12} \qquad (5.2.2)$$

However, in order to obtain an accurate value of I the effect of the groove had to be considered. This was achieved by finding the centre of area and then using the parallel axis theorem for moments of inertia to evaluate I about an axis through the centre of area.

As previously described the 1% R.H. measurements were carried out first. The purpose of these experiments was to evaluate K_{IC}, however, it was found desirable to observe the three stages of slow crack

growth. The reason for this was that the transition from stage II to stage III behaviour is very abrupt, (typically the change occurs with a 50 gms weights change on a 3 k gm load) and only by obtaining a complete picture including stage I and stage II could the position of the transition be found with any degree of success.

Three experimentally prepared glasses were selected for testing. These were 4/1 (electric melt, 110 ppm OH content), 4/3 (gas melt, 356 ppm OH content) and 4/5 (steam bubbled for 5.5 hrs, 763 OH content).

The test procedure used consisted of first introducing the specimen through the transfer chamber shown to the left in Fig,5.4. This chamber had been designed so that it could be evaluated to 0.1 torr and then refilled with nitrogen of the appropriate humidity, thus allowing a rapid transfer of the specimen. The specimen was placed into position as shown in Figs 5.2 and 5.3. A load was then applied to give a K_I of approximately 4.5 $MNm^{-\frac{3}{2}}$ (typically 1.5 kg) and this load was increased in 250 steps until stable slow crack growth (1mm length change) was observed in one hour. The load was then reduced to give a crack velocity of around 1×10^{-8} m_s^{-1} and this crack velocity and the applied load were then recorded. Loading was subsequently increased in 5 g steps and the resultant crack velocities over stage I and stage II were recorded. Towards the end of the stage II region the load steps were reduced to 10 g or even 5 g. Speeds above 5×10^{-3} m_s^{-1} were not in general measured because of the amount of specimen consumed in the 8-10 sec required for an accurate measurement. The experiment was stopped when such velocities were obtained and the specimen unloaded for 24 hours and then the process of testing was repeated. This delay in retesting was to ensure that

the crack tip conditions at the start of the second test were comparable to those at the start of first test. Testing was complete when the crack had propagated about 65% down the length of the specimen. It was observed that at crack lengths much greater than this, complex end effects started to occur and K_I was no longer independant of crack length.

In total at least 4 specimens were tested for each of the glasses selected and then valves A and C (Fig 5.4) were adjusted until the humidity in the glove box was 60% as measured using a commercial horse hair hygrometer accurate to 2% R.H. .

Specimens were prepared for 60% R.H. measurement in the same manner as for 1% R.H. measurements. Testing was carried out using the same technique as previously described with two modifications.

The initial load applied was considerably smaller so that the initial K_I was typically .4 $MNm^{-\frac{3}{2}}$.

The second major difference between the 60% R.H. and the 1% R.H. measurement was that only stage I behaviour was studied. The reason for this was that these slow crack growth measurements were to be compared with the four point bend measurements and Hertzian fracture results where stage I slow crack growth behaviour should dominate. Chandan et al (1978) reported that in their dynamic fatigue measurements no stage II dominated behaviour was observed, (as described in Chapter 2).

In total three specimens were tested for each of the three glasses under study. The results obtained are presented and discussed in Chapter 6.

5.3 FOUR-POINT BEND STUDIES

5.3.1 Introduction

The four-point bend test configuration is a technique for producing a tensile stress in the surface of a glass specimen by the application of a bending moment. The arrangement is shown schematically in Fig. 5.7. The uniform maximum tensile stress σ is achieved on the lower surface between the two inner supports and is given by:-

$$\sigma = \frac{P\,d}{2I} \qquad (5.3.1)$$

where I is the moment of inertia of the cross-section about the neutral axis of loading. (For a rectangular specimen see eqn 5.2.2). The load P is usually applied by a commercial tensile testing machine (of the Instron type) by the application of a constant rate of displacement to the upper support. In the present study four-point bend experiments were to be carried out with three aims in mind.

The first of these was to obtain an estimate of the initial flaw size produced in a glass by a standard abrasion technique. This was to be carried out by performing four-point bend measurements

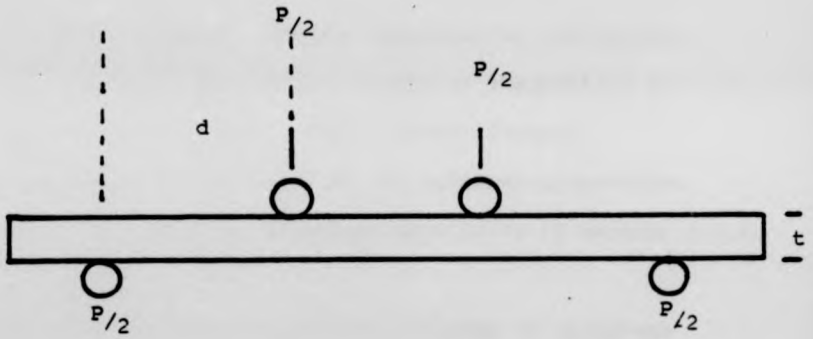

Fig. 5.7 The Four Point Bend Test Arrangement.

under liquid nitrogen (77K) where fatigue effects are absent.

The second aim was to study the strength of glass when fatigue is present by performing four-point bend measurements at 60% R.H. and room temperature. The results obtained can then be compared with theoretical estimates based on fracture mechanics studies and estimates of the initial flaw size.

The third four-point bend study considered necessary was a more detailed examination of microscopic fatigue behaviour by the dynamic fatigue method. In this technique failure stress is examined as a function of the applied loading rate. These dynamic fatigue measurements were necessary in the light of the specimen preparation technique used. This point will be discussed more fully in section 5.3.3.

Within the framework of these objectives a number of decisions had to be taken concerning the parameters which may influence the results obtained from four-point testing. The most important of these were abrasion treatment prior to testing and specimen size and shape. Since these parameters were investigated using both liquid nitrogen and room temperature measurements it is proposed to discuss these two techniques in the following section (5.3.2). Dynamic fatigue studies will then be described in the following section 5.3.3.

5.3.2 Liquid nitrogen and room temperature measurements.

Four-point bend measurements under liquid nitrogen were to be carried out using the apparatus shown in Fig 5.8(a), (b). Fig.5.8(a) shows a photograph of the complete apparatus and Fig,5.8b shows the apparatus schematically. Construction was in stainless steel and the

Fig. 5.8(a) Photograph of Liquid Nitrogen Four Point Bend Stage Removed from the Instron Tensile Testing Machine.

Fig. 5.8(a) Photograph of Liquid Nitrogen Four Point Bend Stage Removed From the Instron Tensile Testing Machine.

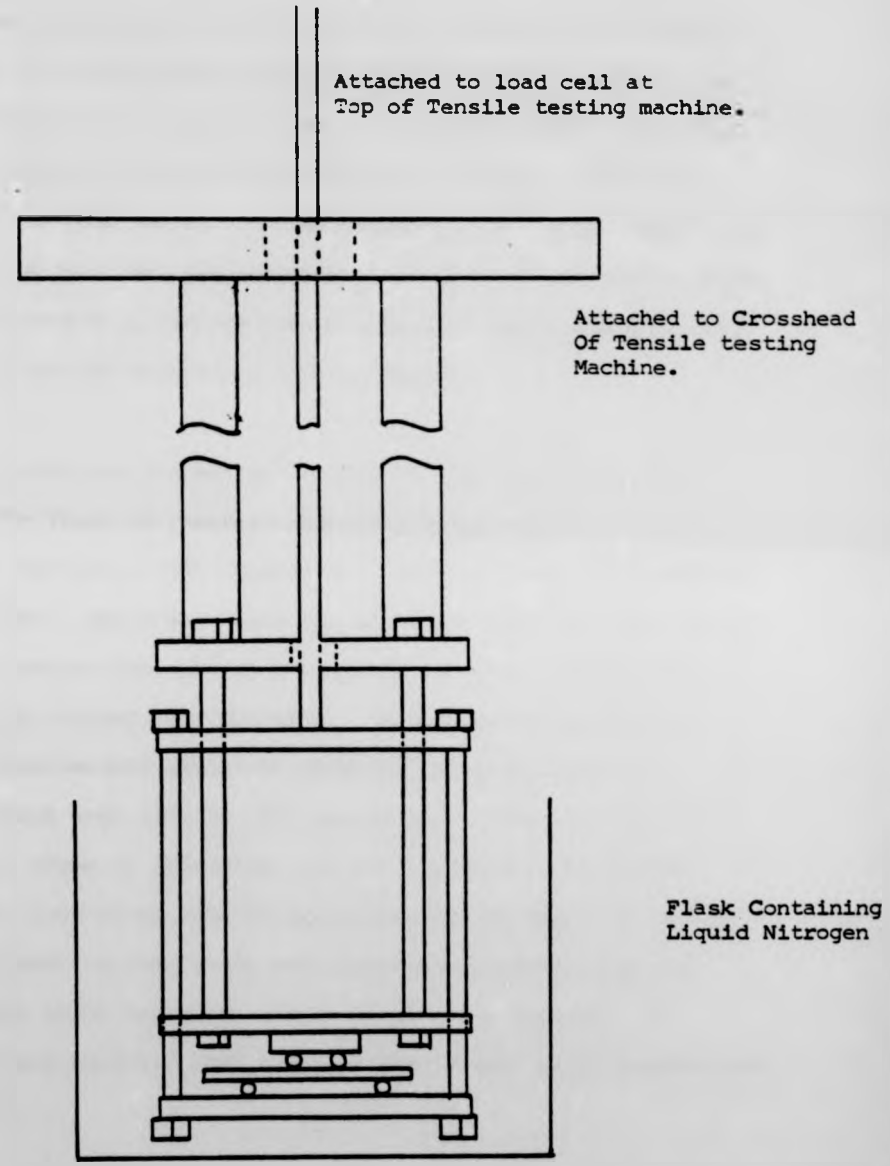

Fig. 5.8(b) Details of the Experimental Arrangement for Four Point Bend Testing under Liquid Nitrogen.

steel rods used for supports had an inner span of 1 cm and an outer span of 4 cm. The entire apparatus below the line shown in Fig 5.8b could be immersed under liquid nitrogen in a vacuum flask. The load was measured using a 5 kN tension/compression load cell which was also used for the room temperature measurements. For room temperature measurements the load cell was mounted in the base of the test machine. Rollers of the same size and spacing were mounted above the load cell with the inner rollers mounted in the crosshead.

In considering the parameters which influence four-point bend measurements the first of these are specimen shape and size. Specimens for four-point bend studies are usually either round rods or rectangular beams. Round rods have the advantage that they can easily be produced to strict dimensional tolerances and with a good surface finish simply by pulling from the melt. Rectangular beams however, require that considerable effort be expended to produce regular specimens in which edge effects (failure by deep flaws introduced by chipping at the edges of specimens) are not a problem. Accordingly, it was decided that round rods of approximately 2mm diameter and 5cm long would be used for this study and these were produced from the series 4 glasses which cover the entire range of OH content. In addition rods were produced from glass of the "float" glass composition (see Chapter 3).

The nature of flaws in glass was discussed in Chapter 2. In experimental studies such as these, flaws will have been introduced by handling of the specimens . Thus if one is to obtain meaningful results then a standard surface treatment must be carried out so that a known surface

condition controls mechanical strength. This need for a standard surface treatment has proven a hindrance to progress in this field precisely because no abrasion treatment has ever been universally adopted, so making comparisons between the results of different workers difficult. As previously described, Mould and Southwick (1959) studied various abrasion treatments and they would classify the flaws present as to whether they were line or point defects. In the present study a number of differing techniques were considered for producing both line and point flaws. Considerable emphasis was placed on producing an unbiased surface treatment with as little human influence as possible. The technique adopted was to place 15 rods into a 0.5 litre screw top jar together with 500 grm of dried 30 mesh silicon carbide. The jar was then rotated at a fixed rate on a ball mill for 2.5 hours. The glasses so prepared were tested at liquid nitrogen temperature. In the meantime, however, the series 5 glasses had been prepared, some with very similar techniques to series 4. It was observed that glasses from the two series prepared by similar techniques did not have the same OH content cf. 4/1 and 5/4. Both of the glasses had been prepared using the presintering technique but glass 4/1 was melted for approximately one hour longer. During the extra hour the crucible was removed from the furnace three or four times for rod pulling. It was felt that this removal of the crucible from the furnace introduced significant OH content changes from 5/4 (72 ppm OH) to 4/1 (110 ppm OH). Thus it was felt that the OH content of the rods might not be the same as in the bulk sample.

The alternative technique investigated was to cut rectangular beams (nominally 2 x 2mm cross-section and 50mm long) from the glass blocks. The glass beams were then polished by staff of Pilkington Brothers Latham Laboratories on all four major sides using the same technique as for infra-red spectroscopy samples (Chapter 4). After polishing the specimen cross-section dimension varied from 1.90mm to 2.30mm between specimens, however, the individual specimens were uniform to better than 40μm. For rectangular beams a new abrasion treatment was evolved with the aim of producing an artificial flaw size distribution which would dominate over the edge flaws present in beams. The new abrasion treatment consisted of sticking the specimens down onto a microscope slide using "Twinstick" a double sided adhesive strip. The microscope slide was in turn attached to the inside of a 500 gm glass jar containing 250 gms of dried 30 mesh silicon carbide and the jar was then rotated at a fixed rate for 3½ hours. For glass abraded in this way the failure stress obtained at room temperature was typically 55.4 ± 13 MPa. Comparable values were obtained for unabraided samples, indicating that failure was due to edge flaws caused by handling prior to abrasion. This was confirmed by optical observation of the fracture origin. Chandan et al (1978) overcame the problem of edge effects by bevelling of the edges. This was attempted, however the small size of the specimens made handling and bevelling difficult and there appeared to be no strength increase after bevelling.

The other method available to remove the edge flaws is by etching in hydroflouric acid. The strength of etched soda-lime-silica rods was extensively studied by Proctor (1962). The etching technique is

based on his work. Proctor reported that a 4% H.F. solution dissolved glass at the rate of 2-3 gm/cm^2/min and would not produce surface deposits which can retard the etching process. This etching rate would remove 30-45μm over a 40 min period. Fig.5.9 shows the specimen holder used by Proctor and in this study.

The etching technique adopted was to first wash 12-15 beams in acetone and then insert them into the holder which was placed into 250 ml of 4% by volume H.F. solution for 40 min. The beams were then removed from the acid solution washed in deionised water and dried using a hot air drier. The specimens were then abra ded using the previously described technique for rectangular beams. After etching specimens had a typical failure stress of 157.0 MPa at room temperature and after abrasion, 87 MPa. This indicates that the standard abrasion treatment now dominated strength rather than random edge flaws.

This then was the specimen preparation technique adopted, all specimens being first etched and then abraided. Specimens for test at 77K were placed under acetone immediately after abrasion (in order to minimise ageing effects) and then tested as quickly as possible afterwards at a crosshead speed of 3.33μm/sec. Specimens for testing under liquid nitrogen were measured at both ends with a micrometer to 0.01mm immediately prior to testing.

For the room temperature, 60% R.H. measurements, specimens were stored in an evacuated dessicator immediately after abrasion. All the specimens from the series 5 and 6 glasses were tested together over a period of 12 hours when the humidity was 60% ± 2%. During

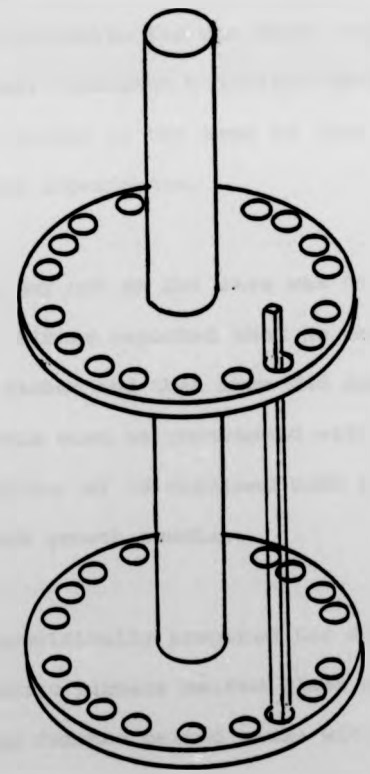

Fig. 5.9 Specimen Holder for Etching of Four Point Bend Specimens.

the testing samples were stored under acetone immediately prior to testing. The crosshead speed used was again 3.33μm sec^{-1}. The dimensions of the specimens were measured after failure and to an accuracy of 0.01mm.

5.3.3 Dynamic Fatigue

Dynamic fatigue studies seek to measure the variation in failure stress as a function of the rate of stress change. In the present work such studies were undertaken for one major reason, i.e. to observe whether the stress corrosion behaviour as defined by the n value obtained in such studies is the same as that obtained from the stage I slow crack growth experiments.

Evidence that this may not be the case was to be found in the work of Ritter (1969). Ritter reported that he observed a value of n equal to 13 for acid etched and then abraded specimens in dynamic fatigue experiments. This must be contrasted with the more typical values for soda-lime-silica of 16 obtained both by dynamic fatigue testing and in slow crack growth studies.

Two glasses were specifically prepared for dynamic fatigue studies. These were 7/1, an electric furnace melted glass with an OH content of 137 ppm and 7/2 a gas furnace melted glass with an OH content of 358 ppm. Specimens were prepared in the previously described manner, with four sets of 10-12 beams from each of the two glasses undergoing the sequence of etching and abrasion. Storage was again in an evacuated dessicator until all of the specimens had been prepared.

The abraded specimens were all tested in one 12 hour period at a relative humidity of 62%.

Four crosshead speeds were used. 0.333, 3.333, 3.33, 33.0 μm/sec giving a range of stressing rates from 0.140–137.0 MPa sec^{-1}. Each set of 10–12 specimens was divided up so that some specimens from each set could be tested at each of the stressing rates used.

5.4 HERTZIAN FRACTURE STUDIES

5.4.1 Introduction

The merits of Hertzian fracture studies were described earlier. Briefly these were twofold. Firstly, because of the small amount of material required to perform indentation studies it is possible to perform a greater number of tests than using conventional 4 point loading. Secondly because the stress field is inhomogeneous a wider range of defect depths would be observed and so the distribution of flaws could more satisfactorily be studied.

In performing Hertzian fracture studies, the fracture event, because it is a microscopic event, is less easily observed than in conventional testing. The restrictions therefore on testing conditions and testing technique are more severe and hence it was decided to carry out Hertzian fracture studies under conditions of room temperature and a relative humidity of 60% which is comparable to the conditions used for 4 point bend studies.

5.4.2 Experimental

The apparatus initially available for Hertzian fracture testing had previously been described by Chlebik, Adams and McMillan (1977). The apparatus had been originally designed for testing opaque materials and had used a transparent corundum indenter. However in carrying out preliminary studies it was observed that the corundum indenters themselves were damaged after approximately 150 indentations. Since it was felt that using a single indenter for all the tests was an important factor in minimising possible spurious effects, an indenter of an alternative material was sought.

Tungsten carbide spheres were obtained in a range of sizes and the test configuration was inverted such that a 4mm diameter sphere was now mounted on the moveable loading system and the specimen was stationary.

The Hertzian fracture testing apparatus in this "inverted" configuration is shown in Figure 5.10. The important parts of the test equipment are: the loading system, the indenter, the specimen and its mountings and the optical system for observing the fracture event.

The loading system consists of a piston and cylinder arrangement constructed of aluminium with the indenter held on a brass support plate above the central axis of the piston. Load is applied by introducing nitrogen under pressure to one side of the piston whilst

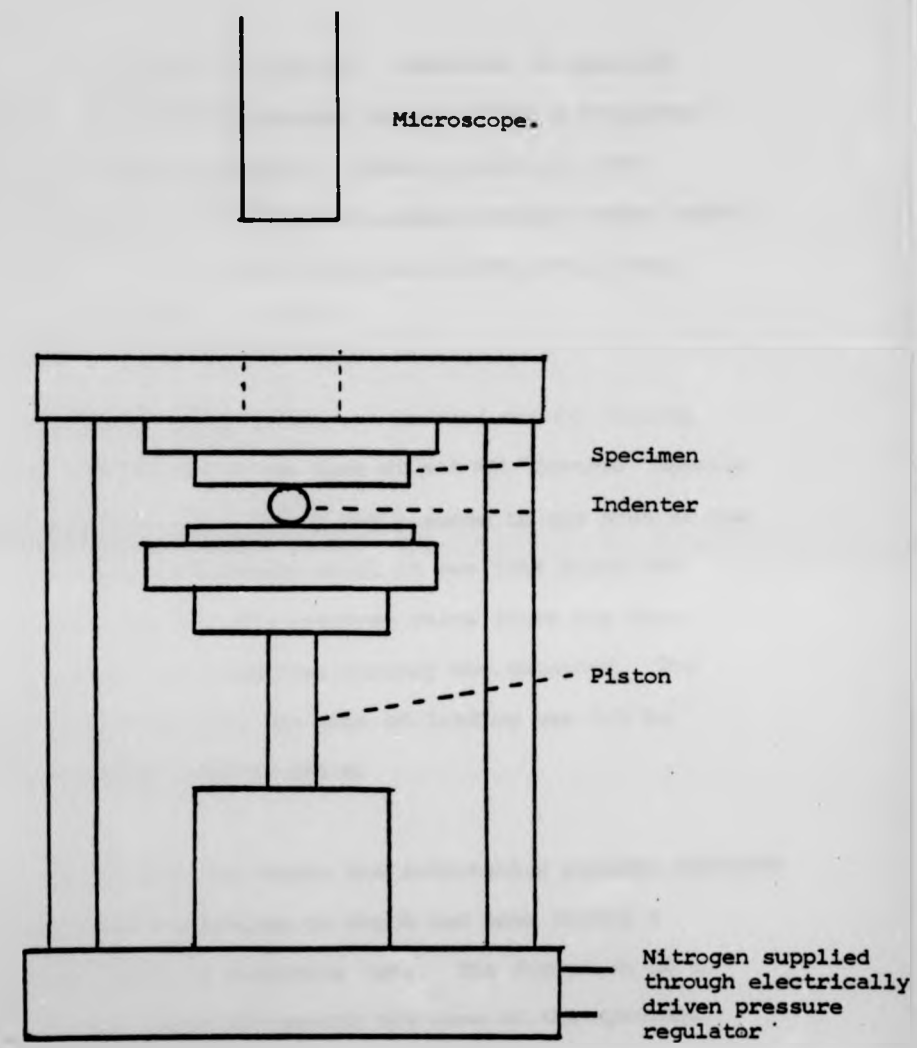

Fig. 5.10. Hertzian Fracture Test Apparatus.

the other side is at atmospheric pressure. Pressure is supplied from commercial gas cylinders containing nitrogen with a regulated outlet pressure of 0.345 MPa (50 psig). This pressure is then further regulated by means of a constant pressure relief valve, which is driven by a small electric motor which was fitted with a dial pressure gauge accurate to ± 0.003 MPa.

Calibration of the loading system was carried out by placing the entire loading assembly onto the base of a 5 KN "Instron" tensile testing machine. The load cell, which was mounted in the base of the crosshead, was then driven downwards until it was just above the loading piston. The motor for the pressure valve drive was then started, and a record of the load/time history was obtained. The load/time history indicated that the rate of loading was 2.9 Ns^{-1} and linear up to a maximum load of 450 N.

The optical system used to obtain the indentation process consists of a "Vickers" binocular microscope to which had been fitted a 10X vernier eyepiece and a 3X objective lens. The formation of a Hertzian ring crack was observed through the base of the specimen and through a piece of 6mm thick plate glass. The image observed was greatly improved by the application of a thin film of silicon grease between the plate glass and the base of the specimen. Calibration of the optical system was carried out by placing an electron microscope specimen-mounting grid between the indanter and the test specimen. The spacing between five grid wires was then measured using the vernier eyepiece. The spacing of the five grid wires was also measured using a travelling microscope with an accuracy of ± 0.01mm, giving

a theoretical precision of ± 0.00167mm per division of the vernier eyepiece. However, in observing a ring crack the diameter could not be accurately measured to better than ± 3 divisions on the vernier eyepiece.

Specimens for Hertzian fracture studies were initially prepared by cutting rectangular parallelepiped blocks, 50mm x 25mm x 8mm, from a large block. The two large surfaces were then polished to a 1 μm finish using the techniques previously described in Chapter 4. Prior to abrasion, specimens were stored in an evacuated dessicator. The technique used to abrade these specimens was very similar to that described for four point bend test specimens. The two differences in specimen preparation technique were: first, two specimens of different glasses were glued to opposite side of the jar and abraded simultaneously. The second difference in preparation technique was that the Hertzian fracture test specimens were not etched in hydroflouric acid because of the experimental difficulties introduced when etching was attempted.

Etching of some Hertzian fracture specimens was tried, however it introduced two experimental difficulties. Firstly the etching process degraded the optical finish of both surfaces of the specimen so making observation of the microscopic fracture event much more difficult. Secondly the etching process introduced pits which were significant in comparison to the indentation stress field, and resulted in the formation of crescent shaped cracks which are indicative of a misalignment between indenter and specimen surface.

Clearly the fact that it proved impossible to use the same abrasion process for Hertzian fracture and four point bend studies can lead to difficulties in the analysis of the results obtained and this point will be discussed in Chapter 8.

After abrasion the two specimens were removed from the glass jar and washed in acetone. The unabraded face of each specimen was then covered in a thin film of silicone grease and the specimens pressed by their edges onto the plate glass specimen support. Indentations were then performed on alternate specimens at the loading rate of 2.9 N^{s-1} and loading stopped the moment a fracture event was observed. The pressure at fracture and the diameter of the ring crack were then recorded. It should be noted however, that the fracture "event" was not always a perfect ring crack which then developed into a cone crack. Occasionally it was observed that the crack,once originated, would propagate down into the bulk of glass before slowly becoming a full circle in direct contradiction of the theories proposed by Langitan and Lawn (1969). This effect was observed on all the glasses tested and the frequency of occurrence of this type of event did not appear to have any systematic relationship to glass composition. In all, approximately 25-35 indentations were performed on each specimen. Care was taken to ensure that the test locations were at least 2mm apart which is over three times a typical diameter of contact, $\sim$ 0.5mm.

Humidity could not be controlled in the Hertzian fracture experiment because of the restrictions that atmospheric control

imposed on the specimen handling. However atmospheric humidity was measured using a horse-hair hygrometer and testing was only carried out when the atmospheric humidity was 62 ± 3% R.H. Because humidity could only be monitored rather than controlled two specimens from different glasses were tested over the same time period by performing indentations on alternative specimens.

In all, at least three specimens of each glass were tested resulting in a minimum of 60 indentation results for each glass. The method of analysis of the results and the results themselves will be reported in Chapter 7.

CHAPTER 6

OTHER EXPERIMENTAL STUDIES

6.1 INTRODUCTION

In this chapter the experimental studies other than the mechanical strength studies are described. A necessary part of the evaluation of Hertzian fracture strength is the definition of the stress field. In order to use the equations given by Johnson et al (1973) which describe the Hertzian stress field under no-slip and complete slip conditions it is necessary to know the elastic constants and the coefficient of static friction. In addition, experiments to examine the structural role of hydroxyl ions are described.

6.2 ELASTIC PROPERTIES STUDIES

The Young's modulus E, the shear modulus G, the bulk modulus K and Poisson's ratio ν are related by the equations:-

$$G = \frac{E}{2(1+\nu)} \qquad (6.2.1)$$

and $$K = \frac{E}{3(1-2\nu)} \qquad (6.2.2)$$

Thus it is only necessary to know any two constants in order to evaluate the other two.

The simplest of the three elastic moduli is clearly Young's modulus, which can be measured either under static or dynamic conditions. Dynamic and static measurements of Young's modulus can give different results because of the anelastic effects which can be significant under dynamic conditions. However, it is easier to obtain precise measurements using dynamic techniques.

Dynamic measurements are in general based on measuring the velocity of sound in a bar or uniform specimen of the glass of interest. The two techniques used are the pulse-echo technique and resonant frequency methods.

The pulse-echo technique relies upon introducing a pulse of ultrasound into a bar of material and measuring the time of flight for the pulse to travel the length of the specimen and echo back. Lynnworth (1973) has described this technique in detail and it has been used extensively by Manghnani (1972) and his co-workers. The pulse of ultrasound can of course be either a longitudinal or a transverse wave, thus allowing an evaluation of the Young's modulus or the shear modulus respectively.

The other method available for obtaining the dynamic elastic moduli is to observe the resonant frequency for a bar of known dimensions. The resonant frequency is a function of the specimen dimensions and

the velocity of sound, which depends on the elastic modulus for the type of stress wave introduced.

Pickett (1945) gives the solution for flexural vibration of a beam with free ends, by:

$$E = 0.078868(f_1^2 L^4 \rho/r^2)T_p \qquad (6.2.3)$$

where f_1 is the fundamental resonant frequency, L is specimen length, ρ is the density, $r = d/\sqrt{12}$ for a rectangular specimen where d is the depth of the beam and T_p is the Pickett correction factor for the effects of shear deformations and rotatory inertia and is given by:

$$T_p = 1 + 6.585(1+0.7528+0.8109\ \nu^2)\ (\frac{d}{L})^2 \qquad (6.2.4)$$

$$- 0.868\ (\frac{d}{L})^4 - \frac{8.340(1+0.2023\ \nu + 2.173\ \nu^3)\ (\frac{d}{L})^4}{1 + 6.338(1+0.14081\ \nu + 1.536\ \nu^2)(d/L)^2}$$

In addition Spinner and Teft (1961) have shown that for torsional vibrations

$$G = \rho\ (2\ L\ f_1)^2\ R \qquad (6.2.5)$$

where R is given by

$$R = R_o\ (1 + (\frac{d}{L})^3)\ 0.01903 \qquad (6.2.6)$$

and R_o is

$$R_o = \frac{1 + (d/a^2}{4\text{-}2.521\ a/d\ (1 - \exp\ (1.991/[(\pi d/a)+1]))} \qquad (6.2.7)$$

with a being the specimen width.

The resonant bar technique is one of the experiments performed in the undergraduate laboratories in the Physics department, and the apparatus used there formed the basis of the equipment used in this study. The apparatus used is shown in Figure 6.1 and consisted of two ceramic gramaphone cartridges which acted as driver and receiver. The cartridges were mounted on counterbalanced arms so as to minimise any possible interaction. The signal generator provided an A.C. signal of approximately 10V. The maximum output voltage was obtained by passing the receiver signal through a high gain amplifier and then measuring the R.M.S. output voltage using a digital voltage meter. The frequency at which this maximum voltage was attained was recorded using the frequency meter (accurate to 0.1Hz). Specimens were rectangular beams measuring approximately 1mm in square section and 100mm long and were measured using a travelling microscope and micrometer gauge. The specimen beams were supported by thin wires at the node positions for the fundamental frequencies which were typically 1.8KHz for bending and 18kHz for torsion. Only the fundamental frequencies were measured and at least three specimens for each

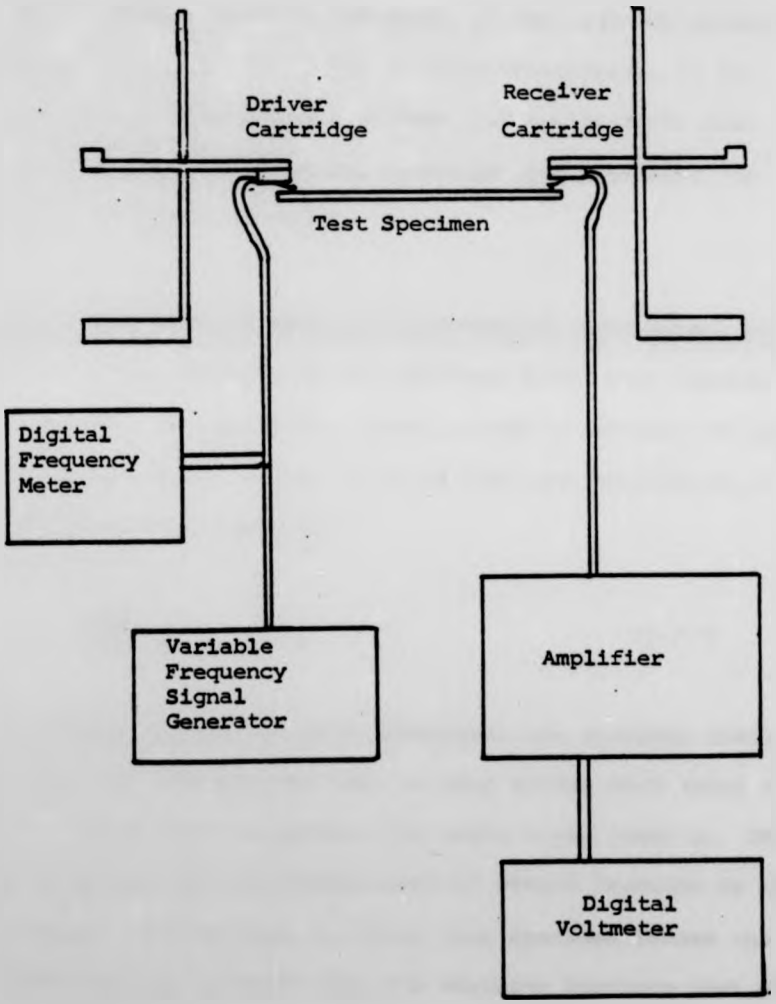

Fig. 6.1 Schematic Diagram of Apparatus For Elastic Moduli Measurement.

glass were investigated. The results obtained are given in Chapter 7.

6.3 COEFFICIENT OF STATIC FRICTION MEASUREMENTS

The other parameter which is required, if the modified stress field proposed by Johnson et al (1973) is to be considered, is the coeffient of static friction. Studman and Field (1973) have described a simple and efficient technique for measuring the coefficient of static friction.

The method they proposed used the experimental arrangement shown in figure 6.2. This consists of the specimen under test forming the inclined plate. The hinge at A being a stop to prevent the upper plate slipping there. It can be shown that the coefficient of static friction μ is again by

$$\mu = \frac{\sin \alpha}{1+\cos \alpha} \qquad (6.3.1)$$

Thus, by simply pushing the ball underneath the specimen until slip occurs, and then allowing the ball to slip slowly back until it sticks, it is possible to measure the angle α and hence μ. This technique was used for the measurement of static friction in the current study. The Hertzian fracture test specimen formed the upper plate and the indenter from the Hertzian fracture test was the sphere. The lower plate was a piece of abraded "float" glass,

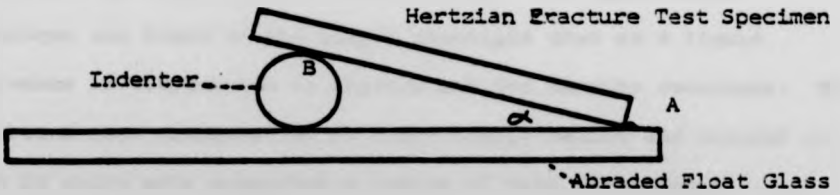

Fig. 6.2 Apparatus for coefficient of static Friction Measurement.

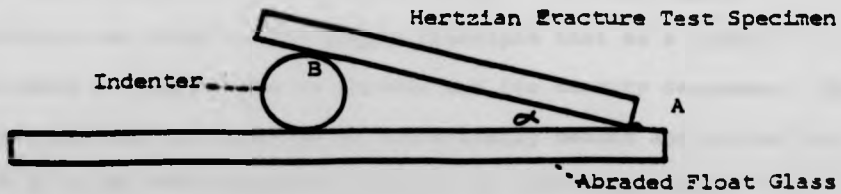

Fig. 6.2 Apparatus for coefficient of static Friction Measurement.

abraded to ensure that slip occurred at B. The angle α was measured by the use of a two way travelling microscope which allowed the accurate measurement (±0.02mm) of the positions A and B in figure 6.2. At least three measurements were taken from each specimen and three specimens of each glass were tested. The results obtained are given in Chapter 7.

6.4 DENSITY MEASUREMENTS

The density of a glass is a useful quantity becuase by combining it with the molecular formula it is possible to obtain the molar volume and hence gain an insight as to the openness of the silica network.

In the present study density measurements were carried out on glasses of series four using a Preston densitometer available at Pilkington Brothers, Lathom Laboratories. The experimental technique was based on the simple principle that as a liquid increases in temperature it expands and its density decreases. The apparatus used consisted of an electrically heated and stirred oil bath in which were supported a number of test tubes and a thermometer accurate to 0.01°C. The test tube was filled with 1.1.2.2 tetra-bromo-ethane which has a density of approximately 2.49g cm^{-3} and a temperature coefficient of density of 0.00195 g cm^{-3} $°C^{-1}$. Two pieces of glass were placed into a test tube, one piece being a sample of a reference glass ie. glass 4/3 and the other piece being the test sample. The temperature of the oil bath

abraded to ensure that slip occurred at B. The angle α was measured by the use of a two way travelling microscope which allowed the accurate measurement (±0.02mm) of the positions A and B in figure 6.2. At least three measurements were taken from each specimen and three specimens of each glass were tested. The results obtained are given in Chapter 7.

6.4 DENSITY MEASUREMENTS

The density of a glass is a useful quantity becuase by combining it with the molecular formula it is possible to obtain the molar volume and hence gain an insight as to the openness of the silica network.

In the present study density measurements were carried out on glasses of series four using a Preston densitometer available at Pilkington Brothers, Lathom Laboratories. The experimental technique was based on the simple principle that as a liquid increases in temperature it expands and its density decreases. The apparatus used consisted of an electrically heated and stirred oil bath in which were supported a number of test tubes and a thermometer accurate to 0.01°C. The test tube was filled with 1.1.2.2 tetra-bromo-ethane which has a density of approximately 2.49g cm^{-3} and a temperature coefficient of density of 0.00195 g cm^{-3} $°C^{-1}$. Two pieces of glass were placed into a test tube, one piece being a sample of a reference glass ie. glass 4/3 and the other piece being the test sample. The temperature of the oil bath

was then slowly increased until the two samples just sank and the temperatures at which they passed a graduated mark was recorded. At least three measurements were made for each glass using different samples of material and then the density of a large piece of glass 4/3 was evaluated using standard volumetric methods. The results obtained from these measurements are given in Chapter 7.

6.5 VISCOSITY STUDIES

It was described in Section 3.5 how the viscosity of glass is known to be influenced by the presence of hydroxyl ions. The effect observed is much greater than could be predicted from a depolymerisation of the silica network, and whilst viscous flow and mechanical strength are not strictly analogous properties, they are both associated with the breaking of bonds in the silica network. Thus, the extent to which the hydroxyl ion content of the glasses used in the current study influences their viscous flow behaviour is clearly of interest.

Low temperature viscosity measurements in the range 10^{10} - 10^{13} poise were conducted using the fibre extension method. The apparatus used is shown schematically in figure 6.3. It consisted of a vertical tube furnace with a long uniform temperature zone in which was contained a fibre of the glass under study, and to which were attached weights by the hook coming from the linear voltage differential transducer (LVDT), the weight of the LVDT internals and lower attachments being included. The LVDT had a sensitivity

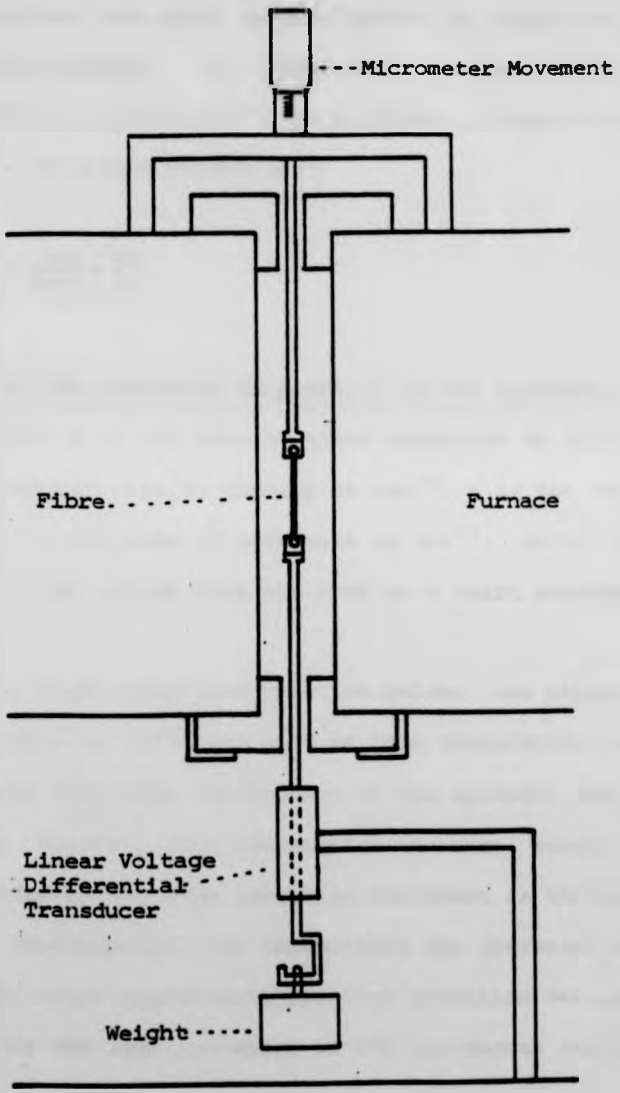

Fig. 6.3 Schematic Diagram of Fibre Extension Viscosity Measurement Apparatus.

of 0.417 mV per μm and was calibrated after every test by the use of the micrometer at the top of the furnace. The temperature of the furnace was measured to ± .1°C using a Chromel/Alumel thermocouple. The specimens used were fibres ~1mm diameter and 80mm long with two small spheres formed at either end for attachment purposes. The fibres were measured using a micrometer and travelling microscope. The equation governing viscous flow in the fibre extension method is:-

$$\nu = \frac{Lmg}{3\pi r^2} \Big/ \frac{dL}{dt} \qquad (6.5.1)$$

where ν is the viscosity in poise, L is the specimen length in centimetres, m is the mass in grams supported by the fibre, g is the acceleration due to gravity in cms^{-2}, r is the fibre radius, and dL/dt is the rate of extension in cms^{-1}. dL/dt was measured by displaying the output from the LVDT on a chart recorder.

The fibre, after insertion into its holder, was rapidly brought to a temperature of 500°C and held at this temperature for 15 minutes. During this time some contraction of the specimen was generally observed. However, this contraction was small because the fibres had experienced the same annealing treatment as the bulk glass blocks. Subsequently, the temperature was increased in 10°C increments until appreciable positive extension was observed; the temperature was then increased in 5°C increments and the applied

load adjusted to give an extension rate typically in the range 1 x 10^{-5} to 5 x 10^{-4} cms^{-1}.

In total two fibres of each of the series four glasses were tested and the results obtained for these glasses are given in Chapter 7.

6.6 CONDUCTIVITY MEASUREMENTS

It was described in Chapters 2 and 3 that the alkali ions present in a glass influence the crack tip pH. The mobility of these ions is of relevance to any discussion of their influence on the subcritical crack growth behaviour present in glass. The ionic motion observed in a sodium silicate under the action of a stress gradient has been studied by Weber and Goldstein (1964), who observed that the alkali ions moved so as to reduce the applied strain. Studies of ionic motion in glasses have in general been undertaken by the application of an electric rather than a stress field and observed as conductivity measurements. Doremus (1973) has provided a simple derivation of the Einstein equation which equates the electrical conductivity to the concentration and diffusion coefficient of the conducting species, thus:-

$$\sigma = \frac{Z^2 F^2 D C}{RT} \qquad (6.6.1)$$

where Z is the ionic charge, F is the Faraday, D is the diffusion coefficient, C is the concentration of the diffusing species and R

and T are the gas constant and temperature respectively. Equation 6.6.1 is often not followed exactly, and the right hand side of the equation must be multiplied by a factor which can vary between .74 and .25 for sodium silicates. Doremus (1964) has, however, reported that equation 6.6.1 is obeyed exactly for a commercial soda-lime-silicate.

Electrical conductivity measurements can be undertaken either under D.C. or A.C. conditions. Both techniques have their advantages and disadvantages, however D.C. conductivity measurements are generally simpler to interpret because there is no frequency dependance, and were accordingly chosen for this study.

Blumenthal and Seitz (1974) have reviewed extensively the techniques for A.C. and D.C. conductivity measurements. In the current study, the three probe configuration described by Blumenthal and Seitz has been used and is shown in Figure 6.4 (a), (b). The specimens used were glass plates 1mm thick and 30mm square which had been polished to a 1μm finish, and subsequently measured using a travelling microscope and micrometer. Gold electrodes were used and were provided by means of argon gas sputtering. Care was taken to ensure a uniform electrode production by wiping the surface with methylated spirits and a lens cleaning tissue prior to sputtering and then applying a constant 10mA current for two minutes. Contacts were attached to the gold electrodes by means of silver paint. The electrode configuration shown in Figure 6.4 was necessary in order to minimise the effects of surface conduction. For this experimental configuration

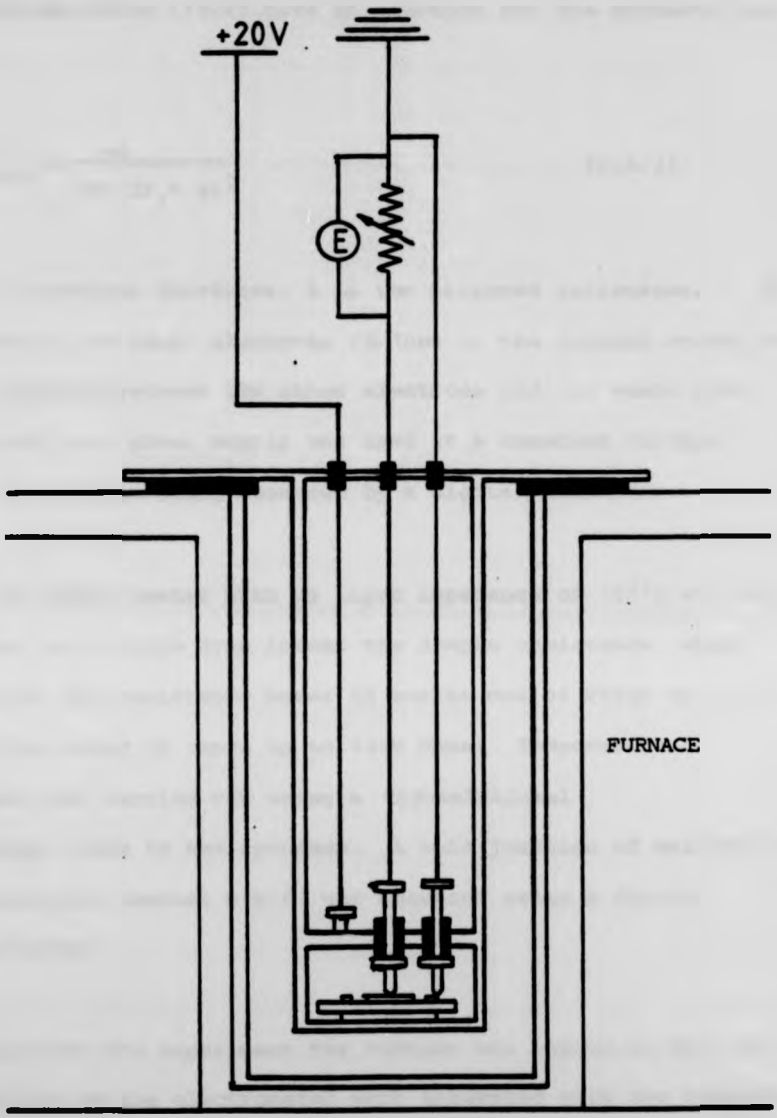

Fig. 6.4a Schematic Diagram of Apparatus for D.C. Conductivity Measurements.

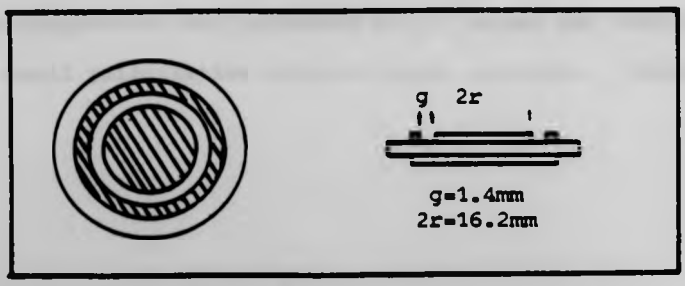

Fig. 6.4b Details of Electrode Configuration.

Blumenthal and Seitz (1974) give an equation for the conductivity of

$$\sigma_{bulk} = \frac{4d}{R\pi\,(2r_1 + g)^2} \qquad (6.6.2)$$

where d is specimen thickness, R is the measured resistance, r_1 is the radius of the inner electrode (8.10mm in the current study) and g is the spacing between the inner electrode and the guard ring. A stabilised D.C. power supply was used as a constant voltage source, the voltage being measured by a digital voltmeter.

An electrometer with an input impedance of $10^{11}\Omega$ was used to measure the voltage drop across the sample resistance, which consisted of two resistance boxes in series one of range up to 10k ohms and the other of range up to 100k ohms. Temperature measurement was carried out using a Chromel/Alumel thermocouple close to the specimen. A cold junction of melting ice was used and the thermal e.m.f. was measured using a digital millivolt meter.

In carrying out the experiment the furnace was heated to 50°C and then readings on the electrometer were attempted with the variable resistance set to 110k ohms. The temperature was then increased in 10°C steps until a reliable voltage reading was obtained at which point the temperature was increased in 5°C steps and measurements recorded until polarisation effects became apparent. Polarisation

effects were minimised by only applying the voltage for the minimum time required. In contrast, at low temperature it was observed that a short time delay of 5 to 10 secs occurred before the maximum current was attained. In order to minimise the diffusion of the gold electrodes into the specimen, the test procedure was carried out as rapidly as possible. In total two specimens for each of the four series glasses were tested. The results obtained are given in Chapter 7.

6.7 HARDNESS MEASUREMENTS

Although the technique of indentation fracture mechanics was considered not sufficiently proven experimentally as a means of measuring fracture toughness, it was considered useful to perform some simple hardness measurements which could give a qualitative insight into the abrasion process.

Accordingly, hardness measurements were carried out using facilities generously provided by Lanchester Polytechnic. The hardness tester was a Vickers microscope fitted with a Vickers microhardness attachment. This attachment consisted of a special 20X lens to which had been fixed the diamond indenter, and by means of a pneumatic system could apply a prescribed load to the indenter. The pressure setting and activation of the pneumatic system was attained by means of an external accumulator. The indentation diagonals were measured by means of vernier eyepiece,

calibrated so that Vickers hardness could be obtained by reference to standard tables.

The specimens, used were polished untested Hertzian fracture specimens on which were performed 10 indentations at a 50gm load applied for 20 seconds. 50 gm was observed to be the maximum load which could be sustained without any cracking occurring. The results obtained from these measurements are given in the subsequent chapter.

CHAPTER 7

RESULTS

7.1 INTRODUCTION

This chapter describes the results obtained in the current study. These results can be classified into mechanical strength results, i.e. those based on the experiments in Chapter 4, and those based on the experiments in Chapter 5, i.e. non-mechanical strength studies. These results were preliminarily reported in the Journal of Non-Crystalline Solids (See Appendix 1).

As described in Chapter 2, the mechanical strength characteristics exhibited by glass have been quantified within a quasi-continuum model. In order to make meaningful comparisons between glasses of different compositions, it is advantageous to examine the results obtained in the current study within the context of the model described in Chapter 2.

7.2 FRACTURE MECHANICS STUDIES RESULTS

The fracture mechanics studies described in Chapter 5 were studies which examined slow crack growth as a function of stress intensity K_I at two humidities 60% and 1% relative humidity. Experiments were performed on those glasses 4/1, 4/3, and 4/5 which had

hydroxyl ion contents of 110, 356 and 763 ppm respectively. The results obtained are shown in Figure 7.1. The characteristic three stages of subcritical crack growth were observed in all three glasses at 1% relative humidity. At 60% relative humidity only the stage I behaviour was investigated because of the large amount of material required to investigate stages II and III at high humidities. The two parameters which may be evaluated from these results are K_{IC}, the critical stress intensity factor, and secondly the stress corrosion parameters.

Considering the critical stress intensity factor K_{IC}, this is difficult to define explicitly for glasses which exhibit subcritical crack growth, even under vacuum conditions. In the present study it is proposed to define K_{IC} as that value of stress intensity factor K_I which results in a crack velocity of $10^{-2} ms^{-1}$. Because of the extreme gradient of the stage III subcritical growth behaviour it is expected that such a definition will introduce an error of less than 1% in K_{IC}. Stage III behaviour at 1% relative humidity was defined as that crack growth which occurs at velocities greater than 3×10^{-5} ms^{-1}, and a least squares fit was carried to K_I against $\log_{10}$ velocity. The results of this analysis are presented in Table 7.1. K_I as a function of $\log_{10}$ velocity was used, rather than $\log_{10}$ velocity as a function of K_I, because the minimisation of the sum of the squares of the difference between the predicted and experimental values of the dependant variable is difficult to achieve, when the dependant variable is very strongly dependant on the independent variable.

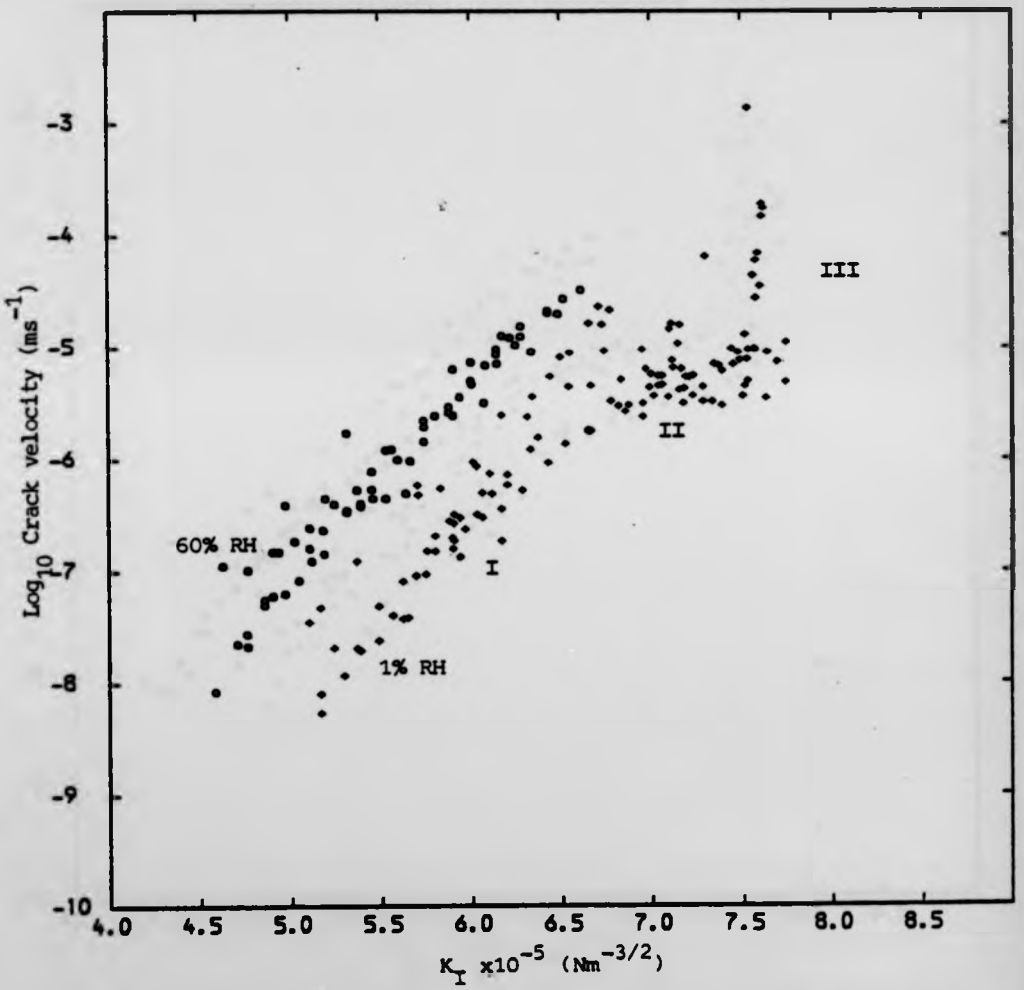

Fig 7.1(a) Fracture mechanics results for glass 4/1 (110ppm OH^- content)

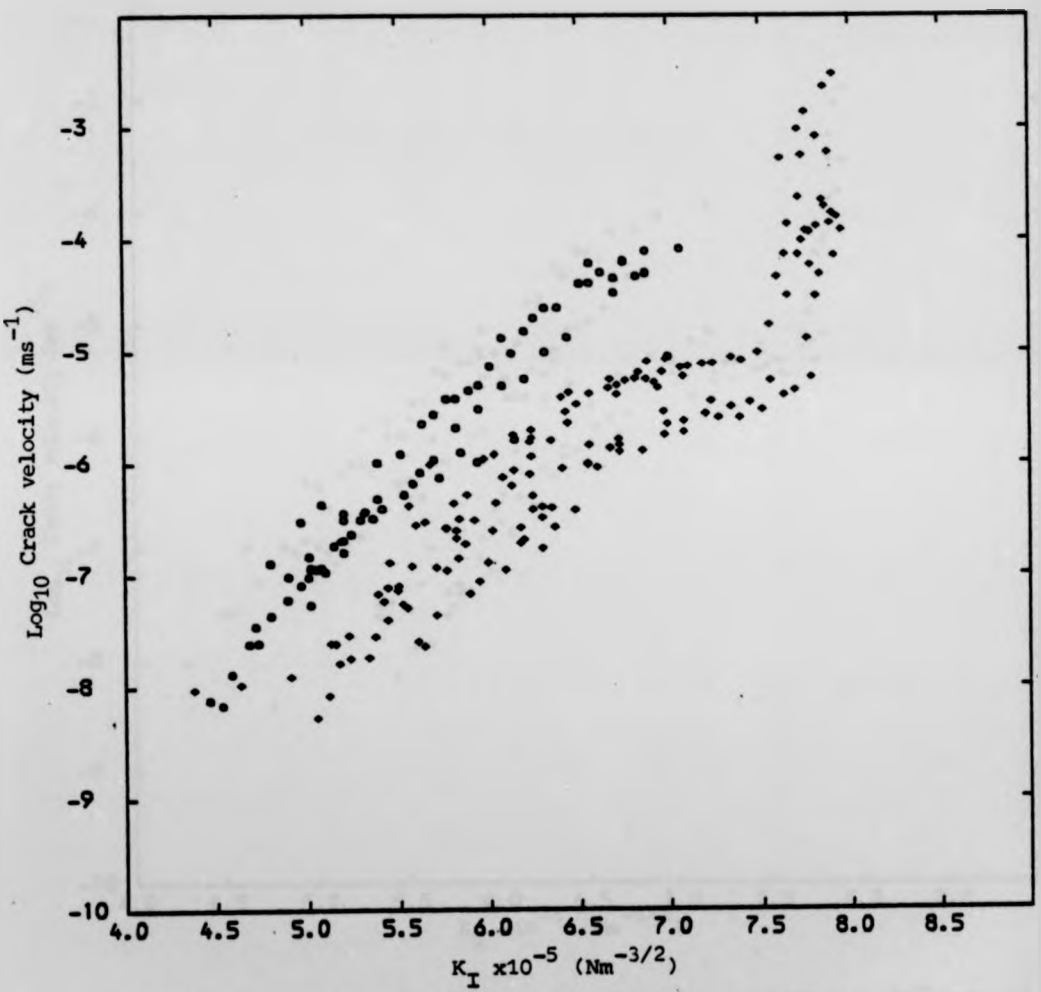

Fig 7.1(b) Fracture mechanics results for glass 4/3 (356ppm OH^- content)

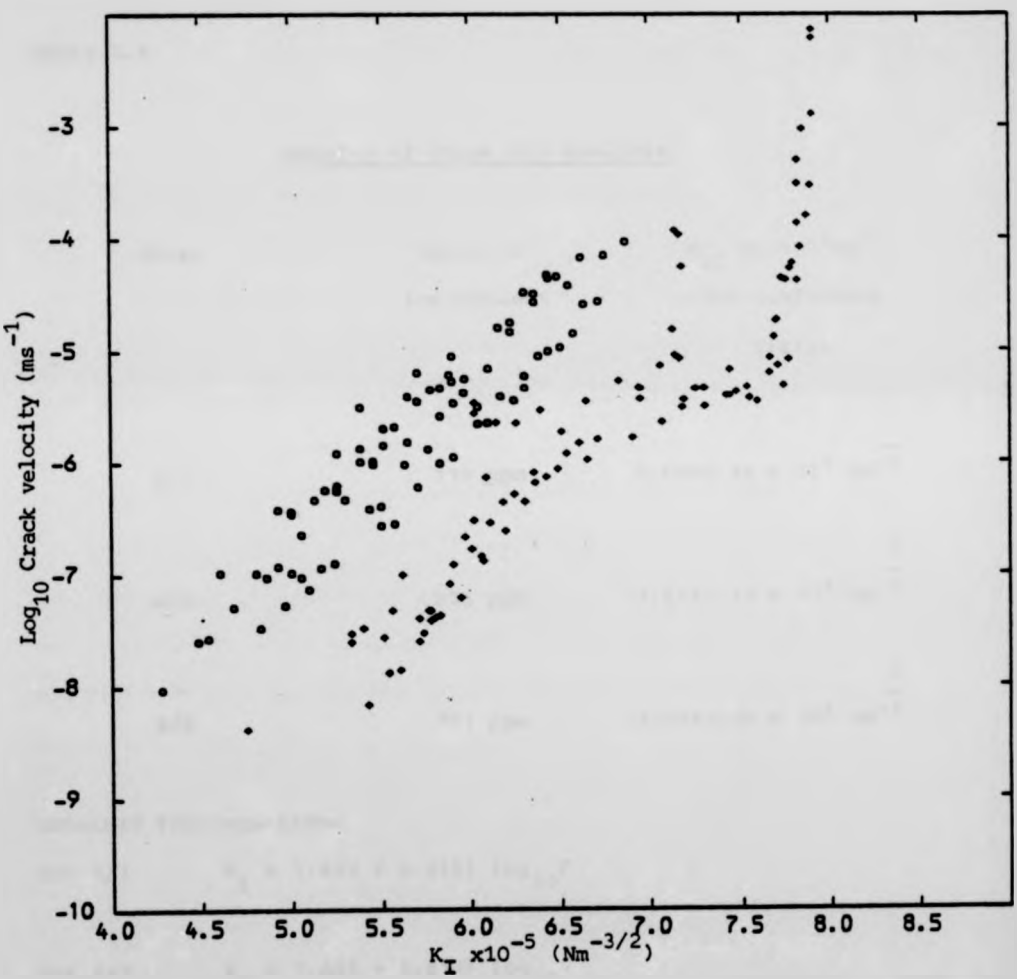

Fig 7.1(c) Fracture mechanics results for glass 4/5(763ppm OH^- content)

The values of K_{IC} obtained are in general agreement with the work of Frieman (1974) who examined crack growth in commercial soda-lime-silicate glasses under a variety of environments, using the constant moment technique.

Table 7.1

Results of Stage III Analysis

Glass	Hydroxyl ion content	K_{IC} at $10^{-2}ms^{-1}$ ±95% confidence limits
4/1	110 ppm	$7.59\pm0.34 \times 10^5$ $Nm^{-\frac{3}{2}}$
4/3	356 ppm	$7.81\pm0.14 \times 10^5$ $Nm^{-\frac{3}{2}}$
4/5	763 ppm	$7.93\pm0.05 \times 10^5$ $Nm^{-\frac{3}{2}}$

obtained from equations

for 4/1 $K_I = 7.629 + 0.0193 \log_{10} V$

for 4/3 $K_I = 7.835 + 0.0137 \log_{10} V$

and for 4/5 $K_I = 8.054 + 0.0605 \log_{10} V$

These results indicate that as hydroxyl ion content increases there is an increase in critical stress intensity factor of 4.5%.

It was described in Chapter 2 that the equation most commonly fitted to crack velocity/stress intensity data is

$$V = AK_I^n \qquad (7.2.1)$$

where A and n are empirical parameters. Wiederhorn (1977) considered the various equations available for fitting to crack growth/stress results, and reported that equation 7.2.1 provided the best fit to the observed data for soda-lime-silica glass. One difficulty that arises in carrying out the fitting process by the method of least squares in a log-log space is that this produces an error structure which is not normally distributed. However, for the case when the range of the dependant variable K_I is small, then the inaccuracy introduced is not severe. The least squares fitting was carried out using routines available in the NAG (Numerical Algorithm Group) library and the results obtained are given in Table 7.2.

Table 7.2 Results of Stage I Slow Crack Growth Analysis for 60% Relative Humidity.

OH^- Content	$\log_{10}A$	n
110	-122.3	20.2±0.6
356	-119.7	19.8±0.8
763	-105.4	17.3±0.8

The three curves obtained from this analysis are shown in Figure 7.2. From Figure 7.2, it can be seen that the results obtained do not show a wide variation in subcritical crack growth characteristics, and it was considered necessary to carry out further statistical tests to assess the significance of these results.

The approach chosen to examine the statistical significance of the apparent variations in the stress corrosion parameters was the dummy variable analysis as described by Draper and Smith (1966).

Considering two sets of experimental observations Y_{1i}, X_{1i} and Y_{2j}, X_{2j} of N_1 and N_2 experimental observations respectively, and which can be fitted independently to an equation of the form,

$$Y = AX + B \qquad (7.2.2)$$

then in order to test whether there is any statistical significance between the two sets of results, two dummy variables are introduced. These two dummy variables D_1 and D_2 form part of a multiple linear regression to the equation

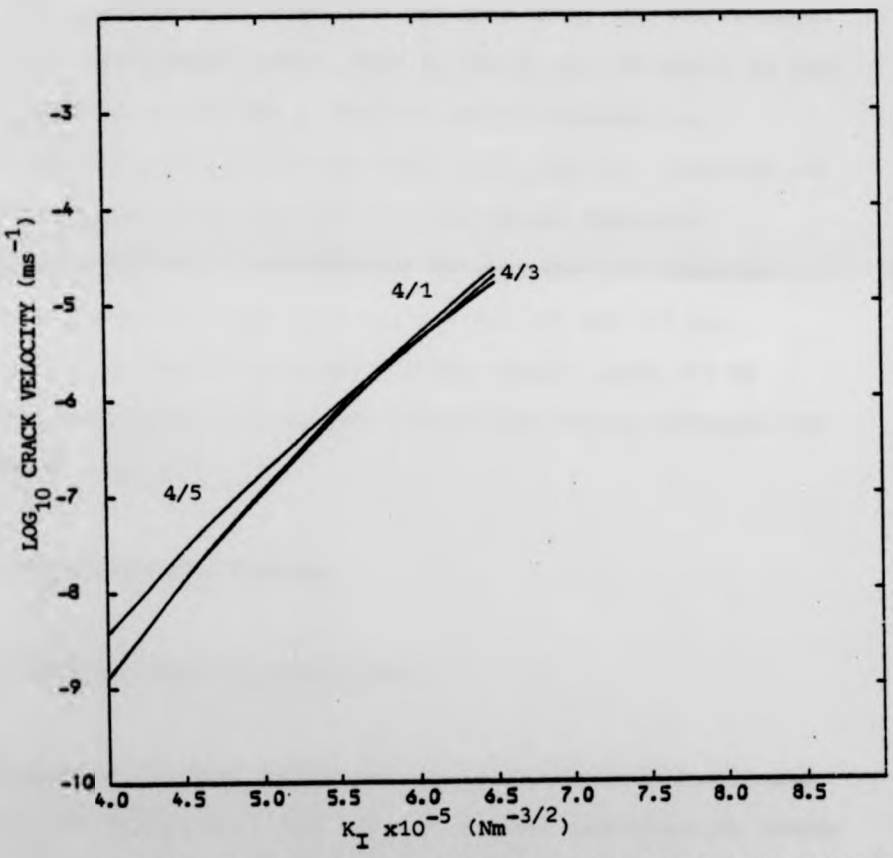

Fig 7.2 Results of Least Squares Fit to Stage I Subcritical Crack Growth at 60% R.H.

$$Y = AX + A_D D_1 + B + B_D D_2 \qquad (7.2.3)$$

for the combined data set $N_1 + N_2$. For the combined data set D_1 and D_2 are given values such that for Y_i, X_i for $i \leqslant N_1$, $D_{1i} = 0$ and $D_{2i} = 0$. Whilst for $N_1 + 1 \leqslant i \geqslant N_1 + N_2$, $D_{1i} = X_i$ and $D_{2i} = 1$

In order to satisfy the null hypothesis that there is no significant difference betwen the two data sets, the coefficients A_D and B_D should equal zero. When A_D and B_D are not equal to zero it is possible to use the student-t test to evaluate the statistical significance of variation in A_D and B_D. Carrying out such an analysis using the T.S.P. (Time Series Processor) statistical package it was possible to show that the observed variations between glasses 4/1 and 4/5 and 4/3 and 4/5 are significant at the 90% confidence level, whilst there was no observed statistical significance betwen the results obtained for glasses 4/1 and 4/3.

7.3 FOUR-POINT BEND STUDIES

7.3.1 Studies Under Liquid Nitrogen

The results of the four point bend studies under liquid nitrogen are shown in Figure 7.3, where it can be seen that there is little evidence of any significant variation with hydroxyl ion content. In assessing such an apparent lack of variation two possibilities exist. Firstly, it is possible that there is no significant

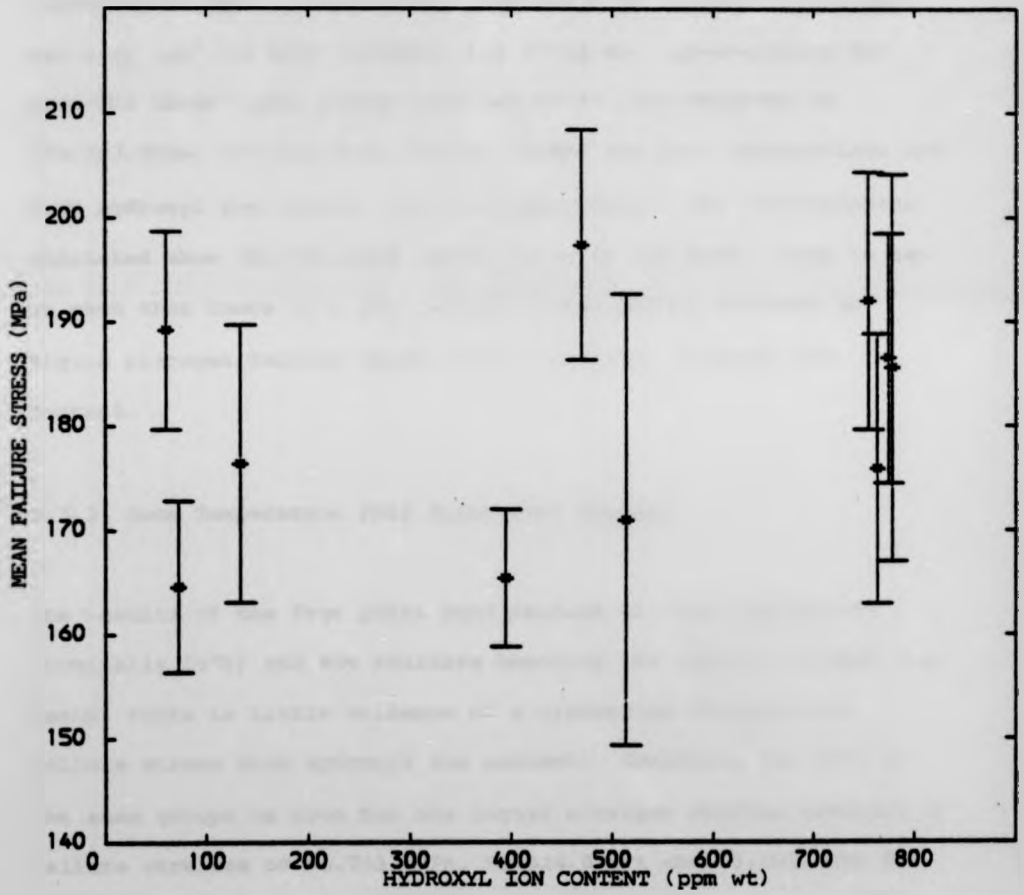

Fig 7.3 Results of four point bend studies at liquid N_2 temperature

variation to be observed, and secondly that the random variation in the data is so great that for the number of samples tested no effect may be observed. In this study, the difficulty of producing the glasses reproducibly, has severely limited the number of specimens that could be prepared. In order to overcome this limitation the data was ordered into three groups of low (OH^- content $\leq$ 250 ppm), intermediate (250 ppm < OH^- content $\geq$ 500 ppm) and high (OH^- content) hydroxyl ion contents. Re-analysing the data for these three groups resulted in failure stresses of 176.7±7.9MPa, 177.2±9.8MPa, 186.9±8.7MPa for the low, intermediate and high hydroxyl ion content groups respectively. The uncertainties indicated show the 95% confidence limits on the mean. Thus it can be seen that there is a statistically significant increase in liquid nitrogen failure stress with increasing hydroxyl ion content.

7.3.2 Room Temperature Four Point Bend Studies

The results of the four point bend studies at room temperature (nominally 20°C) and 60% relative humidity are shown in Figure 7.4. Again, there is little evidence of a systematic variation of failure stress with hydroxyl ion content. Combining the data in the same groups as used for the liquid nitrogen studies resulted in failure stresses of 95.7±3.4MPa, 93.6±4.07MPa and 95.0±2.8MPa for the low, intermediate and high hydroxyl ion contents groups respectively. Thus there appears to be no statically significant variation in failure stress at room temperature with increasing

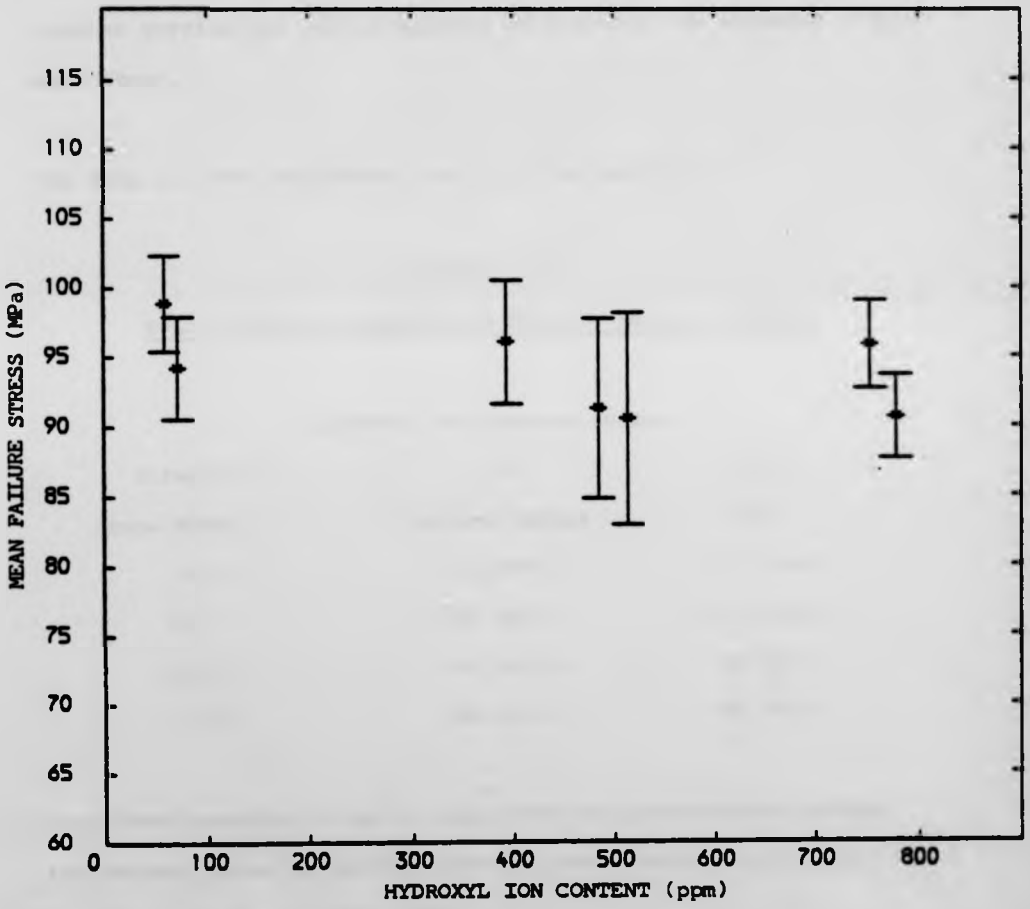

Fig 7.4 Results of four point bend studies at room temperature

hydroxyl ion content, however, the results suggest that a minimum in failure stress at intermediate hydroxyl ion content, may exist.

7.3.3 Dynamic Fatigue Studies

Figures 7.5(a) and (b) show the results of the dynamic fatigue studies carried out on two glasses of hydroxyl ion contents 137ppm and 358ppm.

The mean and 95% confidence limits on the mean are:-

Table 7.3

Mean Failure Stresses from Dynamic Fatigue Studies

	Hydroxyl ion content in ppm	
Stressing rate $MPas^{-1}$	110 Failure Stress MPa	358 MPa
14 3,	118.6±17.1	115.1±6.8
14.2	104.3±9.7	111.3±8.3
1.44	100.1±11.5	96.7±5.0
0.149	90.2±10.1	88.0±6.7

From these results it can be seen that the intermediate hydroxyl ion content glass in general gives a lower failure stress than the low hydroxyl ion content glass.

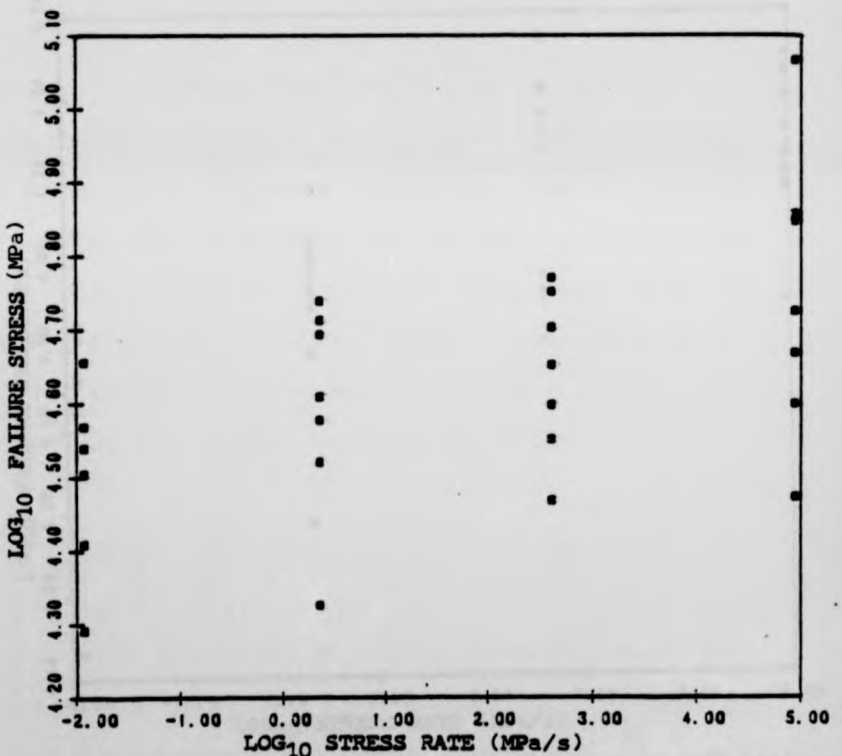

Fig. 7.5(a) Dynamic Fatigue Results for Glass 7/1 (138ppm OH^-).

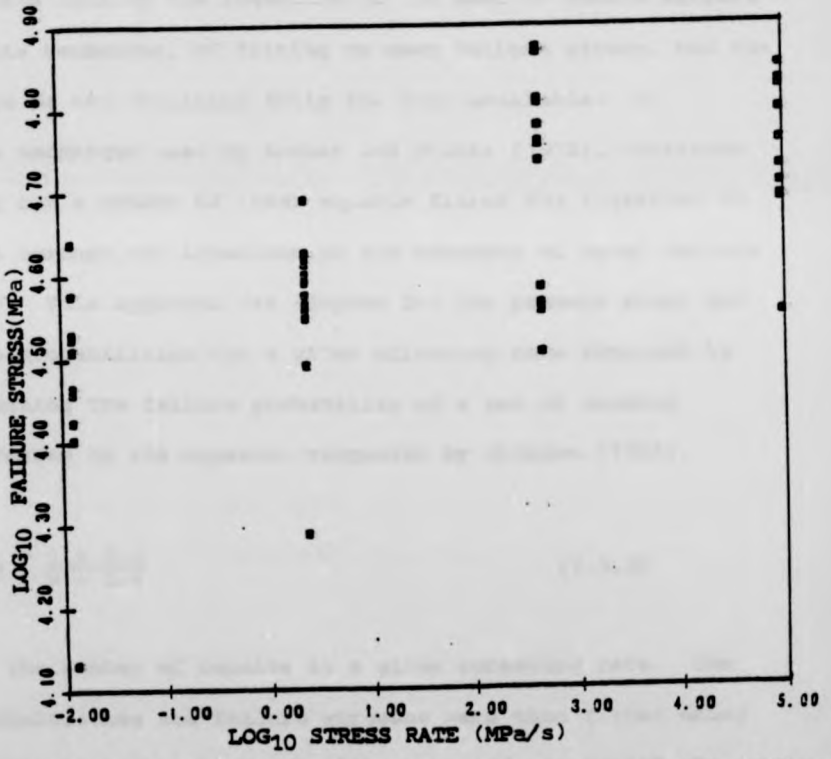

Fig. 7.5(b) Dynamic Fatique Results for Glass 7/2 (358ppm OH^-)

As was described in Chapter 2, dynamic fatigue data is usually analysed by fitting the data to an equation of the form:-

$$\log \sigma = \log \sigma_o + \frac{1}{n+1} \log \left(\frac{\dot{\sigma}}{\dot{\sigma}_o}\right) \qquad (7.3.1)$$

where σ is the failure stress at stressing rate $\dot{\sigma}$, and σ_o is the failure stress at the stressing rate $\dot{\sigma}_o$. In carrying out such an analysis, a least squares fit is performed of the logarithm of the stressing rate against the logarithm of the mean or median failure stress. This technique, of fitting to mean failure stress, has the disadvantage of not utilising fully the data available. An alternative technique used by Rockar and Pletka (1978), consisted of carrying out a number of least squares fits of the logarithm of stress rate against the logarithm of the stresses of equal failure probability. This approach was adopted for the present study and the failure probabilities for a given stressing rate obtained by first evaluating the failure probability of a set of ordered failure stresses by the equation suggested by Johnson (1964).

$$P(\sigma)_j = \frac{j - 0.3}{N + 0.4} \qquad (7.3.2)$$

where N is the number of results at a given stressing rate. The failure probabilities and failure stresses were then fitted using the least squares technique to the linear transformation of the Weibull distribution function.

$$\log \log \frac{1}{P(\sigma)-1} = \log C + m \log \sigma \qquad (7.3.3)$$

where C and m are constants. Having evaluated the stress for a given failure probability the least squares fit to stressing rate for failure probabilities of 40%, 50%, 65% and 75% can be obtained. The gradients of the series of linear equations were then averaged by weighting them in proportion to the reciprocal of their variance. The results of this analysis were:-

For glass 7/1 (137ppm OH^- content) n = 24.05±10.6
and for glass 7/2 (358ppm OH^- content) n = 22.27±12.0

The significance of these results, in the light of macroscopic subcritical crack growth studies will be discussed in Chapter 8.

7.4 HERTZIAN FRACTURE STUDIES

The parameters of the Hertzian fracture data obtained in the current study consisted of the loads at which the ring cracks occur and the diameters of the cracks. The mean failure loads with 95% confidence limits on the mean are shown in Figure 7.6 as a function of hydroxyl ion content. These results indicate a minimum in failure load at intermediate hydroxyl ion contents. Although the failure load gives a good indication of the fracture behaviour of a material, the mean failure load cannot readily be incorporated into the continuum model of mechanical strength, which can more

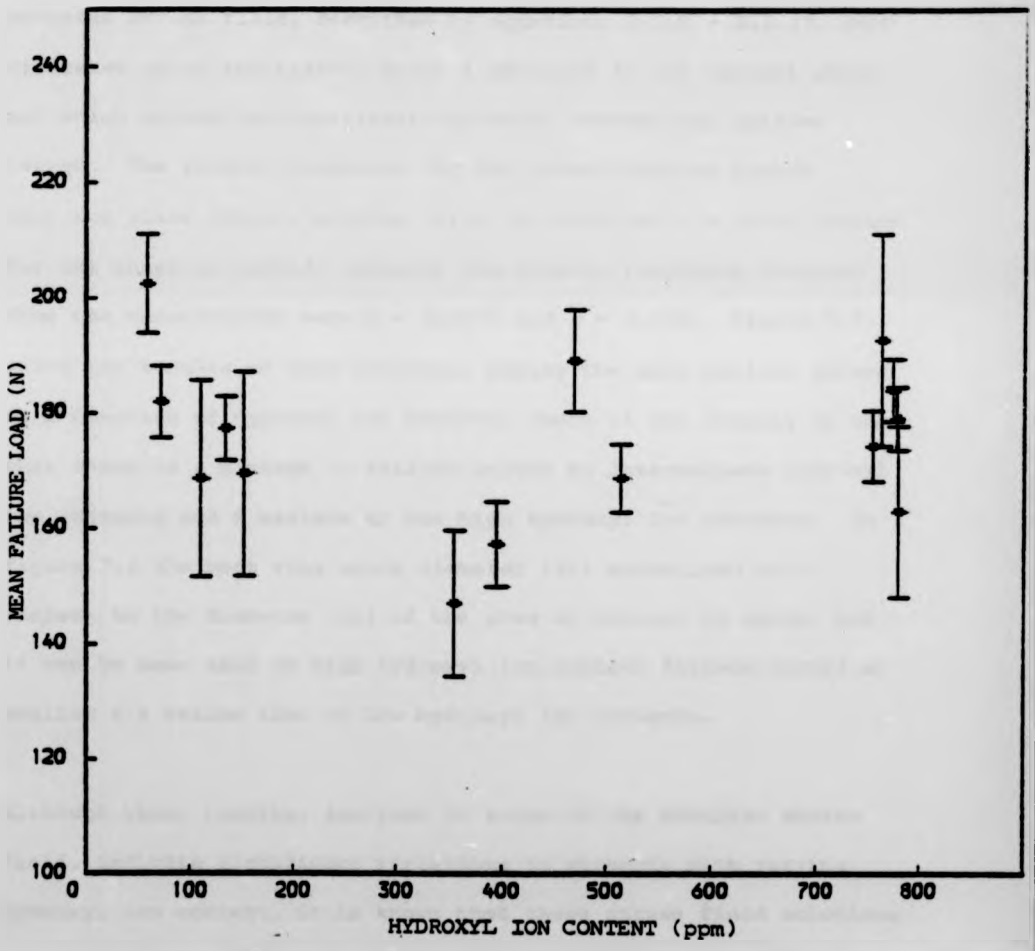

Fig 7.6 Mean Failure Load ± 95% Confidence limits from Hertzian Fracture Test.

simply be considered in terms of the failure stress at individual flaws.

In order to evaluate the failure stress at a specific location in the stress field, the stress field parameters of the classical Hertzian stress field, described by equations 2.2.8 - 2.2.11, were evaluated using the elastic modulii obtained in the current study and which showed no significant variation between the glasses tested. The elastic constants for the glass/indenter system were for glass Young's modulus (E) = 73.13GPa and ν = 0.228, whilst for the tungsten carbide indenter the elastic constants obtained from the manufacturer were E = 650GPa and ν = 0.212. Figure 7.7 shows the results of this analysis, namely the mean failure stress as a function of hydroxyl ion content, where it can clearly be seen that there is a minimum in failure stress at intermediate hydroxyl ion contents and a maximum at the high hydroxyl ion contents. In figure 7.8 the mean ring crack diameter (2r) normalised with respect to the diameter (2a) of the area of contact is shown, and it can be seen that at high hydroxyl ion content failure occurs at smaller r/a ratios than at low hydroxyl ion contents.

Although these results, analysed in terms of the Hertzian stress field, indicate significant variations in strength with varying hydroxyl ion content, it is known that these stress field solutions are not strictly correct. Chapter 2 described how Johnson et al (1973) have shown that the frictional tractions introduced by elastic mismatch between the indenter and specimen can

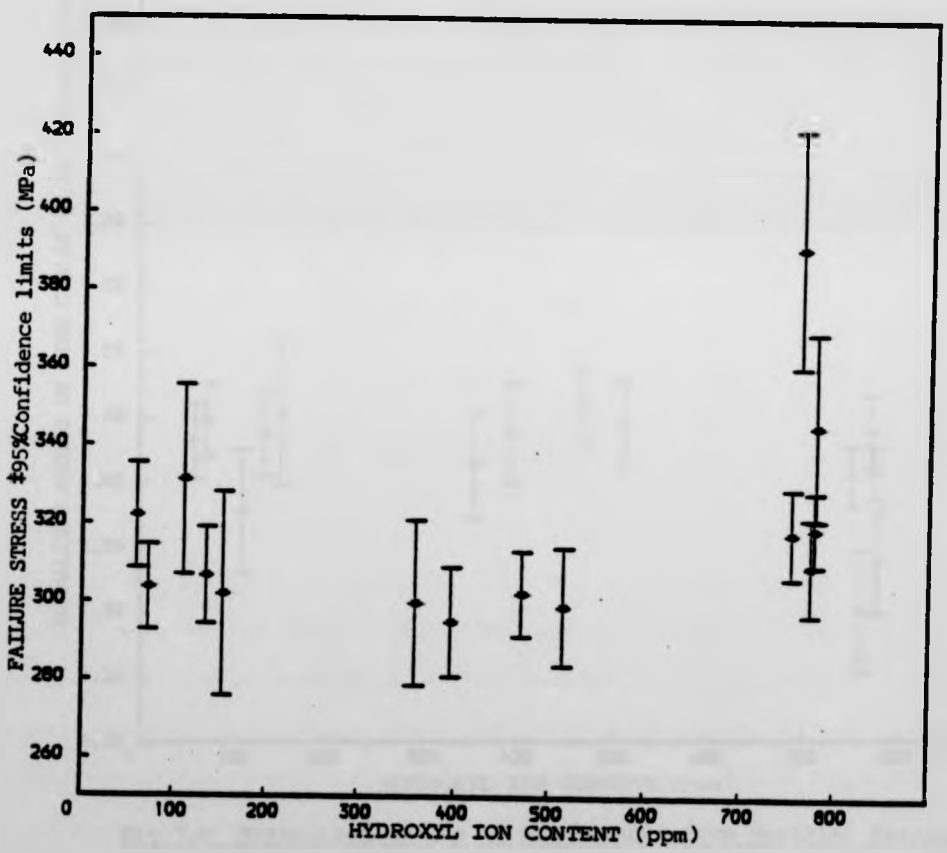

Fig 7.7 Hertzian Fracture Results Analysed using Classical Hertzian stress field.

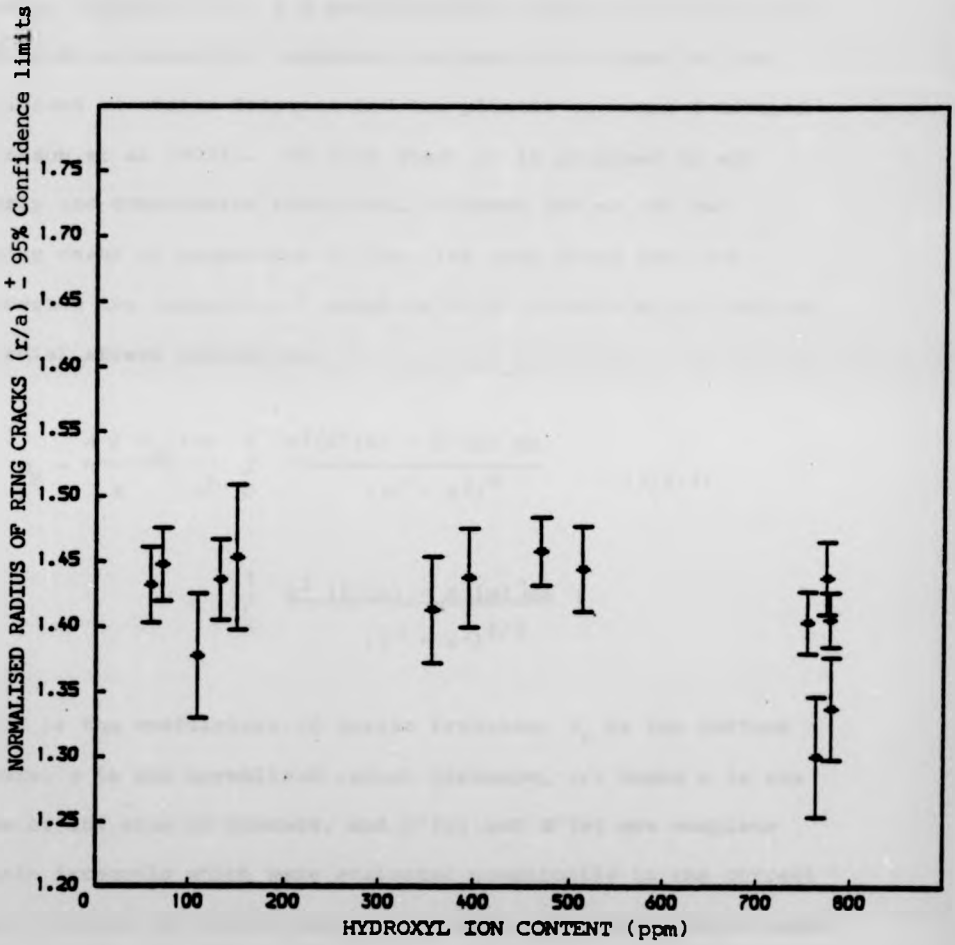

Fig 7.8 Normalised Radius of Ring Cracks from Hertzian Results.

significantly alter the stress field. The two limiting cases they considered were for the conditions of no-slip and for complete slip over the area of contact. In reality, it is probable that part of the area of contact will undergo complete slip whilst the rest will not slip. Spence (1973) has evaluated the radii of the areas over which no slip occurs and tabulated the results in terms of the coefficient of static friction and the plastic constant K defined by Johnson et al (1973). In this study it is proposed to add linearly the compressive tractional stresses due to the two limiting cases in proportion to the area over which they act. Considering the condition of complete slip, Johnson et al, defined the radial stress induced as:

$$\sigma_r = \frac{4 f P_o}{\pi}\left[\frac{1-\nu}{\rho^2}\int_0^1 \frac{x^2\left(K'(x) - E'(x)\right)dx}{(\rho^2 - x^2)^{\frac{1}{2}}}\right. \qquad (7.4.1)$$

$$\left. + \int_0^1 \frac{x^2\left(K'(x) - E^1(x)\right)dx}{(\rho^2 - x^2)^{3/2}}\right]$$

where f is the coefficient of static friction, ρ_o is the surface pressure, ρ is the normalised radial distance, r/a where a is the radius of the area of contact, and K'(x) and E'(x) are complete elliptic integrals which were evaluated numerically in the current study. In fact the entire expression within the square parentheses was evaluated numerically for a range of values of ρ and these results were fitted by a cubic splines routine for subsequent computer analysis of the experimental results. The coefficient of

friction f was obtained from the experiments described in Chapter 6, where it was found that no significant variations existed for the different glasses used and a value of 0.1845 was taken for all the glasses studied

For the condition of no-slip, Johnson et al (1973) gave the equation

$$\sigma_r = (2/3\pi)\ KP_o\left[(2+\nu)(\rho-(\rho^2-1)^{\frac{1}{2}}) + ((1-\nu)\ \sin^{-1}(1/\rho)-(\rho^2-1)^{\frac{1}{2}})/\rho^2\right]$$

$$\text{where } K = \frac{\left[(1-2\nu_1)/G_1\right] - \left[(1-2\nu_2)/G_2\right]}{\left[(1-\nu_1)/G_1\right] + \left[(1-\nu_2)/G_2\right]} \qquad (7.4.3)$$

and was evaluated as 0.558 for the glasses studied.

For these parameters the results of Spence (1973) indicate that the no slip region has a radius of 30% of the radius of contact, and the stress components from the no-slip and the complete slip conditions were scaled accordingly. The resultant stress field is compared with the classical Hertzian solution in Figure 7.9. The main features of the modified stress field are that there exists a region just outside the area of contact where the net stress is compressive and hence failure cannot occur, and that the subsequent maximum stress is lower than that predicted from the Hertzian solutions.

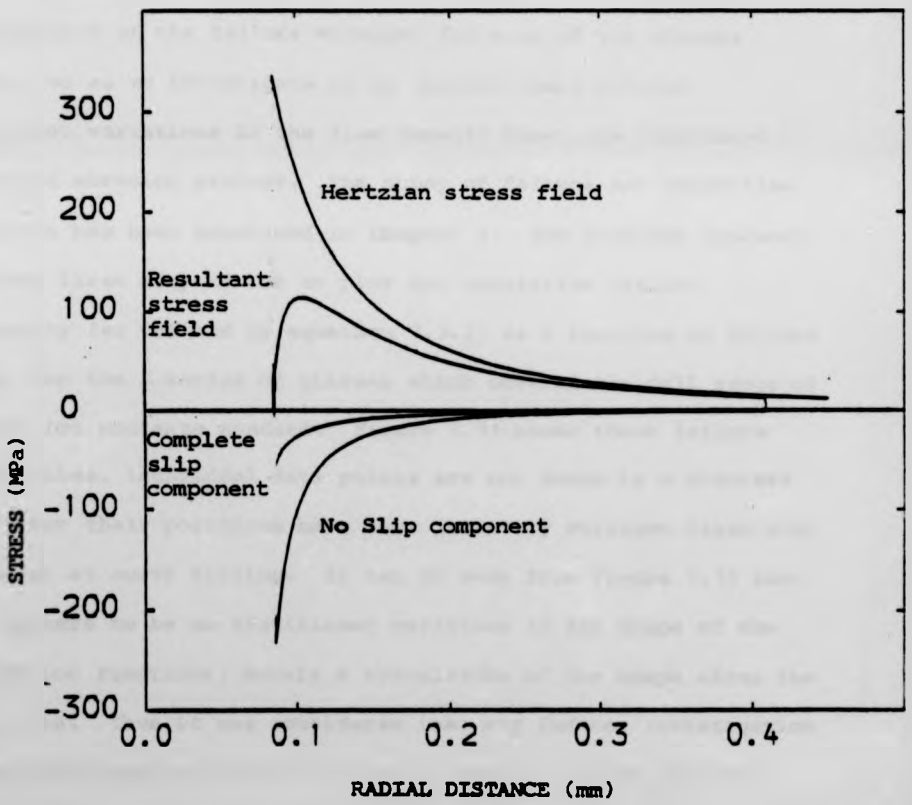

Fig. 7.9 Modified stress field used for Hertzian data analysis.

Re-analysing the experimental data in terms of the modified stress field produces the results shown in figure 7.10. The effects of the modified stress field appear to be twofold: firstly the scatter associated with each glass is decreased, and secondly the trends associated with the variation in failure stress as a function of hydroxyl ion content are generally simplified and appear more consistent.

Finally, it was considered advantageous to investigate the distributions of the failure stresses for each of the glasses studied, so as to investigate as to whether there existed significant variations in the flaw density functions introduced by a standard abrasion process. The study of failure and hence flaw statistics has been described in Chapter 2. The simplest approach which was first adopted was to plot the cumulative failure probability (as defined by equation 7.3.2) as a function of failure stress, for the 4 series of glasses which covered the full range of hydroxyl ion contents studied. Figure 7.11 shows these failure probabilities, individual data points are not shown by a discrete symbol, but their positions have been joined by straight lines with no attempt at curve fitting. It can be seen from Figure 7.11 that there appears to be no significant variation in the shape of the distribution functions, merely a translation of one shape along the stress axis. Thus it was considered that any further investigation of flaw statistics would not lead to a greater insight into the influence of the hydroxyl ion content on the mechanical strength of glass.

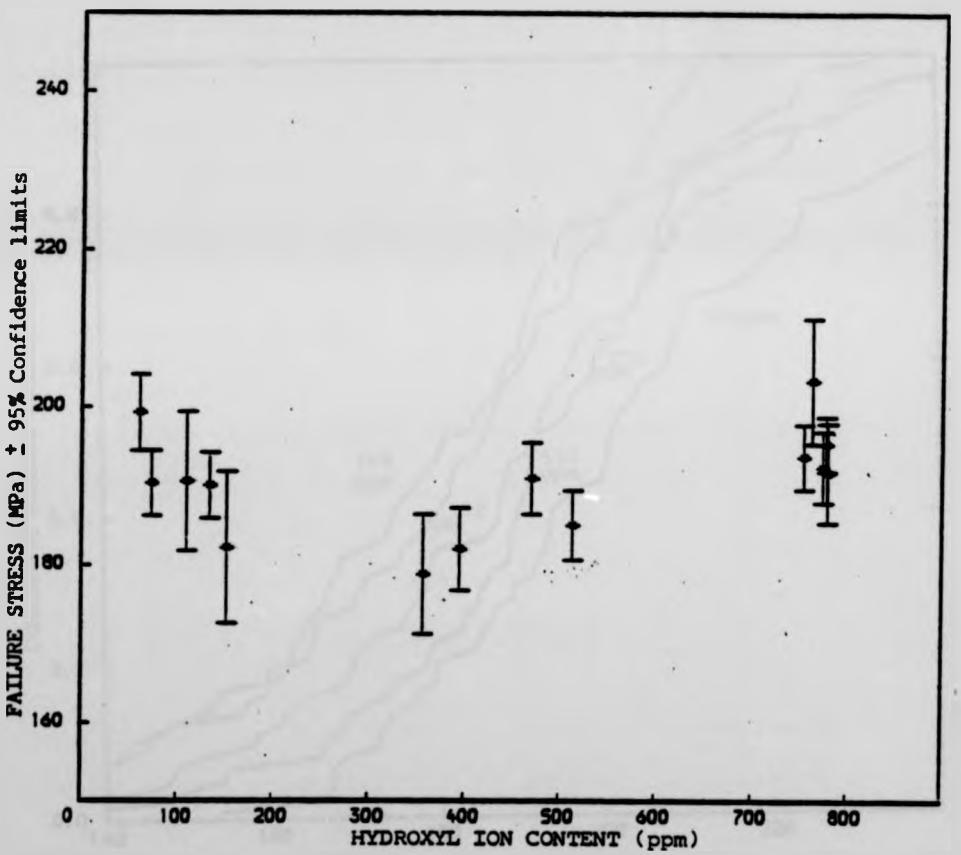

Fig 7.10 Hertzian Fracture Results Analysed using Modified Stress field

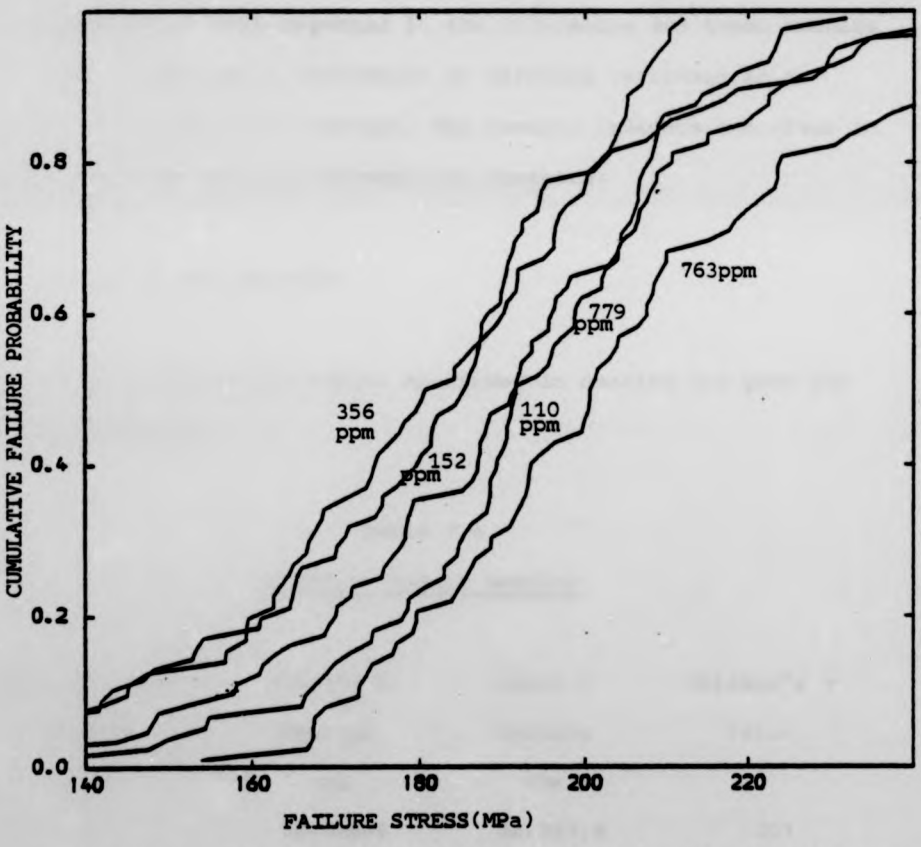

Fig. 7.11 Cumulative Failure Distribiution Functions for Glasses of varying Hydroxyl ion content.

7.5 HARDNESS RESULTS

The results of the hardness measurements obtained at the Lanchester Polytechnic are given in Figure 7.12, which shows the mean hardness and 95% confidence limits on the mean as a function of hydroxyl ion content. Ernsberger (1977) in reviewing mechanical properties, described hardness data as being difficult to obtain reliably. However, the magnitude of the values observed in the current study are comparable to that reported in the literature and these results give a good comparative indication of hardness variation as a function of hydroxyl ion content. The results indicate a maximum in hardness at intermediate hydroxyl ion contents.

7.6 ELASTIC MODULI RESULTS

The elastic moduli measurements described in section 6.2 gave the following results.

Table 7.4

Elastic Moduli Results

Hydroxyl ion Content ppm	Young's E Modulus GPa	Shear G Modulus GPa	Poisson's γ ratio
110	72.8±0.6	30.3±1.6	.201
152	73.3±1.4	29.4±0.4	.246
356	71.8±0.6	29.8±0.4	.206
763	72.8±1.5	30.7±0.1	.202
779	74.2±1.5	29.7±0.1	.248

These results are in general agreement with the published data. There is, however, no systematic variation with hydroxyl ion content and for the stress field calculations described in section 7.4 average values of E = 73.13GPa, G = 29.77GPa and ν = 0.228 were taken.

7.7 DENSITY RESULTS

The results of the density measurements are:-

Table 7.5

Density Results

hydroxyl ion content ppm	Density 10^3 kg m^{-3}
110	2.4945±.0005*
156	2.4951±.0004
356	2.4955±.0002
763	2.4965±.0003
779	2.4965±0.0002

* ± one standard deviation

which indicate a small increase in density with increasing hydroxyl ion content. The value of 2.4955 x 10^3 kgm^{-3} for the glass of 356 ppm OH^- content being evaluated by volumetric methods and the density for the other glasses being evaluated by the comparative method described in section 6.4.

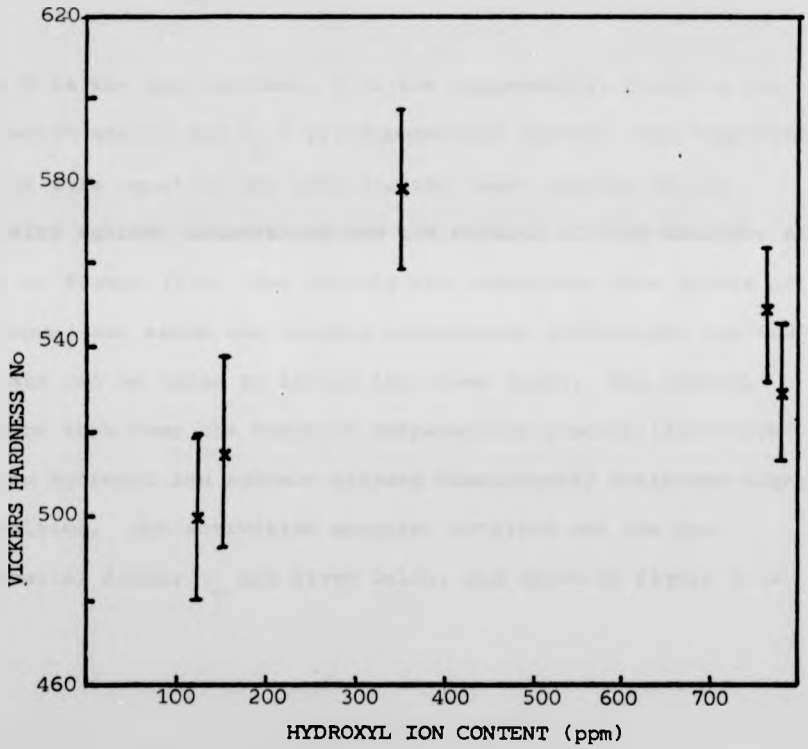

Fig. 7.12 Vickers Hardness results as a function of hydroxyl ion content.

7.8 VISCOSITY RESULTS

It was described in chapter 3 that the hydroxyl ion content of a glass is known to influence its viscosity. The viscosity results obtained in this study were fitted to an equation of the form

$$\nu = \nu_o \exp \frac{Evisc}{RT} \qquad (7.8.1)$$

where R is the gas constant, T is the temperature, Evisc is the activation energy and ν_o a pre-exponential factor. The logarithmic form of this equation was used for the least squares fit of viscosity against temperature and the results of this analysis are given in Figure 7.13. For clarity the individual data points are not shown, and since the minimum correlation coefficient was 0.994, the data can be taken to lie on the lines drawn. The results indicate that over the range of temperatures studied (550°C-620°C) the low hydroxyl ion content glasses consistently exhibited higher viscosities. The activation energies obtained and the pre-exponential factor ν_o are given below, and shown in figure 7.14

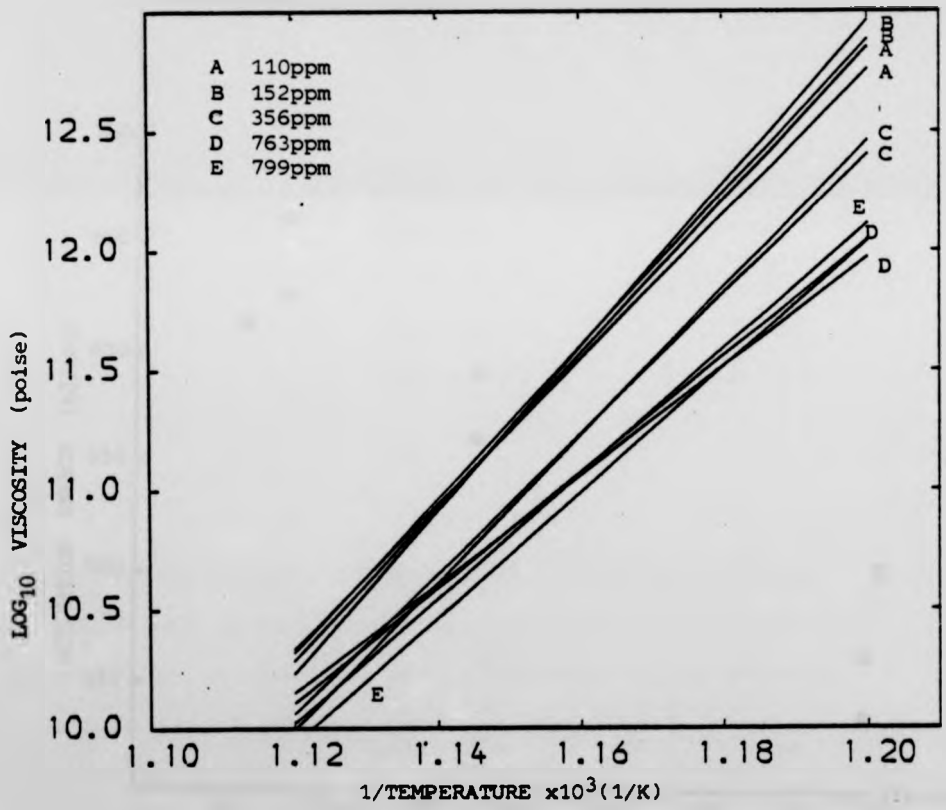

Fig. 7.13 . Results of Least Squares Fit to Viscosity Data for Glasses of varying Hydroxyl ion content.

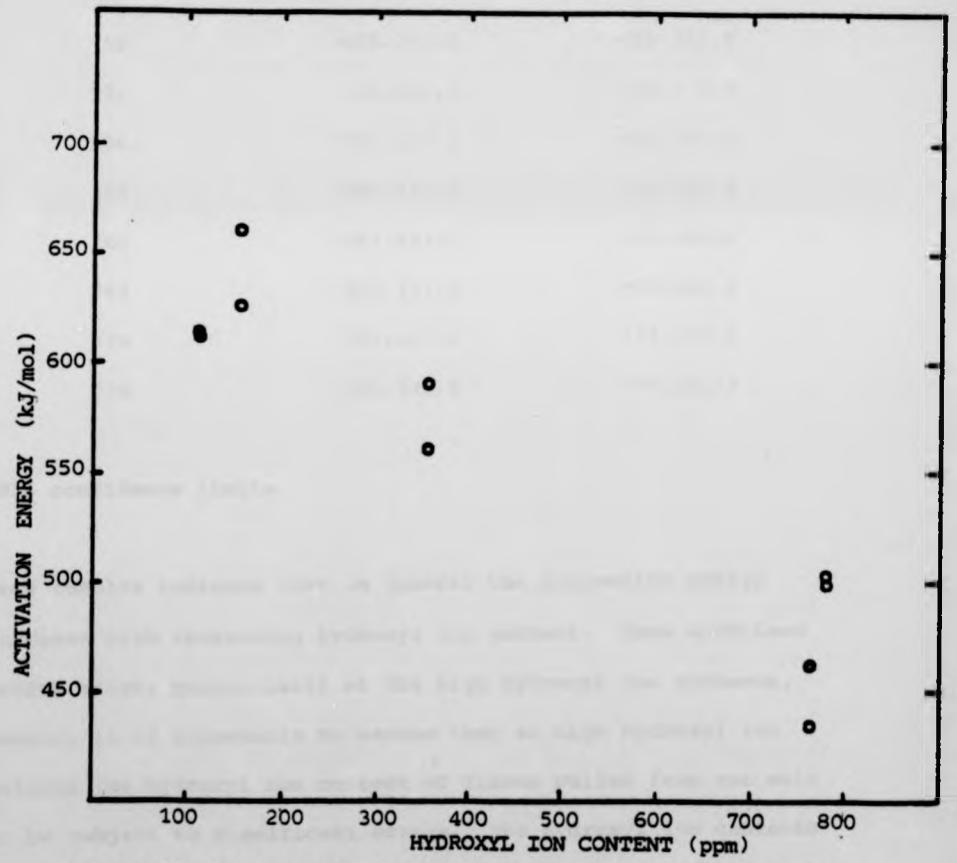

Fig. 7.14 Activation Energy for Viscous Flow as a Function of Hydroxyl ion content.

Table 7.6

Viscosity Measurement Results

Hydroxyl ion content ppm	Activation energy kJ/mol	$-\log_{10} \nu_o$
110	613.8±2.1*	-25.6±2.4*
110	612.8±1.7	-25.3±2.0
152	625.3±3.4	-26.3±4.0
152	660.6±2.4	-28.4±2.9
356	560.2±1.4	-22.7±1.6
356	590.4±2.6	-24.5±2.4
763	435.4±1.2	-15.3±1.4
763	462.7±1.2	-16.9±1.8
779	502.4±1.5	-19.0±1.8
779	499.9±2.8	-19.2±3.3

* 95% confidence limits.

These results indicate that in general the activation energy decreases with increasing hydroxyl ion content. Some anomolous results exist, particularly at the high hydroxyl ion contents, however, it is reasonable to assume that at high hydroxyl ion contents the hydroxyl ion content of fibres pulled from the melt may be subject to significant errors. The hydroxyl ion contents recorded are for the samples taken from the bulk glass.

7.9 D.C. CONDUCTIVITY RESULTS

The conductivity results obtained have been fitted by the least squares method to the log-normal form of the Arhenius type equation:-

$$\sigma = \sigma_o \exp \frac{-Q}{RT} \qquad (7.9.1)$$

where Q is the activation energy, σ_o is a pre-exponential factor and R and T are the gas constant and temperature respectively.

The results obtained from this analysis are given below:-

Table 7.7

D.C. Conductivity Results

OH content ppm	Activation energy kJ/mol	σ_o ohm m^{-1}	Diffusion Coefficient at 20°C m^2 - sec
110	89.74	19.93×10^4	8.78×10^{-22}
152	88.97	9.885×10^4	5.96×10^{-22}
356	88.36	9.162×10^4	7.10×10^{-22}
763	93.29	31.58×10^4	3.25×10^{-22}
779	90.35	10.58×10^4	3.62×10^{-22}

In addition estimates are shown of the diffusion coefficients obtained by evaluating equation 6.6.1. The activation energies given in Table 7.4 are the average for the specimens tested, figure 7.15 shows the activation energies evaluated for individual specimens.

From figure 7.15 and Table 7.4 it can be seen that there is a slight increase in activation energy at increasing hydroxyl ion contents. The estimates of the diffusion coefficients, however, show a more significant trend, with the values for the high hydroxyl ion content glasses showing approximately 50% reduction over the low and intermediate range glasses.

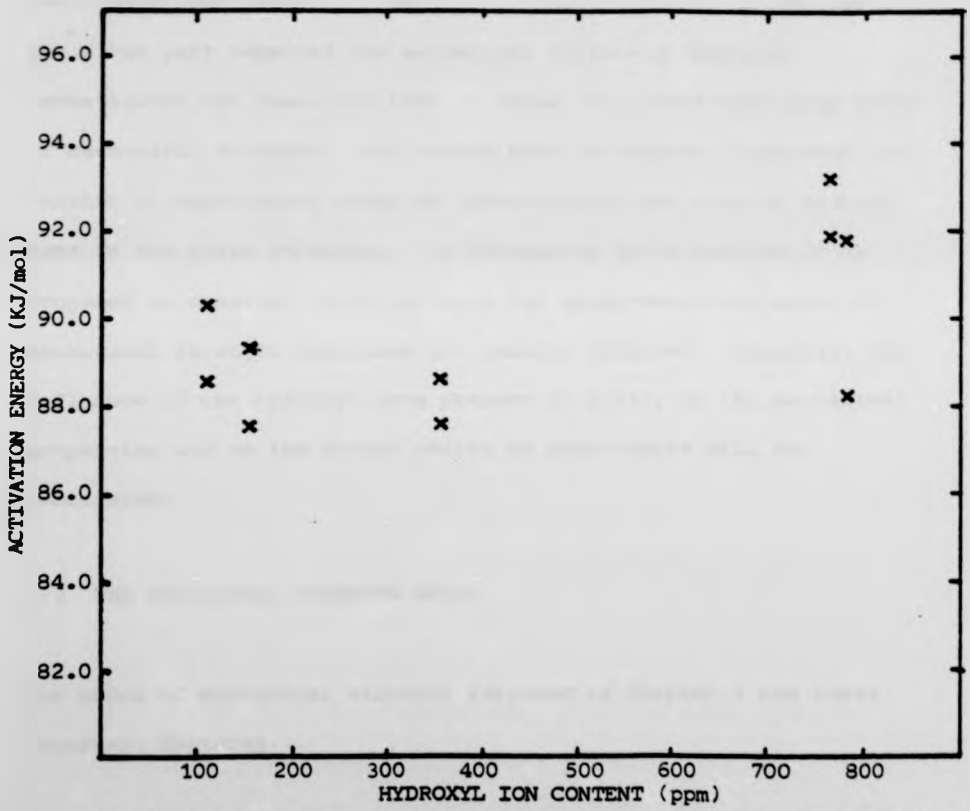

Fig 7.15 Activation Energies for D.C. Conductivity ,by Specimen.

CHAPTER 8

DISCUSSION

8.1 INTRODUCTION

The results described in Chapter 7 can be considered in two parts. The first part reported the mechanical failure properties investigated and described them in terms of a quasi-continuum model of mechanical strength. The second part of Chapter 7 reported the results of experiments aimed at investigating the role of hydroxyl ions in the glass structure. In discussing these results it is proposed to consider first how well the quasi-continuum model of mechanical strength describes the results obtained. Secondly, the influence of the hydroxyl ions present in glass, on the mechanical properties and on the second series of experiments will be considered.

8.2 THE MECHANICAL STRENGTH MODEL

The model of mechanical strength reviewed in Chapter 2 had three important features.

Firstly the critical stress intensity factor K_{IC} was considered to be the parameter which most completely defined the material fracture resistance.

Secondly the stress intensification which gave rise to the stress intensity factor was caused by flaws present in the glass surface and which could be considered as microcracks. These flaws were induced primarily by any form of contact situation, and more usually in the laboratory by means of a controlled abrasion.

The third feature of this model was that fatigue behaviour, ie. time dependant strength variation, occurred. This fatigue behaviour was modelled as a subcritical extension of the microcracks present and was influenced by environmental parameters. The fatigue behaviour was incorporated in the model and investigated primarily in two ways. One method was to investigate the failure behaviour of abraded specimens under varying conditions of load or loading rate. The second method was to investigate the subcritical growth of macroscopic cracks, under conditions of known stress intensity.

Considering the current study in the light of the first of these features ie. the significance of the critical stress intensity factor K_{IC}, there exists a small but statistically significant variation in K_{IC} of approximately 5% over the range of hydroxyl ion contents studied. This variation will have an influence on the failure stress of the four point bending studies at room temperature and at liquid nitrogen temperature, and it will also influence the dynamic fatigue and the Hertzian fracture results. Theoretically the simplest of these experiments is the four point bend studies at liquid nitrogen temperatures (77°K).

The liquid nitrogen four point bend results obtained show a maximum in failure stress at high OH^- contents. The values of failure stress are in general agreement with other studies of failure at 77 e.g. Watanabe et al (1961).

The critical stress intensity factor K_{IC} and the failure stress σ_f are related by

$$\sigma_f = \frac{K_{IC}}{Y\sqrt{\pi a}} \qquad (8.2.1)$$

where a is the crack depth and Y is a geometrical factor which can be approximated as 1.1 for the case of a very short crack. Using equation 8.2.1 the critical crack sizes at failure were evaluated for the three glasses for which K_{IC} was known. The mean crack sizes evaluated were 4.85μm, 5.11μm and 4.74μm for the glasses of 110ppm, 356ppm and 764ppm OH^- content respectively. These crack sizes are of considerable importance because they form an estimate of the initial crack sizes present before fatigue occurs in the room temperature four point bend studies and in the dynamic fatigue analysis. The indication that a maximum in initial crack size occurs at intermediate hydroxyl ion contents is worthy of further investigation.

The indentation fracture mechanics methods, developed by Lawn and co-workers, have been used to study the flaw generation process from a fundamental standpoint. Wiederhorn and Lawn (1979) considered the strength reduction which occurs due to sharp

particles impacting on an annealed surface, and gave an expression for the failure stress after impact in terms of the hardness, K_{IC}, and material and geometrical factors of the particle/glass system. Combining their expression with equation 8.2.1 gives the result that crack size after impact by a sharp particle is proportional to

$H^{2/9} \times K_{IC}^{-2/3}$ where H is the hardness and K_{IC} the critical stress intensity factor. Evaluating this expression, $H^{2/9} \times K_{IC}^{-2/3}$, for the three glasses of interest gives 103, 104.5, and 101.0 (arbitrary units) for the low, intermediate and high hydroxyl ion contents respectively. Thus the indentation fracture mechanics approach also leads to the suggestion that glasses of intermediate hydroxyl ion contents would have the largest initial flaw size, and that the flaw size for low hydroxyl ion content glass would be greater than for the high hydroxyl ion content glass.

This agreement between indentation fracture mechanics and the experimental four point bend studies at 77K° enhances the credibility of the results obtained and the model proposed to fit those results. All of the other mechanical strength studies in this work have included the action of fatigue and it is this effect that will now be considered.

The fatigue behaviour parameters have been investigated by two independent means, fracture mechanics studies and dynamic fatigue measurements.

The fracture mechanics measurements indicated that at high hydroxyl ion contents the fatigue parameter n in equation 7.2.1 decreased. The values obtained are in general in good agreement with those reported in the literature. The dynamic fatigue results, by contrast, were carried out over a limited range of low and intermediate hydroxyl ion contents and showed no significant variation with hydroxyl ion content. The two experiments gave different estimates of the stress corrosion parameter n, 19-20 from fracture mechanics studies and 22-24 from dynamic fatigue measurements. The uncertainties associated with these results are such that the differences between them are not statistically significant. However, the possibility of there being a real difference cannot be ignored.

The most probable source of such a difference is the acid etching process which the dynamic fatigue specimens underwent prior to testing. Ritter and Laporte (1975) have considered the dynamic-fatigue behaviour of abraded and acid etched soda-lime-silica glass and compared the results obtained with crack velocity data. They reported that for testing in distilled water there was no significant variation in the parameter n obtained from the three different tests. Thus it would appear that the most probable cause of any apparent variation between different testing methods can be discounted and the difference can be attributed to chance variations. In considering further experiments it is proposed to use the crack velocity data to define the fatigue crack growth.

It is possible to consider the four point bend studies in terms of the model described so far. The abrasion process that a sample undergoes will introduce an array of initial flaws. The mean value of these initial flaw sizes can be obtained by applying equation 8.2.1 to the results of the four point bend studies and to the K_{IC} values obtained from fracture mechanics measurements. Subsequently under the action of an increasing load, fatigue will occur to increase the effective crack sizes until equation 8.2.1 is again satisfied, this time for the final new flaw size. Evans and Johnson (1975) have considered this solution and derived the following equation for the case when fatigue is dominated by the Stage I slow crack growth.

$$c^{n+1} = \left[\frac{2(n+1)\ \sigma_{fn}^{n-2}}{Y^2(n-2)\ A\ K_{IC}^{n-2}}\right] \dot{\sigma} \qquad (8.2.2)$$

where σ_{fn} is the failure stress at liquid nitrogen temperatures, $\dot{\sigma}$ is the loading rate and A represents the parameters obtained from the slow crack growth data.

Applying this equation to the results obtained for the three glasses 4/1, 4/3, 4/5 of hydroxyl ion contents 110, 358, 736 ppm respectively results in predicted failure stresses of 127.1MPa, 120.2MPa and 124.5MPa respectively. The failure stresses reported for the three groups of results were 95.7MPa, 93.6MPa and 94.99MPa for the low, intermediate and high hydroxyl ion contents

respectively. Again there is only a small variation in failure stress with varying hydroxyl ion content, however there appears to be a large discrepancy between the predicted and observed values of failure stress. In considering this discrepancy it must be remembered that equation 8.2.2 raises some large numbers to very large powers. In fact a systematic error in the slow crack growth parameter n of only 2% would be sufficient to account for the discrepancy between observed and predicted failure stresses. It is unfortunate that the combination of initial flaw size, K_{IC} stress corrosion parameters and the chosen loading rate result in the fatigue behaviour minimising any apparent effects at room temperature. The dynamic fatigue studies were, however, performed at a range of loading rates and so any effects of hydroxyl ions on the behaviour of the model may be more apparent in these studies.

Applying equation 8.2.2 to the dynamic fatigue data resulted in the predicted values given in table 8.1, where there is also reproduced for comparison the dynamic fatigue results.

TABLE 8.1

Predicted and Observed Dynamic Fatigue Failure Stresses

Loading	Predicted Values		Observed Values	
rate $MPas^{-1}$	low OH^-	Intermediate OH^-	low OH^-	Intermediate OH^-
0.14	114.0	107.6	90.2	88.0
1.4	127.1	120.2	100.1	96.7
14.0	141.7	134.3	104.3	111.3
140	157.9	150.0	118.6	115.1

Again there exists the discrepancy in the general level of failure stress between the observed and predicted values. However, the variations between the two glasses as a function of loading rate are significant. The predicted values of failure stress show that the low hydroxyl ion content glass should have a higher failure stress than the intermediate hydroxyl ion content glass over the entire range of loading rates. The observed failure stresses show this behaviour, except at $14MPas^{-1}$. This discrepancy between observed and predicted values can be attributed to the statistical uncertainty associated with the experimental observations and the general agreement between predicted and observed results is good.

To confirm this agreement it would have been desirable to test at more than four loading rates, however, the limitations of specimen numbers precluded this possibility.

The final experimental study of relevance to the proposed model of failure is the Hertzian fracture test experiment. Qualitatively, the Hertzian fracture results exhibit behaviour consistent with the other experimental studies and with the model so far proposed. Firstly a minimum in failure stress and failure load is exhibited at intermediate hydroxyl ion contents. Secondly the high hydroxyl ion content glasses exhibit the maximum failure loads. It is, however, much more difficult to carry out a quantitative assessment

as to the consistency of the proposed model with the observed Hertzian fracture resuts. There are a number of reasons for this difficulty, the first and most important is that it is not possible to be sure that the stress field being used is correct, because of the effects of interfacial friction. Secondly, if the effect of subcritical crack growth is to be considered then the stress rate is position dependant. Thirdly, considerable argument surrounds the failure initiation event, as to whether the initial flaw size has any significance (see Chapter 2).

In an effort to assess the capabilities of the model in analysing the experimental results, the approach adopted was to try and evaluate by numerical means the initial flaw size which would lead to failure by the criterion of equation 8.2.1.
This approach was adopted since it was obvious that the flaw sizes obtained from four point bend studies could not be used as estimates of the initial flaw size.

The relevant material parameters were identical to those used in the four point bend simulation, subcritical crack growth being included in the form obtained from fracture mechanics studies. A computer programme was written to carry out the following procedure:

(1) An initial value of the initial crack size was chosen at a given distance from the point of contact r_f.

(2) The load was increased by an amount $\Delta P = \dot{P}\Delta t$ where Δt is a small increment of time.

(3) The stress acting on the flaw was calculated using the modified stress field.

(4) K_I was evaluated using equation 8.2.1

(5) The crack length increase ($V\Delta t$) for time (Δt) evaluated from $v = AK_I^n$.

(6) Test carried out for $K_I \geq K_{IC}$ or $P \geq P_f$.
If neither of these tests were true then time incremented by Δt and process from step (2) repeated until step (6) was true, and then the initial crack size estimate was altered until a suitably precise estimate was attained. It had originally been planned to carry out this analysis for all the indentation events recorded. However, the excessive computing time required to obtain a precise estimate of the initial crack size i.e. by having Δt very small, precluded this possibility.

An alternative proposal was to carry out the preceeding analysis on the mean values $\bar{P}_f$ and $\bar{r}_f$ for the three glasses 4/1, 4/3, 4/5 for which the fracture mechanics parameters had been evaluated. Performing such an analysis on the mean values of failure load $\bar{P}_f$

and mean radial distance $\bar{r}_f$ is not strictly accurate because of the interaction which exists between P_f and r_f. However, this inaccuracy is not likely to be too severe and can be assessed by comparing the predicted and observed mean failure stresses. Table 8.2 shows the results of such an analysis.

TABLE 8.2

Result of Hertzian Fracture Simulation

glass	$\bar{P}_f$	$\bar{r}_f$	Failure stress Predicted	Failure stress Observed	Initial crack size	Final crack size
	N	(mm)	(MPa)	(MPa)	(μm)	(μm)
4/1	168.8	0.214	192.7	190.1	1.66	3.93
4/2	147.2	0.209	179.0	178.0	1.88	4.82
4/5	192.1	0.211	210.0	204.0	1.15	3.59

From Table 8.2 it may be seen that the mean failure stress predicted generally agrees well with the observed mean failure stress. The estimates of initial flaw size show a similar variation with hydroxyl ion content to that reported for liquid nitrogen four point bend studies. The difference in absolute crack size predicted for the Hertzian fracture results as compared to that reported for four point bend studies could be ascribed to a number of different causes, firstly an inablity to define the stress field correctly, or the fact that because the Hertzian test

samples only small areas of the specimen surface and hence does not encounter the severe flaws which characterise four point bend results. Alternatively, the theories proposed by Lawn (1969) which hold that flaw size is unimportant within a certain range offer a third possible explanation.

8.2.1 Summary of Mechanical Strength Model

The preceeding section has shown that the parameters obtained from the fracture mechanics studies ie. K_{IC} and the crack velocity versus K_I results can be used to explain satisfactorily the other mechanical strength studies i.e. four point bend studies and Hertzian fracture.

The compositional effects isolated from these studies are that K_{IC} increases with increasing hydroxyl ion content. The stress corrosion behaviour (as considered by the slow crack growth) gave a greater crack velocity at a given K_I for high hydroxyl ion content glasses than for low hydroxyl ion content glasses, but the gradient in the crack velocity versus K_I curves was lower for high hydroxyl ion content glasses (see figure 7.2). Finally hardness shows a maximum at intermediate hydroxyl ion contents.

In the following section the experiments performed to elucidate the behaviour of hydroxyl ions in glass will be considered. The model of mechanical strength will then be discussed in terms of the observation concerning the behaviour of hydroxyl ions in glass.

8.3 THE STRUCTURAL ROLE OF HYDROXYL IONS

In the preceeding sections the influence of hydroxyl ion content on the mechanical strength of glass has been discussed. Of the other experiments carried out, density, conductivity, viscosity and hardness have also shown the effects of varying the hydroxyl ion content of the glass. The density results showed a small increase in density with increasing hydroxyl ion content. Bruckner (1971) has suggested that this increase is due to the presence of hydrogen bonding between the hydrogen of a hydroxyl group attached to the glass network and a bridging oxygen. This suggestion is plausible in the light of the fact that infra-red spectroscopy has indicated that such a form of bonding exists (See Chapter 3).

Another of the measured properties which is sensitive to the silica network is viscosity. The results obtained in the present study show a decrease in activation energy of 26% over the range of hydroxyl ion contents. This reduction cannot be due to the increased depolymerisation of the silica network introduced by the addition of hydroxyl ions, there is already approximately one non-bridging oxygen on every second silica tetrahedra and the addition of hydroxyl ions increases the non-bridging oxygen density negligibly. Shelby and McVay have observed similar effects in sodium silicate glasses and attributed this behaviour to a "mixed alkali" effect. In contrast Gonzalez-Oliver et al (1979) in studying the influence of hydroxyl ion content on crystal nucleation and growth in soda-lime-silica glasses, postulated that

viscosity was controlled by oxygen diffusion and that hydroxyl ions in the glass altered the oxygen diffusion coefficient. However, they were unable to offer a real insight into the details of the process.

The mechanism by which hydroxyl ions influence the viscous behaviour of glasses is difficult to speculate upon because the very details of the mechanism of viscous flow are unclear. However it can be proposed that flow must occur by the breaking and reforming of bonds with an attendant reorientation of structural groups. It is difficult to envisage a mechanism by which hydroxyl ions can influence bond rupture and reformation since even in the highest hydroxyl ion content glass only approximately one in every three hundred silica tetrahedra is connected to a hydroxyl ion group. It is therefore more probable that the presence of hydroxyl ions influences the ease with which molecular groups of silica tetrahedra reorientate under the action of an applied stress.

This proposed mode of behaviour is consistent with the current results and also with those of Heatherington et al (1964) who observed that at 1000°C there was a considerable decrease in viscosity for samples of silica with a high OH^- content. They reported however, that at 1400°C there was little difference in viscosity between the two samples of silica. It can be speculated that at lower temperatures the number of silica tetrahedra associated within a molecular group with a hydroxyl ion present will be greater than at high temperatures. At higher

temperatures, the silica network will form smaller molecular groups and the probability that some molecular groups will not contain a hydroxyl ion exists and thus the overall influence of the hydroxyl ions will decrease.

A structural property of interest in this study is the hardness of the glasses produced. In section 8.2 the expression given by Wiederhorn and Lawn (1979) for the defect size after abrasion was used to confirm the variation of defect size with hydroxyl ion content obtained from liquid nitrogen four point bend studies. The form of this variation was also consistent with the results obtained from the Hertzian fracture results. The significance of this expression was that it predicted that flaw size after abrasion was proportional to $H^{2/9}$ (hardness).

In the current study a pronounced maximum in hardness was observed at intermediate hydroxyl ion contents. The actual mechanisms of the hardness measurement are of course open to considerable speculation. Peter (1970) in a careful study of hardness indentations observed that densification, the piling-up of material outside the indentation, and "slip lines" below the indentation all occurred in a soda-lime-silica glass. The amalgamation of all of these effects into a coherent theory is a formidable proposition in itself, without the difficulties of considering compositional variations.

Hillig (1968) considered that viscous flow may play a part in the hardness indentation process. However since the viscosity (a shear deformation process) of the glasses prepared varies so markedly with hydroxyl ion content, it is possible to assess the relevance of this mode of deformation in a description of the hardness of a glass. The variations of hardness and viscosity as a function of hydroxyl ion content are fundamentally different and thus the two modes of deformation must be dominated by different mechanisms. It is probable that the hardness indentation process occurs by the competitive or cooperative action of a number of mechanisms, with one dominating at low hydroxyl ion content whilst another mechanism will be more significant at higher hydroxyl ion contents. Further work, beyond the scope of this study is required to elucidate the nature of these mechanisms.

The experimental results discussed so far have all been dominated by the behaviour of the silica network. In contrast the conductivity measurements were undertaken to investigate the motion of the alkali ions present in the glasses. Conductivity measurements showed a small increase in activation energy and a large decrease in diffusion coefficient over the range 50°-200°C. Considering this behaviour a number of possible structural explanations suggest themselves. The simplest hypothesis is that the observed increase in density with increasing hydroxyl ion content results in a contraction of the silica network about the alkali ions, and hence results in an increase in activation. Unfortunately Charles (1962) has considered the effect of volume

expansion, by quenching from the melt, and volume contraction, by hydrostatic pressure, on the resistivity of a commercial soda-lime-silica glass. Comparing the observed conductivity changes with those recorded by Charles shows that the specific volume changes required to achieve the observed conductivity are an order of magnitude greater than the observed specific volume changes.

A possible explanation of the observed conductivity results is that the hydrogen ions present interact with the alkali ions. The interionic diffusion between hydrogen and sodium ions has been studied by many authors as part of the study of aqueous corrosion (see Doremus (1977) and Hench (1975) for reviews). However, the situation studied in examining aqueous corrosion is more complex than D.C. conductivity because the introduction of protons into the glass is achieved by the formation of alkali hydroxides at the glass surface. Thus there exists a hydrogen rich and alkali depleted layer into which alkali ions diffuse from the bulk glass. In the present work alkali and hydrogen ions are homogeneously mixed and so the interaction process is probably different.

The mixed alkali effect in conductivity was described in chapter 3 as the observed decrease in conductivity which occurs when a second different alkali is added to an alkali silicate. It is possible that the observed behavior is a manifestation of this effect, although the mechanisms of the mixed alkali behaviour are poorly understood.

The experimental results discussed in this section so far were aimed at investigating the influence of hydroxyl ions on phenomena which may play a role in mechanical strength. To this end they have succeeded and some of the effects of hydroxyl ions on the structure and on the alkali ions have been discussed. The fundamental mechanisms which cause the observed results are much harder to elucidate because the basic mechanisms of some of the properties studied are not well understood.

In section 8.2 it was shown that the two parameters which most fully characterised the fracture and fatigue behaviour of the glasses tested were the critical stress intensity factor K_{IC} and the crack velocity stress intensity relationship for the stage I slow crack growth.

Considering the crack velocity stress intensity relationship first, it was described in chapter 2 that Wiederhorn (1973) obtained the pH of ground glass sluries in water (as a measure of crack tip pH) and recorded pH of 11.5 to 12.3 for a soda-lime-silica glass. Wiederhorn and Johnson (1973) also showed that the gradient of the crack velocity stress intensity relationship was a function of the pH of the test solution, and, by comparing the value of the gradient obtained in water with the values obtained for acid and alkali solutions, they suggested that the crack tip pH in the presence of water was approximately 12. Wiederhorn and Bolz (1970) obtained an activation energy for the stage I slow crack growth in

the presence of water which was comparable to that obtained in the current study for D.C. conductivity i.e. ~ 100 KJ/mol.
In the current study it was observed that at low values of K_I the crack velocity was greater in high hydroxyl ion content glasses than in the low hydroxyl ion content glasses, whilst at large values of K_I there was little difference in crack velocity between different glasses. For the glasses studied it was shown earlier that the diffusion coefficient for sodium ion motion was lower in high hydroxyl ion content glasses. Since alkali ions will diffuse to the high tensile stress region at the crack tip, it is possible to postulate that a lower alkali concentration will occur at the crack tip in high hydroxyl ion content glasses. This possible variation in alkali concentration at the crack tip may result in lower pH and hence higher crack velocity in the high hydroxyl ion content glasses.

As described in Chapter 2, at high values of K_I, i.e. at the onset of Stage II slow crack growth, it is to be expected that the external water concentration at the crack tip will limit the reaction process, and then variations due to varying alkali ion concentrations will be inoperative and crack velocities for all the glasses tested will be approximately equal.

This suggested mechanism provides qualitative agreement with the observed behaviour.The quantitative analysis of the postulated mechanism is much harder to attain as it requires further experimentation and a considerably greater theoretical

investigation of stress induced diffusion and the nature of the crack tip region where non-linear behaviour must occur. It is noteworthy that Cox (1969) has produced a theory of mechanical strength which was based on ionic mobility. His theory was fundamentally different in that he proposed that flaws occurred by chance grouping of alkali ions which produced a local weakness and did not consider the possibility of any diffusion to a microcrack tip under the action of stress.

Considering the other important parameter which defines the mechanical strength, ie. the critical stress intensity factor K_{IC}, the experimental results indicate a small increase in K_{IC} with increasing hydroxyl ion content.

The simplest possible explanation for this behaviour would be the hypothesis that the increase in density with increasing hydroxyl ion content will result in an increase in bonds per unit area, and hence the strain energy release rate required per unit crack advance would be greater. However since K_{IC}^2 is proportional to strain energy release rate and bond density is proportional to the two thirds power of the molar concentration, then the density would have to increase by approximately 15% to account for the observed variation in K_{IC}.

The plastic flow theories of Marsh (1964) predict that crack growth occurs at a critical value of plastic zone size. Applying Marsh's equations for flow stress based on hardness measurement predicts a

maximum in flow stress and hence K_{IC} at intermediate hydroxyl ion contents; this is not observed in practice.

The "lattice trapping" theories of fracture of Thomson and co-workers define K_{IC} in terms of complex function of the elastic constants of the models used and hence it is not possible to compare this theory against the experimental observations. However, it must be noted that no significant variation in bulk elastic moduli was observed in the current study. These theories based on the "lattice trapping" concept have however also been used to describe the stage III slow crack growth from which K_{IC} was estimated. Lawn and Wilshaw (1975) in reviewing this model of fracture gave an expression for the crack velocity in a cubic lattice,

$$v = v_o\, a_o \exp\left[-\frac{U_m}{KT}\left[1 + \frac{\pi}{2}\left(\frac{-G + 2y}{2y_t}\right)\right]\right] \qquad (8.3.1)$$

where k and T are the Boltzman constant and temperature respectively, v_o is an atomic vibrational frequency, a_o is a lattice parameter, G is the applied strain energy release rate, y_t is the periodic term of the surface energy, y is the mean surface energy and U_m is the activation energy for movement of a crack front kink pair. Considering this equation in terms of what is known about behaviour of glasses with varying hydroxyl ion contents, a_o the average atomic spacing will decrease with increasing hydroxyl ion content.

The viscosity results were described earlier in terms of a model-in which the effect of increasing hydroxyl ion content was to increase the ease with which the structure was capable of reorientating so as to minimize the effect of stress. If this postulated mode of behaviour is applied to equation 8.3.1 then U_m would tend to increase as reorientation occurs rather than bond rupture.

In conclusion the details of the mechanism by which hydroxyl ions influence the mechanical strength of glass, are difficult to describe. This difficulty is due in part to the fact that the compositional dependance of mechanical strength is itself poorly understood and partly because the influence of the hydroxyl ions present in the glass is extremely complex.

The hydroxyl ion when present in a soda-lime-silicate glass appear capable of exhibiting behaviour, which can be best visualised by considering the hydroxyl or hydrogen ion as behaving as an alkali ion e.g. in D.C. conductivity and in internal friction. However, the hydroxyl ion also appears capable of exhibiting a profound influence on the silica network, e.g. in hardness and viscosity measurements, and it is perhaps necessary to consider the models of these properties as having the hydroxyl group bonded to the network.

CHAPTER 9

CONCLUSIONS AND FUTURE WORK

9.1 CONCLUSIONS

Soda-lime-silica glasses of varying hydroxyl ion content have been prepared. The mechanical properties of these glasses have been studied by experimental measurements of critical stress intensity factor, subcritical crack growth studies, conventional four point bend measurements under conditions of varying temperature and stressing rate. In addition Hertzian fracture tests have been performed.

The results of these mechanical tests have been analysed in terms of K_{IC} and crack velocity K_I relationship. A coherent model of mechanical strength has been described which provides good qualitative and in some cases quantitative agreement between different mechanical tests. The effect of varying the hydroxyl ion content of the glass is to increase K_{IC} for glasses of high hydroxyl ion content and to increase the crack velocity at low values of K_I in the high hydroxyl ion content glasses.

A series of other experiments have also been performed to investigate the structural role of the hydroxyl group. These studies were conductivity, density, viscosity, hardness and elastic moduli. Elastic moduli measurements showed no significant effects,

whilst density conductivity, viscosity and hardness showed complex behaviour as a function of hydroxyl ion content. For these properties it was not possible to provide a single coherent model of hydroxyl ion behaviour, although individual effects could be explained satisfactorily.

Considering the critical stress intensity factor K_{IC} in terms of the basic role of hydroxyl ions in glass, it was not possible to provide a fundamental model to explain the observed behaviour. However, it was possible to show that none of the theories currently available were able to explain the observed behaviour. This was in part due to the fact that for some of the theories proposed the experimental results do not agree with the predicted behaviour, and for the other theories the structural details are either not considered or are considered at such a fundamental level that there is not enough information currently available to compare theory and experiments.

The slow crack growth as a function of stress intensity have been explained in terms of the alkali ion diffusion to the crack tip. It is postulated that this diffusion results in a decrease in crack-tip pH and hence increased crack velocity in high hydroxyl ion content glasses. This theory is supported by the observed correspondence between the observed activation energies for subcritical crack growth and D.C. conductivity. In the current study it was not possible to test this theory by studying the variation in subcritical crack growth as a function of temperature,

because of the limitation of the equipment and the shortage of specimens available.

In this work the fracture mechanics model of mechanical strength has been shown to agree well with the observed results. The model proposed to explain the observed behaviour may appear speculative, however, much of the evidence, although incomplete, provides a good corroboration of the proposed theory.

9.2 FUTURE WORK

In order to test the theories described above, a number of areas of further work suggest themselves.

The study of ionic diffusion under the action of a stress gradient is an area where little work has been performed. Of particular interest is the study of the diffusion mechanism and its relationship to that observed in D.C. conductivity. A sensitive compositional tool in this area would be the mixed alkali glasses, which have been studied experimentally and sophisticated theories proposed to explain their ionic behaviour.

The other area of significance is the study of fracture toughness and stress corrosion behaviour as a function of composition. The theory of subcritical crack growth described above could be tested by studying the behaviour of mixed alkali glasses where ionic

mobilities are known to vary whilst the non-bridging oxygen density remains constant.

In conclusion the compositional dependance of mechanical strength is an area of considerable interest. The use of fracture mechanics techniques can greatly simplify the experimental observations obtained and the material preparation required. However whilst the use of commericially available glasses may hold great appeal, this must be resisted, because the use of these multi-component glasses can lead to much ambiguity in the results obtained. It is the systematic exploration of the fracture mechanics behaviour of two and three component glasses which will ultimately lead to a better understanding of mechanical strength.

REFERENCES

R. ADAMS and P.W. McMILLAN, J. Mater. Sci. 12 (1977) 643.

R.V. ADAMS, Phys. Chem. Glasses 2 (1961) 39.

E.N. ANDRADE and L.C. TSIEN, Proc. Roy. Soc A159 (1937) 346.

F. AUERBACH, Ann. Phys. Chem. 43 (1891) 61.

S.B. BATDORF, in "Fracture Mechanics of Ceramics", Vol.3, edited by R.C. Bradt et al (Plenum Press, New York, 1978).

R.N. BLUMENTHAL and M.A. SEITZ, in "Electrical Conductivity of Ceramics and Glasses" Part A, edited by N.M. Tallen (Dekker, New York, 1974).

E.N. BOULOS and N.J. KREIDL, J. Canad. Ceram. Soc. 41 (1972) 83.

R. BRUCKNER, J. Non-Cryst. Solids 5 (1971) 123.

R.C. BURT, J. Opt. Soc. Amer. 11 (1925) 87.

H.C. CHANDAN, R.C. BRADT and G.E. RINDONE, J. Amer. Ceram Soc. 61 (1978) 207.

R.J. CHARLES, J. Appl. Physics 29 (1958) 1554.

R.J. CHARLES, J. Appl. Physics 29 (1958) 1657.

R.J. CHARLES, J. Amer. Ceram. Soc. 45 (1962) 105.

A. CHLEBIK, R. ADAMS and P.W. McMILLAN, Phys Chem. Glasses 18 (1977) 59.

M. COENEN, Zeit.fur Elektrochem.65 (1961) 903.

S.M. COX, Phys. Chem. Glasses 10 (1969) 226.

D.E. DAY, J. Non-Cryst. Solids 21 (1976) 343.

R.H. DOREMUS, J. Phys. Chem. 68 (1964) 2212.

R.H. DOREMUS, "Glass Science" (North-Holland, New York, 1973).

R.H. DOREMUS, J. Non-Cryst. Solids 25 (1977) 263.

N.R. DRAPER and H. SMITH, "Applied Regression Analysis" (John Wiley, New York, 1966).

F.M. ERNSBERGER, Glass Ind. 47 (1966) 300.

F.M. ERNSBERGER, J. Non-Cryst. Solids 25 (1977) 295.

A.G. EVANS, J. Mater. Sci.7 (1972) 1137.

A.G. EVANS and H. JOHNSON, J.Mater. Sci.10 (1975) 214.

A.G. EVANS and D.P. WILLIAMS J.of Test and Eval. 1 (1973) 264.

K.E. FORRY, J. Amer. Ceram. Soc. 40 (1957) 90.

F.C. FRANK and B.R. LAWN, Proc. Roy. Soc. London A299 (1967) 291.

S.W. FRIEMAN, J. Amer. Ceram. Soc. 57 (1974) 350.

S.W. FRIEMAN, D.R. MULVILLE and P.W. MAST, J. Mater, Sci.8 (1973) 1527.

A.N. GEOROFF and C.L. BABCOCK, J. Amer. Ceram. Soc. 56 (1973) 97.

C.J.R. GONZALEZ-OLIVER, P.S. JOHNSON, and P.F. JAMES, J. Mater. Sci 14 (1979) 1159.

C.H. GREENE AND I KITANO, Glastech. Ber. 32 (1959) 44.

A.A. GRIFFITH, Phil. Trans. Roy. Soc. Lond. A221 (1920) 163.

A.J. HARRISON, J. Amer. Ceram. Soc. 30 (1947) 362.

J. HARRISON and J.WILKS, J. Phys. D:Appl. Phys. 6 (1973) 322.

G. HEATHERINGTON, K.H. JACKS and J.C. KENNEDY, Phys. Chem. Glasses 3 (1964) 130.

L.L. HENCH, J. Non-Cryst. Solids 19 (1975) 27.

H. HERTZ, Reprinted in English in "Hertz's Miscellaneous Papers" (Macmillan, London, 1896) Chs. 5. 6.

R. HILL, "Plasticity" (Clarendon Press, Oxford, 1950).

W.B. HILLIG, Advances in Mater. Res.2 (1968) 383.

W.B. HILLIG and R.J. CHARLES, in "High Strength Materials" ed. by V.F. Zackay (John Wiley, New York, 1965).

C. HSIEH and R. THOMSON, J. App. Phys. 42 (1971) 3154.

M.T. HUBER, Ann. Physik 14 (1904) 153.

C.E. INGLIS, Trans. Inst. Naval Arch. 55 (1913) 219.

G.R. IRWIN, Trans. Amer. Soc. Mech. Engrs, J. Appl. Mech. 24 (1957) 361.

G.R. IRWIN, in "Handbuch der Physik", (Springer-Verlag, Berlin, 6, 1958)

A. ISMAIL, H. ABDEL-LATIF, R.C. BRADT and G.E. RINDONE, J. Amer. Ceram. Soc. 59 (1976) 174.

J.R. JOHNSON, R.H. BRISTOW and H.H. BLAU, J. Amer. Ceram. Soc 34 (1951) 135.

K.L. JOHNSON, J.J. O'CONNER and A.C. WOODWARD, Proc. Roy. Soc. London A334 (1973) 95.

L.G. JOHNSON, "Theory and Techniques of Variation Research", (Elsevier, Amsterdam, 1964).

C.R. KENNEDY, R.C. BRADT and G.E. RINDONE, in "Fracture Mechanics of Ceramics", Vol.2, ed. by R.C. Bradt et al, (Plenum, New York, 1973).

C.R. KURKJIAN and L.E. RUSSEL, J. Soc. Glass Tech. 42 (1958) 130.

W.C. LaCOURSE, in "Introduction to Glass Science", ed. by R.D. Pye et al (Plenum, New York, 1972).

F.B. LANGITAN and B.R. LAWN, J. Appl. Phys.40 (1969) 4009.

B.R. LAWN, J. Mater. Sci. 10 (1975) 469.

B.R. LAWN and A.G. EVANS, J. Mater. Sci. 12 (1977) 2195.

B.R. LAWN, E.R. FULLER and S.M. WIEDERHORN, J. Amer. Ceram. Soc. 59 (1976) 193.

B.R. LAWN and D.B. MARSHALL, in "Fracture Mechanics of Ceramics", Vol.3, ed by R.C. Bradt et al, (Plenum, New York, 1973).

B.R. LAWN, S.M. WIEDERHORN and H.H. JOHNSON, J. Amer. Ceram. Soc. (1975) 428.

B.R. LAWN and T.R. WILSHAW, J. Mater. Sci.10 (1975) 1049.

B.R. LAWN and T.R. WILSHAW, "Fracture of Brittle Solids", (Cambridge University Press, 1975).

J.V. LEWIS and H. RAWSON, Glass Tech. 17 (1976) 128.
L.C. LYNNWORTH, J. Test. and Eval. 1(1973) 119.

M.S. MAKLAD and N.J. KREIDL, Proceedings of the 9th International Congress on Glass, Versailles, France Vol 1 (1971) 75.

D.M. MARSH, Proc. Roy. Soc. London. A282 (1964) 33.

M.H. MANGHANI, J. Amer. Ceram. Soc.55 (1972) 360.

J.R. MATHEWS, F.A. McCLINTOCK and W.J. SHACK, J. Amer. Ceram. Soc. 59 (1976) 304.

O.V. MAZURIN and E.S. BORISOVSKI, J. Tech. Phys. Moscow 27 (1957) 275.

G.S. MEILING and D.R. UHLMANN, Phys. Chem. Glasses 8 (1967) 62.

R.E. MOULD, J. Amer. Ceram. Soc, 43 (1960) 160.

Idem, ibid, 44 (1961) 481.

R.E. MOULD and R.D. SOUTHWICK, ibid, 42 (1959) 542.

Idem, ibid, 42 (1959) 582.

R.L. MOZZI and B.E. WARREN, J. Appl. Cryst. 2 (1969) 164.

W. MULLER-WARMUTH, G.W. SCHULZ, N. NEUROTH, F. MEYER and E. DEEG, Z. Naturforsch, 20A (1965) 491.

I. NARAY-SZABO and J.LADIK, Nature 188 (1960) 226.

H.L. OH and I. FINNIE, J. Mech. Phys. Solids 15 (1967) 401.

H.L. OH and I. FINNIE, Int. J. Fract. Mech. 6 (1970) 287.

E. OROWAN, Weld. Res. Supp. 34 (1955) 157.

E.K. PAVELCHIK and R.H. DOREMUS, J. Mater.Sci. 9 (1974) 1809.

K.K. PETER, J. Non-Cryst. Solids 5 (1970) 103.

G. PICKETT. J. Appl. Phys. 16 (1945) 820.

J.D. POLONIECKI and T.R. WILSHAW, Nature 229 (1971) 226.

B. PROCTOR, J. Phys. Chem. Glasses 3 (1962) 7.

V.P. PUKH, S.A LATERNER and V.N. INGAL, Sov. Phys:- Solid State 12 (1970) 881.

J.E. RITTER AND R.P. LaPORTE, J. Amer. Ceram. Soc. 58 (1975) 265.

J.E. RITTER and J. MANTHURUTHIL, Glass. Tech. 14 (1973) 60.

J.E. RITTER and C.L. SHERBURNE, J. Amer. Ceram. Soc. 54 (1971) 601.

E.M. ROCKAR and B.J. PLETKA, in "Fracture Mechanics of Ceramics", Vol.3 ed. by R.C. Bradt et al (Plenum, New York 1978).

F.C. ROESTLER, Proc. Phy. Soc. B69 (1956) 55.

L.E. RUSSEL, J. Soc. Glass Tech. 41 (1957) 304T.

R.J. RYDER and G.E. RINDONE, J. Amer. Ceram. Soc. 43 (1960) 662.

K. SCHOENERT, H. UMHAUER and W. KLEMM, IN "Fracture", ed. by P.L. Pratt (Chapman and Hall, London, 1969).

H. SCHOLZE, in "Proc. of VIII Int. Cong. on Glass", (Soc. Glass. Tech. Sheffield, 1969).

J.E. SHELBY and G.L. McVAY, J. Non-Cryst. Solids 20 (1976) 439.

D.A. SPENCE, Proc. Camb. Phil. Soc. 73 (1973) 249.

S. SPINNER and W.E. TEFT, Proc. A.S.T.M. 61 (1961) 1221.

J.F. SPROULL and G.E. RINDONE, J. Amer. Ceram. Soc. 57 (1974) 160.

Idem, ibid, 58 (1975) 35.

S.D. STOOKEY, U.S. Patent No.3, 498, 803 (1970).

C.J. STUDMAN and J.E. FIELD, Wear 24 (1973) 243.

M.V. SWAIN and B.R. LAWN, Int. J. Fract. 9 (1973) 481.

J.W. TOMLINSON, J. Soc. Glass Tech. 40 (1956) 25T.

G.G. TRANTINA, J. Amer. Ceram, Soc. 60 (1977) 338.

Y.M. TSAI and H. KOLSKY, J Mech. Phys. Solids 15 (1967) 29.

J.B. WACHTMANN Jr., J. Amer. Ceram. Soc. 57 (1974) 509.

B.E. WARREN, H. KRUTTER and O. MORNINGSTAR, ibid 19 (1936) 202.

M. WATANABE, R.V. CARPORALI and R.E. MOULD, Phys. Chem. Glasses 2 (1961) 12.

N. WEBER and M. GOLDSTEIN, J. Chem. Phys. 41 (1964) 2898.

W. WEIBULL, Ingenioersvetenskapsakad 151 (1938) 45.

G.W. WEIDMANN and D.C. HOLLOWAY, Phys. Chem. Glasses 15 (1974) 68.

A.R.C. WESTWOOD and R.D. HUNTINGDON in Proc. Int. Con. on the Mechanical Behaviour of Materials (Society of Materials Science, Kyoto, 1972).

S.M. WIEDERHORN, J. Amer. Ceram. Soc. 50 (1967) 407.

Idem, Proc. Int. Conf. Fracture 4 (Waterloo, Canada 1977).

Idem, in "Fracture Mechanics of Ceramics" Vol.4, ed. by R.C. Bradt et al (Plenum, New York, 1978).

S.M. WIEDERHORN and L.H. BOLZ, J. Amer. Ceram. Soc. 53 (1970) 543.

S.M. WIEDERHORN, A.G. EVANS and D.E. ROBERTS in "Fracture Mechanics of Ceramics" Vol.2, ed. by R.C. Bradt et al (Plenum, New York, 1973).

S.M. WIEDERHORN AND B.R. LAWN, J. Amer. Ceram. Soc. 62 (1979) 66.

S.M. WIEDERHORN and H. JOHNSON, J. Amer. Ceram. Soc. 56 (1973) 192.

S.M. WIEDERHORN, H. JOHNSON, A.M. DINESS and A.H. HEWER, ibid 57 (1974) 336.

J.P. WILLIAMS, S.U. YAO-SIN and B.L. BUTLER, Proceedings of the 11th International Congress on Glass, Prague (1977).

W.H. ZACHARIESEN, J. Amer.. Chem. Soc. 54 (1932) 3841.

W.A. ZDANIEWSKI, G.E. RINDONE and D.E. DAY, J. Mater. Sci. 14 (1979) 763.

LIST OF SYMBOLS AND ABBREVIATIONS

A, n = Stress corrosion parameters

A_D, B_D = Dummy Variables (Chapter 7)

a = Radius of the area of contact in the Hertzian stress field

$C(\sigma)$ = Flaw distribution function in the Weibull analysis

c = Flaw size

c_f = Critical flaw size

E = Young's modulus

E_{visc} = Activation energy for viscous flow

f, μ = Coefficient of static friction

G = Strain energy release rate (Chapter 2)

G = Shear Modulus (Chapter 6)

H = Vickers Hardness

I = Moment of inertia of a crossection

K_I = Mode I stress intensity factor

K_{IC} = Critical mode I stress intensity factor

P = Hertzian fracture failure load

r = Radius of Hertzian fracture ring crack

Y = Normalised stress intensity factor, typically 1.1

γ = Surface energy

κ = No slip stress field parameter in indentation studies

ν = Poisson's ratio

$\dot{\sigma}$ = Stressing rate

$\dot{\sigma}_f$ = Failure stress

σ_{fn} = Failure stress at liquid nitrogen temperature

APPENDIX A

Journal of Non-Crystalline Solids 38 & 39 (1980) 509-514

THE EFFECT OF HYDROXYL ION CONTENT ON THE MECHANICAL AND OTHER PROPERTIES OF SODA-LIME-SILICA GLASS

P.W. McMillan and A. Chlebik

Department of Physics
University of Warwick
Coventry, CV4 7AL
U.K.

The preparation of soda-lime silica glasses having OH^- contents from about 60 to 780 p.p.m. is described. Measurements of density, electrical conductivity, viscosity, Hertzian fracture, slow crack growth and bending strength are reported. The changes in properties, in particular viscosity, showed effects of the OH^- content upon the glass structure. The Hertzian fracture strength was significantly affected by the hydroxyl ion content and possible reasons are discussed.

1. INTRODUCTION

It has been recognized for a number of years that 'water' present as an impurity in glasses can significantly influence the physical properties and can modify the kinetics of phase-separation and crystallization. The subject has been well reviewed by Boulos and Kreidl(1).

It is generally agreed that the water is accomodated in the glass structure in the form of the hydroxyl ion and a reaction of the type

$$\equiv Si\text{-}O\text{-}Si \equiv + H_2O \rightarrow \equiv Si\text{-}OH\ HO\text{-}Si \equiv$$

is generally postulated. The presence of hydroxyl ions in glasses therefore increases the concentration of non-bridging anions and this would be expected to influence a number of physical properties. Thus with increasing hydroxyl ion content the glass viscosity should decrease and the thermal expansion coefficient should increase.

The exact effect of the hydroxyl ions is determined by the occurrence of hydrogen bonding to adjacent oxygen ions and the strength of hydrogen bonds formed is influenced by the nature of the glass and by the relative concentrations of bridging and non-bridging oxygen ions. The strength of the hydrogen bond formed with a non-bridging oxygen ion is much greater than that formed with a bridging oxygen ion.

It has been established that the concentration of water vapor in the test environment can significantly affect the observed strength of glass, and that the phenomenon referred to as static fatigue depends on the interaction of 'external' water with the glass at the crack tip (2,3). It seems reasonable therefore to determine to what extent 'internal' water in the form of hydroxyl ions might influence the strength and fracture behavior. In addition, other properties such as density, electrical conductivity and viscosity were investigated since changes in these properties as a function of hydroxyl ion content would be expected to cast light upon possible structural effects.

2. EXPERIMENTAL

2.1 Glass Preparation and Characterization

The glass chosen for investigation had the weight percentage composition Na_2O16, CaO10, $SiO_2$74. The glass batch was prepared from pure sodium carbonate, calcium carbonate and crushed quartz and melting was carried out in platinum crucibles at a temperature of 1480-1500°C.

To achieve variation of the hydroxyl ion content, modifications to the melting conditions were adopted:
a) the melt in an electric furnace was bubbled with dry nitrogen for 4-5 hours. This allowed a hydroxyl ion content of 50 - 60 p.p.m. to be achieved.
b) melting was carried out in an electric furnace, usually for 16 hours. The water content of the glass came into equilibrium with the laboratory atmosphere and hydroxyl ion contents of about 70 to 140 p.p.m. were obtained.
c) melting was carried out in a gas-fired furnace. Because of water vapor generated in the combustion process, the hydroxyl ion contents achieved were around 350 to 360 p.p.m.
d) steam was bubbled through the melt from 1½ to 5½ hours enabling hydroxyl ion contents of about 750 to 780 p.p.m. to be obtained.

The hydroxyl ion contents of the experimental glasses were established using IR spectroscopy. The intensity of an absorption band at 2.86 μm due to a stretching vibration of the hydroxyl group is measured and the concentration is derived from

$$I = I_o e^{-\alpha c d}$$

where I_o and I are the incident and transmitted intensities respectively, α is the extinction coefficient, c is the concentration of OH ions and d the specimen thickness. The extinction coefficient used was that derived by Scholze for a glass of identical composition (4).

As a check on the effects of the melting conditions upon the overall glass composition, full chemical analyses of a number of melts were carried out. These indicated that no serious loss by volatilisation of sodium oxide or other significant deviations of the proportions of the major constituents from the intended composition had occurred.

2.2 Property Determinations

2.2.1 Density

This was measured on annealed, bubble free specimens using a Preston density comparator.

2.2.2 Electrical Conductivity

The specimens took the form of 2.5 cm square plates of thickness 1 mm to which gold electrodes were applied by vacuum evaporation. Measurements of d.c. conductivity were carried out over the temperature range 50 to 250°C using an applied voltage of 20V. Precautions were taken to avoid polarization.

2.2.3 Viscosity

The fibre extension method was employed and determinations were made within the temperature range 550 to 620°C.

2.2.4 Hertzian Fracture Strength

The technique used was similar to that described by Jarret and McMillan (5). It was possible to carry out at least 20 measurements of the Hertzian fracture strength for each specimen and three specimens of each experimental glass were used. Testing was undertaken in the normal laboratory atmosphere but constant monitoring of atmospheric humidity was carried out. This showed that for all tests, the relative humidity was in the range 60 to 70 percent. It was not considered that this variation would seriously affect the test results but, as a further precaution, tests on the experimental glasses having different hydroxyl ion contents were conducted in random fashion to eliminate possible bias.

2.2.5 Slow Crack Growth Studies

It was decided to utilize the double cantilever beam technique employing a constant moment system. The apparatus was mounted in a glove box to allow control of the relative humidity of the test environment. This was achieved by passing two streams of nitrogen through the glove box, one of which was dry and the other of which had been bubbled through water. By adjustment of flow rates, control of relative humidity from 1 percent upwards could be achieved. The relative humidity was controlled at 60 ± 2 percent. Measurements of fracture velocity were made using an optical method and this enabled velocities in the range 10^{-9} to 10^{-2} ms^{-1} to be accomodated.

The glass specimens were plates 2.5×9.0 cm of thickness 2.2 to 2.4 mm. To aid stability of crack propagation, the specimens were lightly grooved down the centre of each face and precracked at one end.

2.2.6 Bending Strength Determinations

It was thought useful to carry out strength determinations at liquid nitrogen temperature. It was not possible to carry out Hertzian fracture studies undertaken using an Instron Universal Testing Machine. The specimens were 5 cm long and of 2 mm square cross section and were tested employing an inner span of 1 cm and an outer span of 4 cm using a crosshead speed of 0.2 mm per minute. Initial tests showed an unacceptably large scatter of the strength values and this was attributed to flaws associated with the corners of the specimens. By first etching the specimens in 4 percent hydrofluoric acid for 40 minutes, followed by a controlled abrasion treatment similar to that employed for the Hertzian fracture specimens, the scatter in the results was reduced to an acceptably low level.

3. RESULTS

3.1 Density

Table I indicates a slight upward trend of density as a function of hydroxyl ion content. This is consistent with that by Boulos and Kreidl (1).

Table I - Density as a Function of Hydroxyl Ion Content

OH^- content (p.p.m.)	Density ($g.cm^{-3}$)
92	2.4945
138	2.4951
327	2.4955
745	2.4965
758	2.4965

3.2 Electrical Conductivity

In Figure 1 activation energies derived from the slope of the log conductivity versus reciprocal of absolute temperature plots are shown as a function of hydroxyl ion content. The error bars represent the 90 percent confidence limits. Although the trend of the results is not clearly defined, the indications are that the activation energy increases, particularly for high hydroxyl ion contents. This is similar to that by Zdanilwski et al.(6).

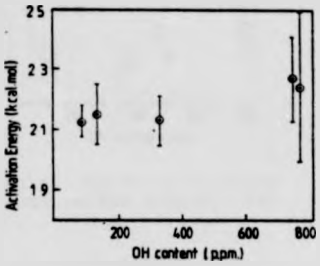

Figure 1. Activation Energy of d.c. conductivity versus hydroxyl Ion Content.

3.3 Viscosity

The marked effect of increasing hydroxyl ion content on viscosity is shown by the results in Figure 2 and in Figure 3 the activation energies of viscous flow as a function of OH^- content are given.

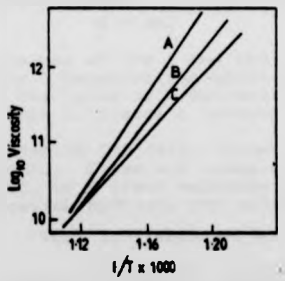

Figure 2. Effects of Hydroxyl Ion Content on Viscosity-Temperature Characteristics, Hydroxyl Ion Contents: A.110 p.p.m., B. 356 p.p.m., C. 763 p.p.m.

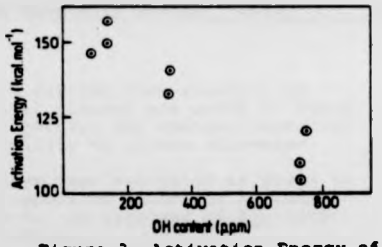

Figure 3. Activation Energy of Viscous Flow versus Hydroxyl Ion Content.

3.4 Hertzian Fracture Strength

In the analysis of the test data it is desirable to take into account frictional effects resulting from slip. Therefore, analysis was carried out using a modified stress field including shear tractions as proposed by Johnson et al. (7). These investigators considered two extreme cases, one when the complete area of contact slipped and the other when no slip occurred. In the analysis used here, the extents of slip and no slip have been taken as proportional to the areas over which each of the effects dominate. These areas have been evaluated by Spence (8).

The results of the anlysis are presented in Figure 4. (The error bars represent 95 percent confidence limts). The Hertzian fracture

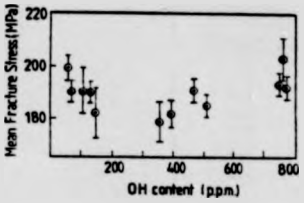

Figure 4. Hertzian Fracture Strength versus Hydroxyl Ion Content.

strength is markedly influenced by the hydroxyl ion content, the most striking feature being the existence of a clearly defined minimum at an OH^- content of 200 to 300 p.p.m.

3.5 Slow Crack Growth Studies

The slow crack growth results in which the logarithm of crack velocity is plotted as a function of the stress intensity factor K_I showed the behavior typical of that found by Wiederhorn (3). Three stages were evident: region I in which the motion of the crack is controlled by the rate of reaction between 'external' water and the glass; region II, where the crack velocity is constant and where the rate of diffusion of water to the crack tip controls the crack motion and region III where the crack velocity is independent of water in the environment and in which the stress intensity factor approaches the value of K_{IC}, the critical stress intensity factor. Crack motion in region I is represented by

$$V = AK_I^n$$

The values of log A and the exponent n derived from analysis of region I behavior for three experimental glasses are given in Table II. The value of n decreases as the hydroxyl ion content increases and this indicates a reduced susceptibility to stress corrosion.

From region III data, values of K_{IC} have been estimated as given in Table II. These are taken as the extrapolated values of K_I corresponding to a crack velocity of $10^{-2} ms^{-1}$. An increase of K_{IC} with increasing hydroxyl ion content is evident.

TABLE II - Parameters Derived from Slow Crack Growth Studies

OH^- Content (p.p.m.)	log A	n	K_{IC} ($Nm^{-3/2}$)
110	-122.3	20.2 ± 0.7	7.66 x 10^5
356	-119.7	19.7 ± 0.8	7.81 x 10^5
703	-105.4	17.3 ± 0.8	7.95 x 10^5

3.6 Bending Strength Determinations

The mean values and 90 percent confidence limits for bending strength determination are given in Table III. No clear cut relationship between the strength at liquid nitrogen temperature and hydroxyl ion content is evident from these data.

TABLE III - Mean Bending Strengths at Liquid Nitrogen Temperature (90% Confidence Limits are Indicated)

OH^- Content (p.p.m.)	Bending Strength (MPa)
59	189.2 ± 9.5
72	164.6 ± 8.2
134	176.4 ± 13.2
394	166.4 ± 6.6
469	197.4 ± 11.1
513	171.0 ± 21.7
754	192.0 ± 12.4
769	170.9 ± 12.9
778	185.6 ± 18.6

References

[1] Boulous, E.N. and Kreidl, N. J., J. Canad. Ceram. Soc. 41 (1972) 83.

[2] Charles, R. J., J. Appl. Phys. 29 (1958) 1554.

[3] Wiederhorn, S. M., J. Amer. Ceram. Soc. 50 (1967) 1049.

[4] Scholze, H., Glass Ind., 47 (1966) 546.

[5] Jarrett, D. N. and McMillan, P. W., J. Phys. E., 7 (2974).

[6] Zdanilwski, W. A., Rindone, G. E. and Day, D. E., J. Mater. Sci. 14 (1979) 763.

[7] Johnson, K. L., O'Connor, J. J. and Woodward, A. C., Proc. Roy. Soc. Lond. A334 (1973) 95.

[8] Spence, D. A., Proc. Camb. Phil. Soc. 73 (1973) 249.